Development of a Crystallization Step for Monoclonal Antibody Purification: Screening, Optimization and Aggregation Control

zur Erlangung des akademischen Grades eines

DOKTORS DER INGENIEURWISSENSCHAFTEN (Dr.-Ing.)

der Fakultät für Chemieingenieurwesen und Verfahrenstechnik des

Karlsruher Instituts für Technologie (KIT)

genehmigte

DISSERTATION

von

Yuguo Zang

Referent: Prof. Dr.-Ing Jürgen Hubbuch

Korreferent: Prof. Dr. Hans Kiefer

Tag der mündlichen Prüfung: 25.06.2013

Acknowledgments

At first I would like to thank Prof. Dr. Jürgen Hubbuch for accepting me as his PhD student and taking the time to be the referee of my thesis.

Prof. Dr. Hans Kiefer, for providing me the opportunity to attend this BMBF-project and, the enormous time he spent with me for supervision, scientific discussion, useful advices and revision of manuscripts, for giving me the freedom to develop my topic and helping to grow as an independent researcher.

Maike Eisenkolb for the great teamwork, her support and encouragement to my thesis. I will surely miss our cook community.

Dr. Bernd Kammerer for giving me advices and teaching me how to work with HPLC.

Albrecht Weber who helped me getting started with the Äkta, and for the hot, friendly discussions about light scattering.

Dr. Andreas Witt who helped me a lot in downstream processing, and for the happy barbecue time in his house.

Dr. René Hendrick for his practical suggestions to my thesis und every warm dinner we had with his kind family.

All staff of pharmaceutical biotechnology faculty at Biberach University of applied Sciences for always giving me a helping hand when needed, which was very important for a foreign studend.

My parents and my sister, who gave me courage, took care of me and alway stand behind me. Without their support, I could never make my first step on Germany.

Especially I would like to thank my wife, Qian Zhang, for always supporting me and giving me strength.

Abstract

Therapeutic monoclonal antibodies (mAbs) are a rapidly growing category of pharmaceutical proteins. For the recovery of mAbs from fermentation broths, protein A affinity chromatography is a dominant process used as a capture step to reduce harvest volume and remove the majority of impurities. However, protein A resin is highly expensive. Therefore, biopharmaceutical industry also tries to find new non-chromatographic techniques to replace protein A chromatography and thus to meet the ever-increasing market of therapeutic mAbs.

The objective of this PhD thesis is to explore the possibility of implement crystallization in the early downstream process for the recovery of monoclonal antibody conforming to GMP requirements. A detailed phase diagram, which is required for the control of crystallization process, was established for an intact mAb after identifying crystallization conditions. Conditions were adapted to crystallize the antibody directly from concentrated clarified cell culture supernatant. The purification efficiency in a single crystallization step was similar to that of protein A chromatography, though with lower yield and a long incubation time. The crystallization rate and crystal yield of mAb were determined in the presence of various model contaminating proteins. The spiking proteins exhibited different impacts on the crystallization of target mAb. Light scattering experiments indicated that this protein-specific difference may be related to the sign of the protein surface charge, where proteins with uneven charge sign as target protein had stronger influence on crystallization process than proteins with the same sign due to electrostatic interactions. The results also suggest interaction analysis as a useful tool to predict whether a specific contaminating protein will have adverse effects on crystallization and should help in the future to develop methods overcoming those adverse effects.

In addition, since amorphous aggregates compete with the formation of crystals, stabilization potency of different osmolyte classes (polyols, amino acids and methylamine groups) was examined focusing on hen egg white lysozyme as an example of a folded globular protein. It was found that polyols increased both thermal and kinetic stability in a concentration-dependent manner, whereas most compounds from the amino acids and

methylamine groups led to destabilization. Furthermore, it was observed that there was similar but not identical effects of particular osmolytes on both types of stability. Kinetic stability therefore cannot solely be predicted by thermal stability. Such information may help to control aggregation and thereby, benefits crystallization.

Zusammenfassung

Monoklonale Antikörper (mAbs) sind eine schnell wachsende Gruppe therapeutischer Proteine. Die Protein A-Affinitätschromatographie ist dabei das dominierende Verfahren bei der Aufreinigung der mAbs aus Kulturübständen. Sie ermöglicht die Reduzierung des Puffer-Volumens und die Entfernung der meisten Verunreinigungen in nur einem *Capture*-Schritt, das Säulenmaterial ist allerdings sehr teuer. Die biopharmazeutische Industrie sucht daher nach neuen, nicht-chromatographischen Verfahren, die die Protein A-Chromatographie ersetzen und so den immer steigenden Markt von therapeutischen mAbs befriedigen können.

Das vorrangige Ziel dieser Dissertation ist die Untersuchung der Möglichkeit eines GMP-konformen Aufreinigungsprotokolls für mAbs mittels technischer Proteinkristallisation. Nach Ermittlung der Kristallisationsbedingung wurde ein detailliertes Phasendiagramm erstellt, mit dem die Kristallisation im Batch kontrolliert werden kann. Die Kristallisationsbedingung wurde erfolgreich auf die Kristallisation aus Fermentationsüberstand übertragen. Die Reinheit des mAbs nach Kristallisation war vergleichbar mit der nach Protein A Chromatographie, jedoch mit einer niedrigeren Ausbeute und einer langen Inkubationszeit. Die Wachstumsgeschwindigkeit und Ausbeute des mAb-Kristalls wurde in Anwesenheit von Modell-Kontaminanten (Proteine unterschiedlicher Größe und Ladung) bestimmt. Dabei zeigten sich erhebliche proteinspezifische Unterschiede. Untersuchungen mittels Lichtstreuung wiesen darauf hin, dass der Einfluss von Kontaminanten mit der Oberflächenladung des Proteins korrelieren: Fremdproteine mit der gegengesetzten Ladung zum Zielprotein beeinflussten den Kristallisationsprozess stärker als solche mit gleicher Ladung. Diese Ergebnisse zeigen, dass die Analyse der Wechselwirkung zwischen Proteinen ein nützliches Werkzeug sein könnte, um ungünstige Einflüsse von Fremdproteinen auf Kristallisation vorherzusagen. Außerdem könnte sie bei der Entwicklung eines Verfahrens zur Beseitigung von nachteiligen Einflüssen hilfreich sein.

Weil amorphe Aggregate mit der Bildung des Kristalls konkurrieren können, wurde anhand des globulären Modellproteins Lysozym aus Hühnereiweiß die potentiell stabilisierenden Effekte von unterschiedlichen Gruppen von Osmolyten (Polyole,

Aminosäuren, Methylamine) untersucht. Polyole erhöhten dabei sowohl die thermische als auch kinetische Stabilität auf konzentrationsabhängige Weise, wohingegen die meisten Aminosäuren und Methylamine zu einer Destabilisierung des Proteins führten. Des Weiteren zeigten bestimmte Osmolyte ähnliche aber nicht identisch Effekt auf beide Stabilitätsarten, kinetische Stabilität lässt sich daher nicht lediglich durch thermische Stabilität prognostizieren. Auf Basis dieser Informationen könnten die Aggregation kontrolliert werden, was dem Kristallisationsprozess hilfreich sein könnten.

Abbreviations

AFM	atomic force microscopy
BSA	bovine serum albumin
CEX	cation exchange chromatography
CG-MALS	composition-gradient multi-angle static light scattering
CHO	Chinese hamster ovary
COS	choline-O-sulfate
CVC	cross-virial coefficient
DLR	double linear regression
DLS	dynamic light scattering
Exp.	Experiments
HCP	host cell protein
HPLC	high performance liquid chromatography
IgG4	immunoglobulin G, subclass 4
LRV	Log reduction value
mAb	monoclonal antibody
PEG	polyethylene glycol
RT	room temperature
RI	refractive index
SEC	size exclusion chromatography
SLR	single linear regression

SLS   static light scattering

SVC   self-virial coefficient

ThT   Thioflavin T

TMAO   trimethylamine-N-oxide

Symbols

A_2 second virial coefficient

A_{11} second cross virial coefficient

adj. r^2   adjusted correlation of determination

c   concentration

dn/dc   specific refractive index increment

I_θ scattered light intensity of solution

$I_{\theta, solvent}$ scattered light intensity of solute

K*   optical constant

Mw   weight-average molar mass

n_0 refractive index of solvent

N_A Avogadro's number

$R(\theta)$ excess Rayleigh ration at the angle θ

$P(\theta)$ particle scattering factor

T_m protein melting point

V_θ detector signal voltage of solution from light scattering

$V_{\theta, solvent}$ detector signal voltage of solvent from light scattering

V_{laser} detector signal voltage of laser from light scattering

Contents

1

Introduction

1.1 Background

Biopharmaceuticals are protein or nucleic acid based pharmaceutical substances used for therapeutic or in vivo diagnostic purposes, which are produced by means other than direct extraction from a native (non-engineered) biological source (Walsh G. 2003; Walsh G. 2001). They constitute about one-third of drugs currently in development (Sekhon BS. 2010). Currently approved biopharmaceuticals and proteins are now widely used to treat diseases as diverse as cancer, autoimmune disorders, myocardial infarction and various growth factor deficiencies (Anicetti V. 2009).

During the past two decades, in upstream processing cell culture densities and cellular productivity have been improved considerably. Fermentation runs longer than it did a decade ago, and protein titers have risen to several grams per liter. The advances in recombinant DNA, metabolic engineering and hybridoma technologies have permitted the large-scale production of virtually any biomolecule at increased titer through a fermentation route (Walsh G. 2000). However, improvements have not occurred correspondingly in downstream processing. Frequently, a "high product" upstream process cannot be matched by scaling up the downstream process correspondingly without increasing the specific production cost or losing yield. The downstream processing, therefore, has been the bottleneck in the overall production process.

Therapeutic monoclonal antibodies (mAbs) are a promising and rapidly growing category of pharmaceutical proteins. Antibody, also called immunoglobulin (Ig), plays a very important role in the immune system. The Igs are produced by the immune-competent cells and secreted by the β lymphocytes of the immune system in response to foreign -

proteins or macromolecules (antigens). The specific antibody-antigen interaction is widely used in analytical methods, such as ELISA and Western Blot. The first monoclonal antibody product was licensed in 1986 (Birch JR and Racher AJ. 2006). Since then, therapeutic monoclonal antibodies are broadly used as a major part of treatments in various diseases including transplantation, oncology, autoimmune, cardiovascular, and infectious diseases (Nissim A, Chernajovsky Y. 2008) and have become a driving force of growth in the biopharmaceutical industry. In 2009, mAbs maintained their ranking as the best-selling class of biologics, with their US sales reaching ~ $ 16.9 billion — an 8.3% growth over their 2008 sales (Aggarwal S. 2010). As of March 2011, 29 mAbs have been approved by FDA (Upreti D. 2012).

The majority of these commercial mAbs are produced from Chinese Hamster Ovary (CHO) and NS0 cells by recombinant DNA technology (Yoo EM, et al. 2002), followed by a sequence of filtration and column chromatography process steps. Several preparative modes of chromatography have been employed for the process-scale purification of mAbs to achieve an overall yield of about 80 %. A typical procedure is depicted in Figure **1**. Protein A affinity chromatography, by which the mAb purity can exceed 95 %, is a dominant process used as a capture step to reduce harvest volume and remove the majority of impurities. The use of protein A chromatography has greatly simplified the recovery process of monoclonal antibodies. Direct capture by this step followed by ion exchange chromatography and size exclusion chromatography has been employed for purifying monoclonal antibodies from fermentation broths (Shukla AA, et al. 2007). However, protein A chromatography has also some drawbacks. First, protein A resin is highly expensive (ca. US $ 10,000 per liter), which can be several times as expensive as other chromatographic materials. Second, Protein A ligand may be cleaved by proteases present in the cell culture supernatant and become an impurity in itself. Finally, elution of mAb occurs at low pH, which can lead to aggregation of mAb and loss of activity. Aggregation usually leads to inactivation of the drug and can even trigger an immunogenic reaction in the organism (Arosio P, et al. 2011). Although much progress has been made to increase dynamic binding capacity of protein A material and make the media resistant to alkaline exposure damage, the media still remains expensive and sensitive to product residence time (Fahrner RL, et al. 2001).
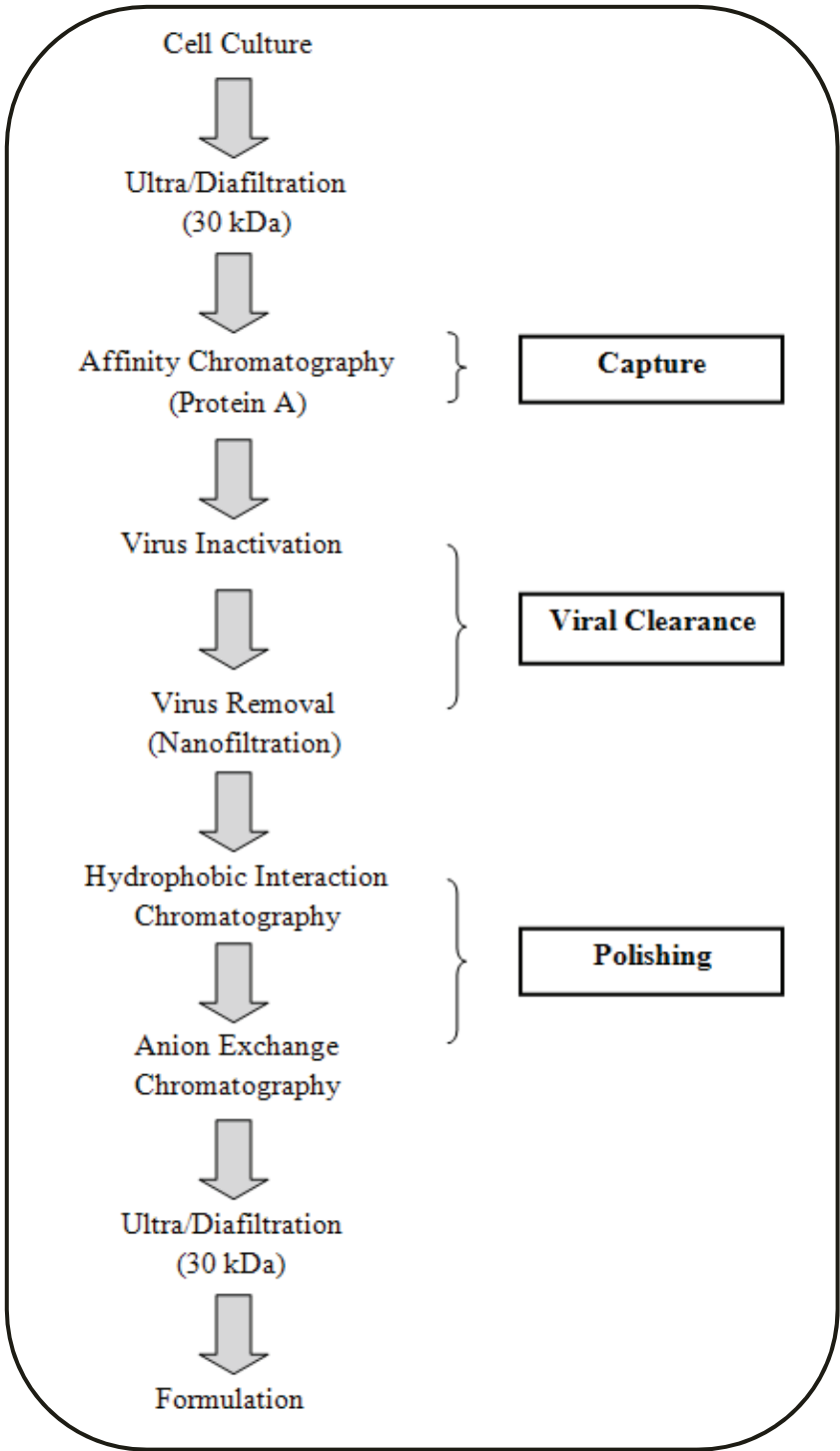
Figure 1. A typical procedure for the recovery of mAb from cell culture. A sequence of chromatographic processes are used for the antibody purification.

In the past decade, CEX as an alternative capture step to protein A chromatography has been evaluated for manufacture of monoclonal antibodies. During CEX, antibody binds to column media because of the positive net charge if the pH value is below its isoelectric point and elutes through increase of pH value or competition from increased salt concentration. While older CEX media were low capacity (20-30 g mAb/L), nowadays, CEX media can reach a dynamic binding capacity of more than 100 g/L for mAbs. (Urmann, et al. 2010; Lain B, et al. 2009; Jackewitz A. 2008). The progress of increased capacity of CEX media has made CEX a viable alternative for protein A chromatography. However, capacity of chromatography matrices cannot increase unlimitedly because of the steric hindrance of protein molecule and the absorption kinetics of the proteins to gel matrices. (Werner RG. 1998.). To meet the ever-increasing productivity in cell culture, for a long-term strategy, biopharmaceutical industry therefore tries to find new non-chromatographic techniques or revisit older technologies with a new application (Chon JH and Zarbis-Papastoitsis G. 2011). Crystallization is one of such technologies to be considered as potential operation to meet the damands and reduce cost during production of mAb.

Crystallization is a separation and purification process widely used in chemical technology for the production of small molecules from bulk chemicals. For macromolecules such as proteins, crystallization is mostly applied in X-ray structure analysis. However, as one of the oldest chemical purification technologies, crystallization is also attracting increasing interest as a protein purification process. Many reports of purification of enzyme from bulk fermentation through crystallization have been published (Fukumoto J, et al. 1963; Kitazono A, et al. 1992; Pitts JE, et al. 1993). Several enzymes, such as cellulase, glucose isomerase and alcohol oxidase, have been crystallized for commercial production (Aehle W. 2007) A purification process of an industrial enzyme using crystallization is illustrated in Figure **2**.
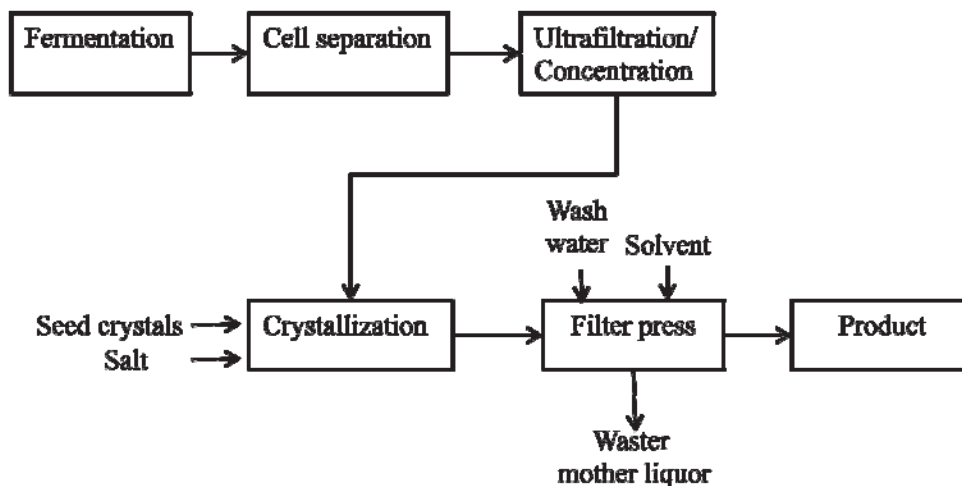
Figure 2. A schematic diagram for recovery of subtilisin from fermentation broth using crystallization (Becker T and Lawlis VB. 1991).

1.2 Objective and research methodolgy

The objective of this research is to develop a process for monoclonal antibody purification using crystallization. To achieve this goal, a monoclonal antibody of the immunoglobulin G subclass 4 (IgG 4), was employed to evaluate the feasibility of recovery of mAbs using crystallization as a capture or intermediate step conforming to GMP requirements. Different unrelated proteins were added to crystallization batches of protein-A-purified mAb in order to understand the influence of impurities on the crystallization process. Because amorphous aggregates compete with the formation of crystals, protein stability is a critical prerequisite for successful crystallization. Therefore, the effect of different osmolyte, a class of small organic molecules used by living organisms to respond to cellular stress, on protein stability was investigated.

Purification of mAb by crystallization

In **Chapter 3**, suitable crystallization conditions for a IgG4 type antibody BImAb04c, which was partially purified by protein A chromatography, were found using the sparse matrix and subsequently grid screen strategies. The phase diagram, which is important for predictive development of an efficient purification step, was determined from microbatch experiments. Crystallization was inspected by microscopy to distinguish amorphous

precipitate and crystal through birefringence. BImAb04c was then purified from culture supernatant through crystallization. Recovery yield and product purity from the crystallization process were compared to that of protein A chromatography. Different analytical techniques, such as UV_{280} absorption, SDS-PAGE and high performance size exclusion chromatography (HP-SEC), were applied to determine protein concentration and sample purity. Surface plasmon resonance spectroscopy served to verify intact Fc-binding activity of crystallized antibody. To meet regulatory requirements for biopharmaceuticals, the ability of the process to remove critical contaminants was investigated by crystallizing mAb in the presence of spiked bacteriophage (virus model) or genomic DNA.

Influence of contaminating proteins on crystallization

The presence of impurities is a critical problem in X-ray structure determination, because incorporation of impurities into protein crystals may affect defect densities, crystal morphology, crystal size, and diffraction resolution (Plomp M, et al. 2003; McPherson A, et al. 1996). For bulk protein crystallization, crystal quality is less important. However, impurities can cause undesirable interactions on the surface of growing crystals (Anderson WF, et al. 1988; Caylor CL, et al. 1999; Kurihara K, et al. 1999) and are often associated with "step pinning", where they adsorb to the surface of a growing crystal and impede the addition of desired components (McPherson A, et al. 1996.; Plomp M, et al. 2003). The presence of impurities may affect both nucleation and growth rate of crystal and may lead to lower rate and yield of protein crystallization. In **Chapter 4**, different unrelated proteins, such as bovine serum albumin (BSA), lysozyme, etc., were used as model contaminants in spike test to investigate how protein impurities affect antibody crystallization. Since the crystal quality requirements are quite different for purification purposes compared to protein structure determination, only growth rate and recovery rate were investigated in this work.

To corroborate these results with direct interaction studies in solution, static light scattering was measured. Different types of interactions occur between proteins, including ionic, hydrophobic, van der Waals and polar interactions such as hydrogen bonds (Lodish H, et al. 2000). Both solvent composition and protein concentration influence the degree of the macromolecular interactions. The strength and direction of the interactions (repulsive

or attractive) can change drastically depending on buffer conditions. The overall interaction between molecules in dilute solution can be described by osmotic virial coefficients, which appear as coefficients in the osmotic pressure equation. A positive value reveals repulsive interaction between molecules, while a negative value suggests attractive interaction. A multi-angle light scattering detector (MALS) for static light scattering (SLS) measurement was employed in this work to study interactions between proteins in solution. SLS allows determining molecular weight, size and osmotic virial coefficients.

For the study of interaction between antibody and contaminating proteins, cross-virial coefficients A_{11} (CVC) were determined through composition gradient - multiangle static light scattering (CG-MALS). The CG-MALS technique consists of preparing solutions of each of the required compositions, delivering each to an SLS instrument automatically, recording the scattered intensity and concentration values in batch module, and analyzing the data through Zimm or Debye Plots (Some D, et al. 2008). In this work, monoclonal antibodies were mixed with different contaminating proteins at varying ratios in crystallization buffer, and interactions between proteins were characterized by CG-MALS.

Effect of osmolytes on protein stability

Protein stability is an issue of consideration in crystallization. The formation and growth of amorphous aggregates, which are often irreversible, competes with the formation and growth of crystals. Denaturation, formation of oligomers or conformational change should not occur or at least be minimized during the crystallization process. Storage solvents for proteins are optimized not only by studying the effect of pH value and ionic strength on protein stability, but also the effect of additives. Osmolytes, such as sugars and amino acids, are a class of small organic molecules used by living organisms to respond to cellular stress (Harries D, Rösgen J. 2008). They can influence thermal and kinetic stability of protein in solution resulting from volume exclusion (hard interactions), or, electrostatic-, hydrophobic-, and van der Waals interactions (soft interactions) (Saunders AJ, et al. 1999). In **Chapter 5**, 21 selected osmolytes from different classes (polyols, amino acids and methylamine groups) was chosen and their thermal and kinetic stabilizing potencies were determined as a function of osmolyte concentration. Thermal stability was studied by

recording thermal denaturation curves with differential scanning fluorimetry using SYPRO Orange. Kinetic stability was investigated using fibrillation of lysozyme as a model system for aggregation, because its kinetics can be manipulated easily by adjusting experimental conditions. The fluorescent dye Thioflavin T (ThT) was used to monitor fibrillation kinetics of lysozyme in real-time. ThT fluoresces strongly with excitation and emission maxima at approximately 440 and 490 nm respectively in the presence of samples containing β-sheet-rich deposits (LeVine H III, 1993; Nilsson MR, 2004). It was also attempted to correlate thermal and kinetic effect.

2

Theory

2.1 Protein Crystallization

Crystallization is a means by which a metastable supersaturated solution can reach a stable lower energy state by reduction of solute concentration (Weber PC. 1991.) and is widely used in the chemical industry for separation and purification purposes. Unlike crystallization of small molecules, crystallization of macromolecules such as proteins has a history of only about 160 years. The first published observation of the crystallization of hemoglobin by Hünefeld in 1840 in Germany (McPherson A. 1991). In the 1930s, X-ray diffraction was applied to protein crystals (Bergfors TM. 2009). Since then, protein crystallization is mostly applied in X-ray crystallography for protein structure analysis. The growth of macromolecular crystals from solution may appear similar to conventional solution grown organic and inorganic crystals, however, there are many differences in physical and mechanical properties.

1. Dimension. Organic and inorganic crystals can often be grown with dimensions of several centimeters. Protein crystals rarely exceed an edge length of one millimeter and are therefore much smaller.

2. High solvent content. Mostly, protein crystals contain 40-60 % solvent by volume (Matthews BW. 1968.), which is contained in channels and gaps that pass among the molecules in the crystal lattice. In some extreme cases such as tropomyosin, solvent content can be as high as 90 %. (Caspar DL, et al. 1969.). Because of the high solvent content, the structure of protein crystals would be destroyed by any prolonged exposure to air due to dehydration.

3. Mechanical properties. Protein crystals are extremely fragile. For example, protein crystals crush if pressed with a metal edge, whereas conventional crystals crack when so challenged. This unique feature is often employed during the screening process in order to examine whether crystals are related to salt or protein.

Because of the aforesaid nature of macromolecular crystals and the conformational flexibility and microheterogeneity of proteins in solution, protein crystallization is not straightforward. The average crystallization success rate (i.e. preparation of X-ray quality crystals) is about 20 % for proteins that express in soluble form (Hui A and Edwards A. 2003). By now, technical progress makes the task of crystallizing proteins much easier. However, protein crystallization is still a complex, multiparametric process (Klyushnichenko V. 2003).

2.1.1 Physical aspects of protein crystallization

Despite some different properties, proteins crystallize following the same process seen with lower molecular weight molecules. Crystallization is a phase transition phenomenon. The knowledge of protein solubility and the phase diagram is therefore essential to understanding and controlling the protein crystallization process. Figure **3** illustrates a generic phase diagram for protein crystallization, which can be obtained experimentally by varying two parameters, such as protein concentration and precipitant concentration, or protein concentration and temperature, at a time. The phase diagram is composed of four zones: in the undersaturated zone, the protein is dissolved and crystallization will never occur; in the metastable zone, protein solution is supersaturated, but no spontaneous nucleation will happen. However, crystal seeds are stable and will grow until system equilibrium has been reached; in the zone of moderate supersaturation (labile zone), protein forms crystals spontaneously; in the precipitation zone, where the protein is highly supersaturated, precipitate (amorphous form) is formed. The thick solid line in Figure **3** is the thermodynamic solubility curve of protein. Only soluble proteins and crystals are thermodynamically stable on this curve. For a defined solution, the maximum crystal yield will be $(c_0 - c_{eq})/c_0$, where c_0 is the initial protein concentration and c_{eq} is the protein concentration on the solubility curve.
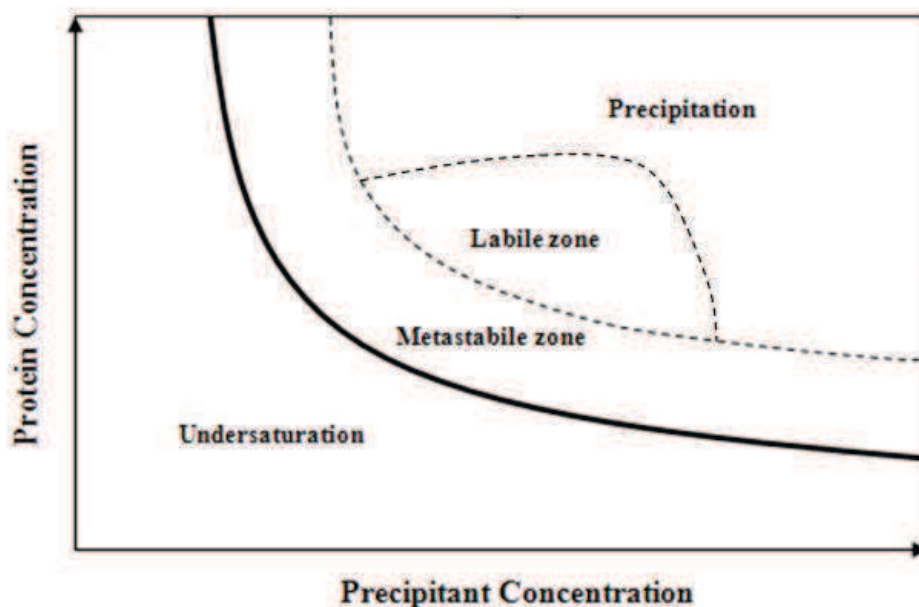
Figure 3. Schematic illustration of a typical protein crystallization phase diagram. The ordinate value is the concentration of protein; the abscissa value is the concentration of a crystallizing agent (precipitant). Other adjustable solubility parameters could be pH and temperature. The phase diagram can be divided into one undersaturated region and three supersaturated zones: precipitation, labile and metastabile zone. The thick solid line represents the solubility curve. The liquid and crystal phases of the protein are in equilibrium on the curve.

There are three phases during crystallization: nucleation, growth of crystal and cessation of growth (Feher G. 1986). Nucleation and growth of crystal occur in supersaturated solutions, in which the protein concentration exceeds its equilibrium solubility value. If no crystal seed is added, nucleation is a prerequisite for a successful crystallization process. As illustrated in Figure **4**, protein molecules have a higher chance of encountering each other in the nonequilibrium state of supersaturation and produce dimers and higher oligomers. Solute protein molecules are continuously added to the aggregate, while others dissociate. However, very small aggregates are not stable due to the high surface tension, which results from a high surface-to-volume ratio (S/V ratio). If the dimension of the ordered aggregate reach a critical value, the S/V ratio has decreased enough to result in stable aggregates, association of the aggregate with new molecule will now be more rapid than dissociation and a crystal nucleus will be formed. The energy

required to result in such critical nuclei is the critical activation free energy for nucleation. The system will remain in a nonequilibrium state for a long time, if the activation energy is high. The initial free energy level can be increased through higher supersaturation of the solution, resulting in reduced activation energy. Thus, supersaturation is the driving force for crystallization. Nucleation occurs typically at a supersaturation 2-10 fold higher than the equilibrium solubility (McPherson A. 1993). Crystal growth rate is also increased at higher supersaturation. However, disordered amorphous aggregates will be favored over crystals if the degree of supersaturation becomes too high.
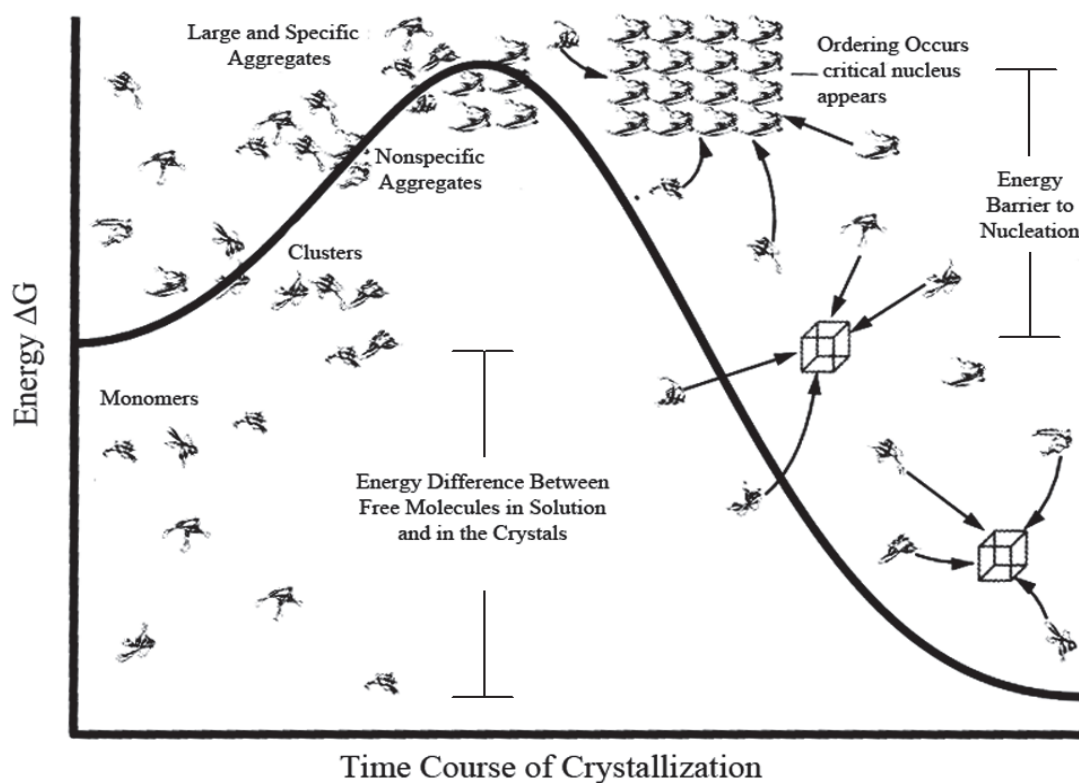
Figure 4. Formation of protein crystals from solution (McPherson A. 1999). As shown here, a supersaturated solution (at the left) is at a higher energy state than crystalline state the system must surmount an energy barrier to get to reach the lowest energy equilibrium state (at the right).

After nucleation, the nucleus will continue to grow through the addition of monomers or small aggregates from solution. Three dominant growth mechanisms were reported by observation of different protein crystals using atomic force microscopy (AFM) (Malkin AJ, et al. 1995.; Kuznetsov YG, et al. 1996): 1) two-dimensional nucleation on surfaces and lateral expansion; 2) spiral dislocations; 3) irregular and rough growth of crystal surface, known as normal growth. Crystals stop growing once the protein concentration reaches its thermodynamic solubility.

2.1.2 Considerations and procedures for protein crystallization

Protein solubility can be affected by different factors, including type and concentration of precipitant, pH value, ionic strength and solution temperature. The chemical composition (precipitant) of the solution is one of the extensively investigated factors during screening of crystallization conditions. As shown in Table **1** (McPherson A. 1999), different salts, polymers, organic solvents and nonvolatile alcohols are used in crystallizations.

Table 1: Frequently used precipitants in macromolecular crystallization (McPherson A. 1999)

Salts	Organic solvents	Polymers
ammonium sulfate	Ethanol	PEG 1000, 3350, 6000, 8000,
Lithium sulfate or chloride	Propanol and isopropanol	Jeffamine T
Sodium or ammonium citrate	1,3-Prapanediol	PEG monomethyl ester
sodium phosphate	2-methyl-2,4-pentanediol	PEG monostearate
sodium or ammonium chloride	Dioxane	Polyamine
Sodium or ammonium acetate	Acetone	
Magnesium or calcium sulfate	Butanol	
Cetyltriethyl ammonium salts	Acetonitrile	
Calcium chloride	Dimethyl sulfoxide	
Ammonium or sodium nitrate	2,5-Hexanediol	
Sodium or magnesium formate	Methanol	
Sodium or potassium tartrate	1,3-Butyrolactone	
Cadmium sulfate	Ethylene glycol 400	

As salt concentration in solution is increased, solubility of most proteins is reduced because of the "salting out" effect. The reason for "salting out" is the competition of salt ions and protein molecules for water, since they all require hydration layers to maintain solubility (Baldwin RL. 1996). Less water molecules are available for proteins at high ionic concentrations. As a consequence, protein molecules self-associate through hydrophobic interaction. The ability of salting out is proportional to the square of the valences of the ionic species composing the salt (Cohn EJ and Ferry JD. 1943). Divalent ions, such as sulfates and phosphates, are the most efficient precipitants. In addition to salting out, there are also specific protein-ion interactions that may have important consequences (Hofmeister F. 1888; Ries-Kautt M and Ducruix A. 1989). It is therefore not sufficient to screen only one or two types of salt.

Polyethylene glycol (PEG), which is a polymer of ethylene oxide produced in various lengths, is another commonly used precipitating agent. In fact, PEG ranks first in the list of successfully used protein precipitants, and over 50 % of published protein crystals were obtained using PEG (Tanaka S and Ataka M. 2002; Roussel A, et al. 1990). PEG induces the attractive interaction between protein molecules by volume exclusion, as first explained in Asakura and Oosawa's depletion model (Asakura S, Oosawa F. 1954; Asakura S, Oosawa F. 1958; Budayova M, et al. 1999). Because of the high molecular weight (MW) and the long structure of PEG, protein molecules in solution are excluded from the hydrodynamic volume of PEG, resulting in concentration of protein. Once the solubility is exceeded, protein precipitation occurs. This depletion force rises with increasing MW and concentration of the polymer in solution. Therefore, control of MW and polymer concentration is needed for protein crystallization. The most useful PEGs have been those in the range MW of 2000-8000 Da, and most protein crystallize within a narrow range of 4-20% (w/v) PEG concentration (McPherson A, 1999).

Organic solvents, such as ethanol, acetone and acetonitrile, can be used to decrease protein solubility efficiently. Such organic solvents lower the dielectric constant of bulk solvent and increase the effective strength of electrostatic interaction, both repulsive as well as attractive (Arakawa T, et al. 2011). This leads to intermolecular polar interactions that allow self-association of protein molecules (Fennema OR. 1996): first, the increased repulsive intramolecular electrostatic interactions cause protein unfolding; next, interior

peptide groups of protein are exposed; at last, intermolecular attractions occur between oppositely charged groups, which results in a reduction of protein solubility. To minimize denaturation of the protein, organic solvents should normally be used at low temperatures ($\leq 4°C$) and ionic strength should be maintained as low as possible (McPherson A, 1999).

The most generally used nonvolatile alcohols are methylpentanediol (MPD) and hexanediol.

In addition to precipitating agent, pH value and temperature of solvent are also factors to be investigated in searching crystallization conditions. Proteins carry negative or positive charge due to the acid and basic side chains of their amino acids. In the acidic pH range, lysine, arginine and histidine for instance protonate, thus protein molecules carry a positive charge, while in the basic pH range, protein is negatively charged due to deprotonation of aspartic and glutamic acid. In solution, protein molecules repel each other because of the like-charge on surface. This electrostatic repulsion will be minimized at isoelectric pH (pI), at which the charge of side chains compensate each other. The lack of net charge makes protein molecules more likely to aggregate and may cause protein precipitation. For many years it was assumed that the optimal pH value for protein crystallization should be its pI, since the solubility of protein is minimal at the pI value. However, some reports indicated that there is no correlation between pI value and the pH at which proteins were crystallized (Gilliland GL. 1988), probably because protein incline to form amorphous aggregate instead of crystal at its pI. Thus, screening a broad pH range is still necessary. In comparison to pH value, solution temperature may have little impact on crystallization. For most proteins, the dependence appears to be rather shallow (McPherson A, 1999). From a practical standpoint, temperature is almost always set near room temperature (22°C-25°C), and all trials are generally duplicated at 4 °C, i.e. in a cold room (Kundrot CE. 2004). The different solubility behavior may give information as to whether temperature is likely to play an important role (McPherson A, 1999). In addition, studies of protein crystallization using AFM (Malkin AJ, et al. 1996a, 1996b, 1996c), have indicated that temperature may have a major effect on the growth mechanisms of the crystals (see **Chapter 2.1.1**). Thus, temperature can have a major influence on the crystal quality.

As mentioned above, many factors affect protein solubility, and protein crystallization still remains a trial-and-error process. To find preliminary crystallization conditions, factorial designs such as sparse matrix and grid screens are used to screen a wider range of conditions (pH, buffer, precipitant, additive, etc) with a modest number of experiments. Sparse matrix screens are employed to evaluate a large number of parameters with a limited amount of protein sample. Prefabricated sparse matrix screening kits are mostly composed of reagent cocktails that are biased toward previous successes (Jancarik J and Kim SH. 1991), which might increase the success rate of initial crystallization screenings. However, because protein and precipitant concentrations are not extensively sampled, it is then difficult to make a statistical conclusion of protein solubility using this screening procedure if no crystal is formed in crystallization trails. Grid screen is another approach, in which several precipitant types are screened more systematically, varying pH-value and concentration (Bergfors TM. 2009). Through experimental design, crystallization trials can be easily and rapidly designed and interpreted in a grid screen experiment. However, DoE requires more experiments to cover a relatively narrow parameter range. Therefore, this method is mostly employed for the optimization of crystallization conditions after initial screen. In this work, different commercial sparse matrix screening kits were used for initial setups. Grid screen was employed for fine-tuning or optimization once initial crystallization conditions had been found.

When searching for crystallization conditions, an undersaturated protein solution is produced initially. Then, solvent properties are altered such as to slowly reach the supersaturation region. This is important to avoid a sudden rise of free energy of the system, which would result in the formation of amorphous aggregates. There are a number of devices, procedures, and methods for attaining a supersaturated protein solution by changing chemical and/or physical properties of the system in a gentle and continuous manner. The most common methods are presented in Table **2** (McPherson A, 1999). Among them, the most used methods in this work were batch crystallization and vapor diffusion.

Table 2. Crystallization methods (McPherson A, 1999).

1. Bulk crystallization
2. Batch method in vials
3. Evaporation
4. Bulk dialysis
5. Concentration dialysis
6. Microdialysis
7. Liquid bridge
8. Free interface diffusion
9. Vapor diffusion (sitting drops)
10. Vapor diffusion (hanging drops)
11. Sequential extraction
12. pH-induced crystallization
13. Temperature-induced crystallization
14. Crystallization by effector addition

Vapor diffusion is the most widely used crystallization technique, due to its convenience and the diversity of variables that can be controlled. Virtually all vapor diffusion trials are carried out at microliter scale with volumes of mother liquor solution from 2 to 20 µl (Weber PC. 1997). Two common procedures, sitting drop and hanging drop, are involved in this approach, depending on the position of the experiment drop. Figure **5** illustrates the hanging drop approach as an example. At the beginning of the trial a crystallization drop containing protein sample and precipitant is dispensed onto a surface in an airtight chamber with a reservoir solution containing the same precipitant but a higher concentration than it is found in the droplet. Thus, vapor pressure of water over the reservoir solution is lower than that over the crystallization drop. Water will be transported from droplet to reservoir until equilibrium between the two is achieved. Meanwhile, nonvolatile chemicals (PEG, salts, protein) will remain in the drop. Since the volume of reservoir is much larger than that of the drop, the ultimate precipitant concentration in the droplet will correspond to the initial concentration of precipitant in the reservoir. The

increased concentration of chemical components in the drop will drive the protein into supersaturation.

$[C_p]_{drop} < [C_p]_{reservoir}$
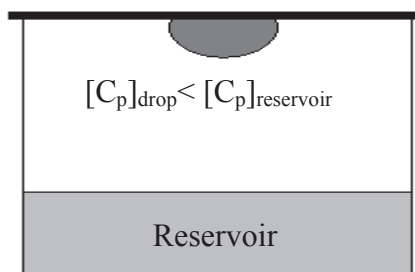
Reservoir

Figure 5. Schematic representation of the hanging drop method. A protein containing drop is sealed in a closed system with a reservoir that is much larger in volume. Since the initial concentration of precipitant in drop ($[C_p]_{drop}$) is lower than that in reservoir ($[C_p]_{reservoir}$), water will be transported from droplet to reservoir until equilibrium is achieved. The concentrations of all nonvolatile chemicals inclusive protein rise thus due to the decrease of volume.

Batch crystallization is the simplest and oldest technique used for the protein crystallization (McPherson A, 1999). This technique is attractive, because it is simple to set up and reproducible. Two or more solutions are mixed together for each experiment, and unlike in vapor diffusion, the protein concentration will not change unless protein molecules are transferred from solution into amorphous aggregates or crystals. For batch processes at laboratory scale (several microliters), a paraffin oil layer is used to prevent dehydration. Because of its simplicity, the technique is amenable to interface with different observational systems designed to monitor and record the process of protein crystal growth. Examples are light scattering studies of nucleation (Malkin AJ, et al. 1993; George A and Wilson WW. 1994; Veesler S, et al. 1994), time lapse photography (Koszelak S, et al. 1991), or AFM (Land TA, et al. 1995; Kuznetsov YZ, et al. 1997). Moreover, a batch process is the method of choice for many industrial-scale production crystallizations (Bergfors TM. 2009), because it can be easy up- or downscaled.

2.1.3 Bulk crystallization for purification

Protein crystallization is mostly applied for structure analysis. For this application, protein purity is an important factor for growth of highly ordered crystals. However, proteins indeed can crystallize from impure solutions, since the specific protein-protein interactions associated with the growth of crystals appear to preclude the inclusion of contaminating species (Przybycien TM. 1998). Although crystallization was used early as a protein purification method (Jakoby WB. 1971), this application has been ignored for a long time, perhaps due to the difficulty in seeking conditions to obtain protein crystals with high quality. The experience from crystallography indicates that the presence of impurities makes crystallization very difficult (Giege R, et al. 1986.; Lorber B, et al. 1993; McPherson A. 1985). However, biochemical engineers have different requirements on crystals than crystallographer. Defect densities and diffraction resolution of crystals, which are important for structure determination, are irrelevant for bulk crystallization. Thus, crystals unsuitable for structural characterization may be suitable as a final product form (Przybycien TM, 1998). In addition, because of advances in fermentation technology over recent years, recombinant techniques allow the creation of strains where few other proteins are secreted and fewer impurities are therefore found in the product stream (Jacobsen C, et al. 1997). Such progresses make protein crystallization more amenable to purification at process scale. Besides the quality of crystals, requirements regarding precipitant, growth rate and crystallization yield are also different between structure analysis and purification applications. Some differences are summarized in Table **3**.

Table 3. Success criteria for crystallography vs. bioseparation processes (Peters J, et al. 2005)

Criterion	Crystals for crystallography	Crystals for processes
Precipitants	Free choice	Nontoxic, nonhazardous
Precipitant costs	No issue	Important
Process compatibility	Not important	Essential
Crystal size	Large is best (150-500 μm)	small okay (10-20 μm)
Packing quality (unit cells)	High resolution	Not important
Crystallization yield	Not important	Very importang
Growth kinetics	Often slow (days to months)	Fast (hours to days)
Redissolution	Not necessary	Necessary
Scalability of conditions	Not important	Very important
Protein available for screening	Critical restriction	No restriction

To date, proteins purified by crystallization are mainly found among industrially produced enzymes. Lipase crystals and subtilisin crystals, for example, both have been produced from a fermentation broth that was only clarified by centrifugation and concentrated by ultrafiltration and diafiltration prior to the crystallization process (Shukla AA, et al. 2007; Jacobsen C, et al. 1998; Becker T and Lawlis VB. 1991). There are only a few such examples in biopharmaceutical processes one of which is the production of insulin using crystallization (Brange J. 1987.). However, the crystallization process is carried out late in the purification sequence where most of the impurities have already been removed (Jacobsen C, et al. 1997.). Because of the challenge from the increased protein titer to downstream processing, as a cheap and easily scaled-up separation and purification process, bulk crystallization has recently drawn more attention again for the recovery of pharmaceutical proteins.

Due to the possible influence of impurities present in fermentation broths, it is practical to place a crystallization step late in downstream processing. Implementation of crystallization as an intermediate or polishing step into the large-scale production of

aprotinin, a protease inhibitor used to decrease blood loss during surgery, has been described by Peters *et al*. (Peters J, et al. 2005.). Their work showed that crystal yield increased if crystallization was performed as a final step as opposed to an intermediate step. They also concluded that there were several advantages for proteins formulated in crystalline form: (1) high proteins concentration; (2) crystalline protein is stable and can be stored for years without significant product degradation. It was also reported that crystalline suspensions provide an improved method of delivery for therapeutic proteins, because of their low viscosity at high concentration (Yang MX, et al. 2003).

Placement further downstream provides a more pure and controlled feed solution to the crystallization process. However, placement earlier in the process would provide more advantages, because crystallization both concentrates and purifies the feed solution (Shukla AA, et al. 2007.), and moreover, this operation unit is cheaper than many chromatographic processes (e.g. protein A chromatography), which are commonly used in routine purification. Judeg *et al*. (Judge RA, et al. 1995) successfully crystallized ovalbumin from a solution containing lysozyme and conalbumin, which were added to the solution intentionally as impurities. The results indicate that conalbumin and lysozyme molecules were excluded from crystalline ovalbumin. The purity of ovalbumin was increased from 86% (w/w) to 99% of total protein by one crystallization step. Although components in fermentation broths are mostly more complex, this study still demonstrates that protein crystallization may be carried out closer to cell culture and fermentation, with the benefit of very high enrichment.

2.2 Characterization of protein protein interactions through virial coefficients

2.2.1 Osmotic virial coefficients

The osmotic virial coefficients appear as coefficients in the osmotic virial equation (Moon YU. 2011):

$$\frac{\pi}{cRT} = \frac{1}{M} + A_2 c + A_3 c^2 + \cdots \tag{1}$$

where π is the osmotic pressure, A_2 and A_3 are the second and third virial coefficients, c is the solute concentration, M is the molar mass, R is the gas constant, and T is the absolute temperature. The second virial coefficient A_2 can be determined through the Zimm equation (**Chapter 2.2.3**), and reflects the magnitude and sign of two body interactions in dilute solution (Neal BL, et al. 1998). If the determined A_2 has a positive values of magnitude $\geq 10^{-4}$ mol·mL/g^2, repulsive interaction is dominant between molecules, which implies that solute molecules in solution prefer to interact with the solvent over interacting with themselves. A slight negative value on the other hand indicates attractive interactions. Solute molecules then tend to aggregate and precipitate from solution. Very large negative A_2 values do not occur, because such thermodynamically poor solvents would not dissolve polymers at all (Podzimek S. 2011). George and Wilson (George A and Wilson WW, 1994) correlated the second virial coefficient with increased an probability of protein crystallization and stated that crystallization only occurs when A_2 is within a narrow range of slightly negative values between about -1.0 to -8.0×10^{-4}mol·ml·g^{-2}, the so-called "crystallization slot". If A_2 is strongly negative, formation of amorphous aggregation is more favorable because of the strong attraction between protein molecules. A_2 therefore becomes a suitable parameter to predict protein crystallization, although cases of proteins crystallizing outside this slot have also been found (Bonnete F, Vivares D. 2002; Ebel C, et al. 1999; Hitscherich C, et al. 2000).

2.2.2 Static light scattering

Elastic or Raleigh light scattering is a phenomenon that occurs when molecules or particles with a diameter more than 1 nm present in solution (Ahrer K, et al. 2003). There are two main techniques for measurement of scattered light. Static light scattering (SLS) measures the average intensity of scattered light at a given scattering angle and is applied for the determination of absolute molecular mass, molecule size and virial coefficients. Dynamic light scatting (DLS) or quasi-elastic light scattering measures the fluctuation of the scattered light intensity over time, due to the Brownian motion of the scattering particles (Ahrer K et al. 2003). In this work, only SLS is discussed and used.

In a dilute polymer solution, the intensity of scattered light depends on (1) the intensity scattered by the solvent, and (2) the intensity scattered by the solute, i.e. the macromolecules. The difference between the two scattered intensities is defined as excess scattering, which provides information about the dissolved macromolecules (Podzimek S. 2011). Excess scattering intensity depends on the molar mass M, the solute concentration c, and the interaction between macromolecules in solutions.

The basic equation that relates the intensity of scattered light with the properties of the macromolecules in solution is the Zimm equation (Zimm BH. 1948).

$$\frac{K^* \cdot c}{R(\theta)} = \frac{1}{M \cdot P(\theta)} + 2A_2 \cdot c + \cdots \qquad (2)$$

In the above equation, K^* is an optical constant equal to $[4\pi^2 n_0^2 (dn/dc)^2]/(\lambda^4 N_A)$, n_0 is the refractive index of solvent at the incident wavelength λ, *dn/dc* is the specific refractive index increment of scattering macromolecules, N_A is Avogadro's number, $R(\theta)$ is the excess Rayleigh ratio at the angle θ (the angle between the scattering direction and the incident light), $P(\theta)$ is the particle scattering factor, A_2 is the second virial coefficient. Macromolecules do not have a single molar mass, therefore molar mass M here is the weight-average molar mass Mw, which is defined as follows:

$$Mw = \frac{\sum_i n_i M_i^2}{\sum_i n_i M_i} \qquad (3)$$

where n_i is the number of mass point with molar mass M_i.

The specific refractive index increment *dn/dc*, appearing in the optical constant K*, characterizes how the refractive index of a solution changes with the concentration of the solute (Huglin MB. 1972). Thus, *dn/dc* can be defined as the slope of the dependence of the refractive index of a polymer solution on its concentration. For the majority of soluble proteins *dn/dc* has approximately the same value, i.e. 0.185-0.187 mL/g (Ball V, Ramsden JJ. 1998; Wen J, et al. 2000) and is constant over a wide range of the protein concentration.

The excess Rayleigh ratio R(θ), named after the physicist Lord Rayleigh, who discovered light scattering phenomenon, describes the angular dependence of scattered light and is defined as:

$$R(\theta) = \frac{(I_\theta - I_{\theta,solvent})r^2}{I_0 \cdot V} \qquad (4)$$

where I_θ is the scattered light intensity of the solution, $I_{\theta,\ solvent}$ is the scattered light intensity of the solvent, I_0 is the intensity of the incident light, V is the scattering volume of sample, r is the distance between the scattering volume and the detector. In practice, the light scattering intensity is measured as voltage yield by photodiodes:

$$R(\theta) = f\frac{V_\theta - V_{\theta,solvent}}{V_{laser}} \qquad (5)$$

here, V_θ, $V_{\theta,\ solvent}$ and V_{laser} are detector signal voltages of the solution, solvent and laser, respectively, f is an instrumental constant related to the geometry of the scattering cell, the refractive indices of the solvent and the scattering cell. This calibration constant is determined by a solvent of well-known Rayleigh ratio, e.g. toluene.

The scattered light from different mass points of a large particle can interfere with each other. Therefore, the intensity of the resulting radiation is smaller than the sum of particular intensity of light scattered by all the individual mass points. This phenomenon is called intramolecular interference of scattered light, which is described by the particle scattering factor P(θ) in equation (2). P(θ) is defined as the ratio of the intensity of light scattered at an angle of observation to the intensity of light scattered at zero angle (where incident light enters) (Podzimek S. 2011) and is decreased with increasing angle, if the diameter of the particle is larger than λ/20 (anisotropic scattering). Thus, the study of P(θ) leads to knowledge concerning the shape of the macromolecules and more specifically to a measurement to the mean square radius of gyration (Albrecht AC. 1957; Zimm BH. 1948).

In addition to intramolecular interference, light scattered by different macromolecules also interferes. The intermolecular interference effect is characterized by the second and higher virial coefficient (A_2, A_3…) and provides information on thermodynamic properties

of the protein-solvent system. Although Equation (2) contains further terms with the third and higher virial coefficients, they can be neglected if light scattering is measured at low concentrations (Podzimek S. 2011). A_2 represent non-ideality in dilute solution, and characterizes the result of macromolecular interactions between particles in solution (Bonnete F, Vivares D. 2002), contributed by electrostatics, van der Waals interactions, excluded volumes, hydration forces, and hydrophobic effects (Curitis RA, et al. 2001; Haas C and Drenth J. 1999).

2.2.3 Determination of virial coefficient by static light scattering

To obtain the second virial coefficient A_2, a Zimm plot (Figure **6**), that is, a plot of $K^*c/R(\theta)$ versus $[\sin^2(\theta/2)+kc]$ is constructed according to Equation (2). The constant k is set to spread out the experimental data points and affects thus only the visual appearance of the plot, but has no influence on the obtained results (Podzimek S. 2011).
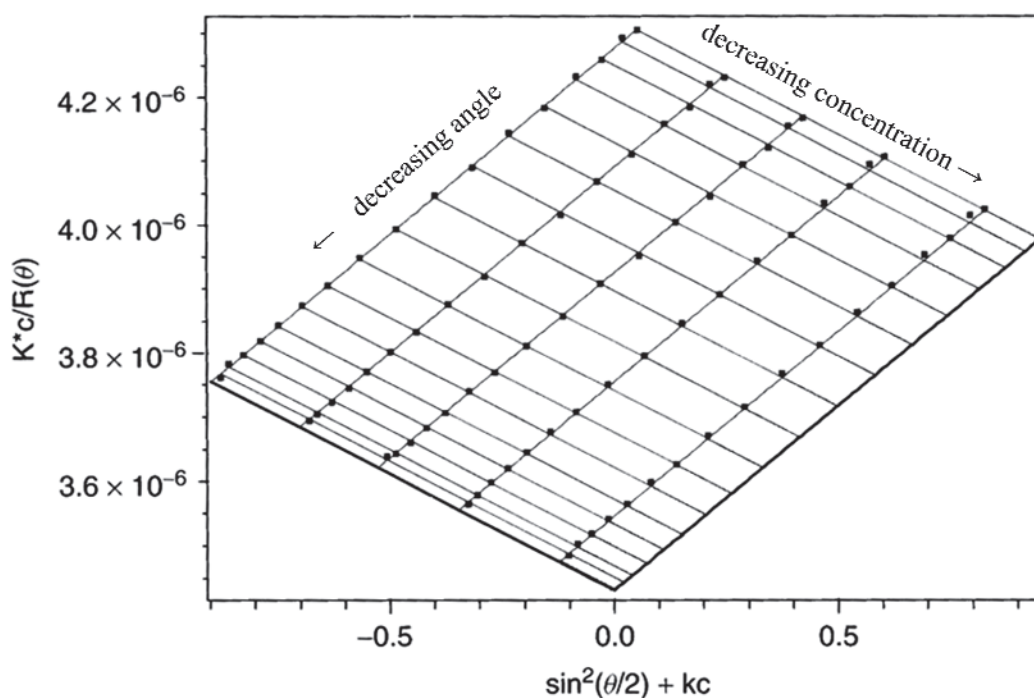
Figure 6. Typical Zimm plot, showing light scattering intensity $R(\theta)$ as a function of concentration c and scattering angle θ (Podzimek S. 2011).

The Zimm plot processes the three-dimensional function R(θ) versus c and θ using a two-dimensional plot and allows simultaneous extrapolation of the concentration and angular dependence of the light scattering intensities to zero angle and zero concentration. The molecular mass, virial coefficients are obtained through a global fit of angular dependence of the light scattering data at different solute concentration and a subsequent extrapolation of the data at zero concentration and zero angle. The slope of the concentration dependence at zero angle yields then the second virial coefficient according to the following equation:

$$\left(\frac{K^* \cdot c}{R(\theta)}\right)_{\theta=0} = 2A_2 \cdot c + \frac{1}{M} \qquad (6)$$

Multi-protein systems require not only information for self interaction between protein molecules of the same species, but also for cross interaction between protein molecules of the different species. In analogy to the aforementioned second self virial coefficient A_2 (SVC), which was used to represent interactions in one protein system, second cross virial coefficient A_{11} (CVC) are employed to characterize the magnitude and direction (repulsive or attractive) of cross interactions in multi-protein system. A_{11} may help to determine optimum conditions to precipitate or crystallize a target protein from an aqueous protein mixture (Choi HS, Bae YC. 2009.) and can also be obtained through light scattering measurement in batch mode.

2.3 Impact of osmolytes on protein stability

Protein stability can play an important role in determining crystallization behavior. Protein aggregation can occur through a number of distinct mechanisms (Philo JS, Arakawa T. 2009): 1. reversible association of the native monomer due to complementary areas on the protein surface; 2. aggregation caused by chemical degradation or modification, which may create new sticky patches on the surface or change the electric charge and reduce electrostatic repulsion between monomers; 3. conformation change due to binding of the native monomer to a surface, which leads to partial unfolding and protein self-association; 4. association of unfolded proteins promoted by environmental stress. Among them,

mechanism 4 represents the most common form of all possible deteriorations (Wang W. 2005) and is mainly considered in this work. Partially or fully unfolded proteins reduce the probability of crystallization. (Price WN, et al. 2009). In addition, aggregation of pharmaceutical proteins, which could occur during downstream process, also results in activity loss and immunogenic adverse reactions. Therefore, protein aggregation must be avoided in general when working with biopharmaceuticals and specifically during a crystallization process step.

Several environmental factors may induce protein aggregation through unfolding, including temperature, ionic strength, pH, salt type and concentration and mechanical stress. Issues of protein stability arise when cells are subjected to such environmental changes that under ordinary circumstances may cause proteins to precipitate (Bolen DW. 2004). Numerous eukaryotic organisms have successfully adapted to such stresses through making and accumulating significant concentrations of small organic molecules (Hochachka PW, Somero GN. 2002). These so-called osmolytes have the ability to stabilize proteins against denaturation stresses in order to maintain cell viability. Most of them belong to three substance classes (Yancey PH, et al. 1982): (1) polyhydric alcohols and sugars (polyols), such as glycerol, sorbitol, sucrose; (2) amino acids and their derivatives such as proline, glycine, glutamine, alanine; and (3) methylamine compounds such as trimethylamine-N-oxide (TMAO). The basic mechanism for their stabilizing property has been shown to correlate with the preferential exclusion of osmolytes from the vicinity of the protein (Bolen DW. 2001). Exclusion of stabilizing osmolytes decreases the entropy of the osmolyte / protein system in the unfolded state, because less volume is accessible to the osmolytes if the unfolded protein occupies a larger volume. Thus compaction of the (folded) protein is energetically more favorable when these osmolytes are present.

Protein stability comes in two flavors: (i) thermodynamic stability, which is equal to ΔG_{unf}, the free energy of unfolding; (ii) kinetic stability, which is related to a high free-energy barrier "separating" the native state from the unfolded or aggregated forms, when the latter are at a lower free energy level. (Sanchez-Ruiz JM. 2010). The effect of osmolytes on thermodynamic stability has been studied extensively (Yancey PH et al. 1982; Taneja S, Ahmad F. 1994; Santoro MM, et al. 1992). However, thermodynamic stability may not be the critical factor for many protein applications of (Rodriguez-Larrea

D, et al. 2006) and does not necessarily correlate with "stabilization" in the sense of preserving functionality over extended periods. In many cases, the kinetic stability of proteins is thus relevant, because it relates more directly with practical parameters of interest, such as shelf-life or half-life time for degradation (Pey AL, et al. 2008). Kinetic stability has also been addressed in osmolyte studies, for instance, osmolytes were able to slow down insulin fibrillation (Nayak A, et al. 2009) or to increase the storage half-life of human recombinant growth factor (Chen BL, Arakawa T. 1996).

It is important to note that osmolytes do not always exhibit protein-stabilizing properties. On the one hand, protecting osmolytes can sometimes be protein-specific: osmolyte that stabilize one protein may have a destabilizing effect on other proteins. For example, glycine betaine has been reported to stabilize RNAse A, but destabilizes α-lactalbumin at low pH (Singh LR, et al. 2009). On the other hand, osmolytes can also be stress-specific. It was reported that TMAO is a potent stabilizer at neutral pH but destabilizes proteins at low pH (Singh R, et al. 2005).

3

Towards Protein Crystallization as a Process Step in Downstream Processing of Therapeutic Antibodies Screening and Optimization at Microbatch Scale

Zang Y, Kammerer B, Eisenkolb M, Lohr K, Kiefer H

Institute of applied Biotechnology, Biberach University of applied sciences

Abstract

Crystallization conditions of an intact monoclonal IgG4 (immunoglobulin G, subclass 4) antibody were established in vapor diffusion mode by sparse matrix screening and subsequent optimization. The procedure was transferred to microbatch conditions and a *phase diagram was built showing surprisingly low solubility of the antibody at equilibrium.* With up-scaling to process scale in mind, purification efficiency of the crystallization step was investigated. Added model protein contaminants were excluded from the crystals to more than 95 %. No measurable loss of Fc-binding activity was observed in the crystallized and redissolved antibody. Conditions could be adapted to crystallize the antibody directly from concentrated and diafiltrated cell culture supernatant, showing purification efficiency similar to that of Protein A chromatography. We conclude that crystallization has the potential to be included in downstream processing as a low-cost purification or formulation step.

Key words: protein crystallization, antibody, purification, protein A chromatography

Introduction

Therapeutic monoclonal antibodies (mAbs) were introduced into the market in 1986. Since then, processing technologies for this class of therapeutics have seen enormous progress as exemplified by recombinant cell lines producing titers in the range of 10 grams per liter of cell culture. Downstream processing technology currently relies heavily on protein A chromatography, a fast and highly selective capturing step, followed by additional chromatographic procedures such as ion exchange or hydrophobic interaction chromatography. Although the purity of mAb achieved after Protein A chromatography usually exceeds 90 %, further purification steps are required to meet the exceptionally high purity targets of biopharmaceuticals. The major drawback of chromatographic procedures is the high cost of adsorption media, which can amount to more than ten thousand US dollar per liter of Protein A resin. Therefore, more economic procedures able to replace at least one chromatographic operation are subject to extensive research.

Protein crystallization, which has been mostly applied in protein structure analysis, has been recognized in principle as a method of protein purification [1, 2]. Within a crystal, protein molecules form a regular lattice able to exclude other proteins as well as misfolded protein molecules of the same type. Therefore, as routinely applied to small molecules, crystallization can also be used as a cheap and scalable purification procedure [3]. Earlier work has demonstrated the feasibility of protein purification by crystallization e.g. for an industrial lipase [4] or the model protein ovalbumin [5]. However, the only biopharmaceutical routinely crystallized at industrial scale and with excellent recovery yields is insulin [6]. Insulin is a small and extraordinarily stable peptide able to refold easily into its native structure even after exposure to organic solvents. It is crystallized late in the purification sequence where most of the impurities have already been removed [4].

Additional benefits of protein crystallization from a formulation perspective are the higher stability of crystalline proteins in comparison to protein solutions, making crystalline formulations an attractive alternative with potentially longer shelf life, and the possibility to control delivery of a protein by making use of crystal dissolution kinetics [7]. The latter has been investigated extensively in the context of insulin formulations [8].

For immunoglobulin, the use of this technique as a means of purification or formulation is not yet a routine procedure. Several authors studied phase behavior of mAbs with the goal to identify a rational approach leading to crystallization conditions [9-11]. The work has been complicated by the fact that in addition to crystallization other phenomena such as precipitation, phase separation and the formation of gel-like phases can occur that kinetically trap the system far from equilibrium and as a consequence reduce the yield of crystalline protein or inhibit crystal formation completely.

In our study, we chose an IgG4 mAb that readily crystallizes under a range of conditions, allowing us to optimize the procedure with respect to mass and activity recovery and degree of purity. Focusing on a simple system composed of solvent and crystals, we were able to identify the solubility limit in a phase diagram and use this as the starting point for up-scaling to a process step conforming to GMP requirements. The aim of this work is to show how initial crystallization conditions can be improved and optimized to result in a process step that delivers high purity and high recovery. We want to point out however, that for any individual antibody, those initial conditions have to be identified by screening. There is yet no method available that allows predicting crystallization conditions from protein sequence or general physico-chemical parameters. Nor can crystallization conditions be transferred from one protein to another even if they are very closely related in sequence. [12] The osmotic virial coefficient B_{22}, which has been shown to often adopt values within a certain range ("crystallization slot") under conditions promoting protein crystallization [13], has not proven to become a general predictor for proteins difficult to crystallize [10] [14].

Materials and Methods

Antibody

Clarified cell culture supernatant of a CHO derived cell line secreting monoclonal IgG4 type antibody mAb04c as well as Protein A-purified mAb04c were kindly provided by Boehringer Ingelheim Pharma GmbH (Biberach, Germany).

Crystallization technique

Wizard™ I, II, III Crystal Screen kits were from Emerald BioSystems (Bainbridge Island, US). Basic and Extension Kits were from Sigma (Taufkirchen, Germany).

For protein crystallization, both vapor diffusion and microbatch techniques were utilized. The methods were performed according to Bergfors [15]. 96 well crystallization plates from Corning (Amsterdam, The Netherlands) and Crystalbridge™ (45 µl) from Greiner bio-one (Germany) were used for sitting drops. 24 wells plate (Greiner bio-one) were used for hanging drop and 60 wells plate (Greiner bio-one) for microbatch crystallization. The protein solution was filtered through 0.2 µm filter (Sartorius, Germany) before crystallization.

Concentration and buffer exchange

Protein A-purified mAb was dialyzed overnight against 20 mM Tris buffer pH 7.0 at 4 °C, and was then concentrated to the desired concentration with Vivaspin™ 500 centrifugal filter (30 kDa MWCO, Sartorius) by centrifugation (15000g, 4°C). Cell culture supernatant was diafiltrated using 7 volumes of 20 mM Tris, 50 mM Histidine, pH 7, and 30 kDa MWCO membrane cassettes (Hydrostat, Sartorius, Germany). Next, mAb was concentrated with Vivaspin™ 500 to the required concentration.

Concentration of purified mAb was determined photometrically at 280 nm using a NanoDrop® 1000 (Thermo Scientific, US) photometer, whereas mAb concentration of culture supernatant was measured by size exclusion HPLC (SE-HPLC) on a Tosoh TSK-GEL 3000 SWXL column at 25 °C. HPLC system was HP1100 from Agilent (Waldbronn, Germany). Elution buffer was 0.05 M Tris/0.15 M NaCl, pH 7, the flow rate was 1 ml/min. Chromeleon® software (Dionex, Sunnyvale, US) was applied for chromatogram recording. Protein was detected at 225 nm and integrated elution peaks were compared to a mAb standard calibration curve.

Purity of mAb was estimated by SE-HPLC and by SDS-PAGE on 12.5 % Laemmli gels. SDS gels were stained with Coomassie Blue or silver.

Distinction of crystals and amorphous precipitate

Crystals and amorphous precipitate were distinguished through birefringence using a microscope (Nikon Eclipse 80i, Düsseldorf, Germany) equipped with polarizing filters. Birefringent protein crystals change color upon rotation of the polarizing filter, while amorphous precipitate does not show this behavior.

Harvest of protein crystal

Crystals were separated from the mother liquor by 10 min centrifugation at 4 °C and 10,000g and washed 3 times with reservoir solution, each volume of the wash reservoir being the same as that of the original sample of crystal suspension. The crystals were redissolved in 100 mM sodium acetate pH 4.0, and stored at 4 °C for further analysis.

Determination of phase diagram

The apparent phase diagram was obtained from microbatch experiments in 60 well plates at room temperature (about 22 °C). 1.5 µL of protein solution were mixed with an equivalent volume of crystallization reagent and covered by paraffin oil (Hampton Research, Aliso Viejo, US). Experiments were monitored visually under microscope over a period of five days. No visual changes were detected starting from day three.

In the metastable zone spontaneous nucleation does not occur, and therefore equilibrium cannot be reached through the growth of crystals starting from a supersaturated solution. The solubility limit of mAb04c was therefore measured by dissolving crystals in a protein-free solution until equilibrium reached. MAb04 was first crystallized as controlled by microscopy at 8 mg/ml protein, 8 % w/v PEG 8000, 0.2 M Ca(OAc)$_2$, 0.1 M Imidazol, pH 7 using microbatch process. Crystals were harvested, homogenized with Seed Bead™ (Hampton Research), and resuspended in deionized water. 20 µl Aliquots of this suspension were added to 1.5 ml centrifuge tubes. Subsequently, 100 µl of precipitant solution as above, but with varying PEG 8000 concentrations was added to each aliquot. The amount of crystallized protein was in excess so that crystals would not dissolve completely. After five days mixing in a Thermomixer Campact (RT, 300 RPM, Eppendorf,

Germany), the protein concentration in the supernatant was determined via A_{280} measurement in a NanoDrop photometer following 10 min centrifugation at 10,000 g. Control experiments showed that equilibrium had been attained at this time.

Binding activity measurement

The functional integrity of the Fc portion of crystallized mAb was confirmed by binding to immobilized Protein A on a Biacore® T100 SPR instrument (GE Healthcare, Germany) as described by the manufacturer.

Spiking experiments with protein contaminations, DNA and bacteriophage

Host cell proteins (HCPs), virus and DNA are critical impurities in the production of biopharmaceuticals. Therefore, spiking experiments using model protein impurities, genomic DNA and bacteriophage T7 as a virus model were carried out.

For HCP spiking, purified mAb (8.6 mg/ml) was mixed with lysozyme (14.3 kDa, 10 mg/ml, Fluka, Schwitzerland) or BSA (bovine serum albumin, 66 kDa, 10 mg/ml, Carl Roth, Germany) and then crystallized by sitting drop vapor diffusion. Precipitant solution was 10 % w/v PEG 8000, 0.2 M Ca(OAc)$_2$, 0.1 M Imidazol, pH 7 as above.

For DNA and phage spiking, DNA at a concentration of 25 µg DNA/mg mAb or phage at a concentration of 6.4×10^7 PFU (Plaque Forming Unit)/mg mAb were added to mAb04c. Crystallization was carried out as above.

Bacteriophage T7 and *E. coli* strain B were kindly provided by A. Kuhn (Hohenheim University, Germany). Bacteriophage concentration was determined by plaque counting following the online protocol [16]. *E. coli* was cultured in LB-Medium pH 7.5. Phage was diluted in 0.85 % *phosphate buffered saline (PBS buffer: 8 g/l NaCl, 0.2 g/l KCl, 1.44 g/l* Na$_2$HPO$_4$, 0.24 KH$_2$PO$_4$, pH 7.4). *Agar plates contained 20 g pepton, 3.5 g NaCl, 15 g agar, 1.5 % w/v glucose, 6.75 mM* Na$_2$HPO$_4$, 8 ml 1 % w/v aniline blue (filtered through 0.2 µm sterile filter) *per liter*. Soft top agar was 7 g agar per liter. All solutions were autoclaved.

DNA concentration was measured using a 96 wells microplate (Greiner bio-one) SYBR® Green I (Invitrogen, Germany) assay [17]. Chromosomal DNA was from salmon

sperm (Fluka, Germany). SpectraMax[®] microplate reader was from Molecular Devices (US). Excitation: 488 nm /Emission: 520 nm.

Results and Discussion

Seven hits (microcrystals or crystals) were found in sparse matrix screening using commercial screen kits. After 3 repetition tests with the 7 conditions found, the most robust condition (10 % w/v PEG 8000, 0.2 M Ca(OAc)$_2$, 0.1 M Imidazol, pH 7) was chosen as the starting point of a phase diagram. Crystals obtained were coffin-shaped structures (Figure **7**). Mechanical rigidity, as qualitatively assessed by micromanipulation using "Crystal tools" (Hampton Research) under microscope, was high compared to "needles" found in other screening experiments. When the seeding stock was prepared (see above) omission of the "Seed bead", acting as a ball mill, even vigourous vortexing resulted in a preparation that contained relatively large crystals and fragments. We therefore expect that those crystals will not fragment extensively under mechanical stress, e.g. in a stirred crystallizer, and will be suitable for subsequent solid-liquid separation. Protein solubility was studied as a function of the concentrations of protein and PEG 8000 in 0.1 M Imidazol 0.2 M calcium acetate pH 7 at RT (Figure **8**). The solubility of mAb decreased with increasing precipitate concentration. Crystals were observed at PEG 8000 concentrations exceeding 5 % (w/v). In the protein concentration range between 10 and 14 mg/ml, there was a broad crystallization region between 5 and 9 % PEG 8000.
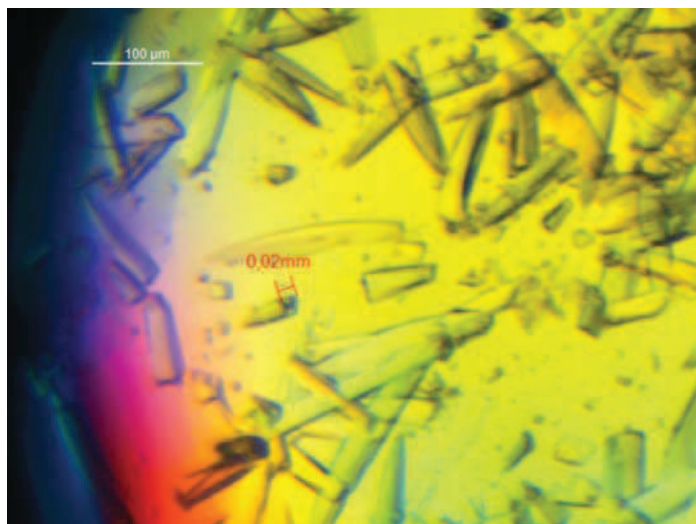
Figure 7. Micrograph of crystals of mAb04c under polarized light. 3 µl microbatch. Conditions: 1.5 µl 20 mg/ml mAb04c in 20 mM Tris, 50 mM Histidine, pH 7 plus 1.5 µl 12 % (w/v) PEG 8000, 0.4 M calcium acetate in 0.2 M Imidazol, pH 7, RT. The broken crystal (intentionally) indicates that the dimension of crystal is about 100~150 µm × 10~20 µm× 10~20 µm.
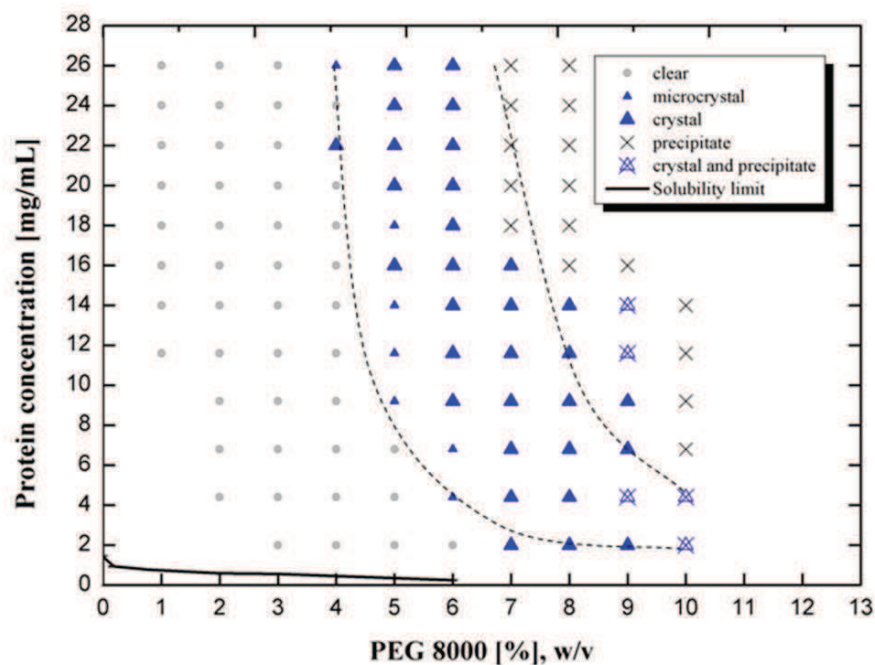
Figure 8. Phase diagram of mAb04c with PEG 8000 as precipitant. Buffer: 0.1 M imidazol, 0.2 M calcium acetate, pH 7.0, RT.

However, this method does not provide the solubility limit, as crystallization does not occur spontaneously in the metastable region where kinetic effects prevent nucleation [12]. Therefore, the solubility limit was determined by preparing saturated solutions in equilibrium with crystalline protein and measuring the protein concentration in the supernatant. The solubility limit (solid line in Figure **8**) was found to be located far away from the crystallization zone at protein and precipitant concentrations at least one order of magnitude below the limit of spontaneous crystallization. This result indicates that mAb04c crystallizes spontaneously only at high supersaturation.

The crystallization of mAb04c in the presence of contaminating protein was examined by spiking with model protein impurities as described by Judge et al [5]. Crystals appeared after 2 days and the crystal shape was indistinguishable from crystals of non-contaminated mAb04c. Crystals were harvested after 5 days and then redissolved in 100 mM Sodium Acetate pH 4. On SDS-PAGE, neither Lysozyme nor BSA still present in the mother liquor was detected in the redissolved mAb crystals (Figure **9**, lanes 3 and 6). The only bands detectable resulted from the original mAb protein (IgG light and heavy chains), plus a band probably resulting from partially degraded heavy chain. The contaminants Lysozyme and BSA were only present in the mother liquor (lanes 2 and 5) and in the wash solutions (lanes 4 and 7). Silver staining is reported to detect individual bands exceeding 10 nanograms, indicating that more than 90% of the protein contaminations had been removed.
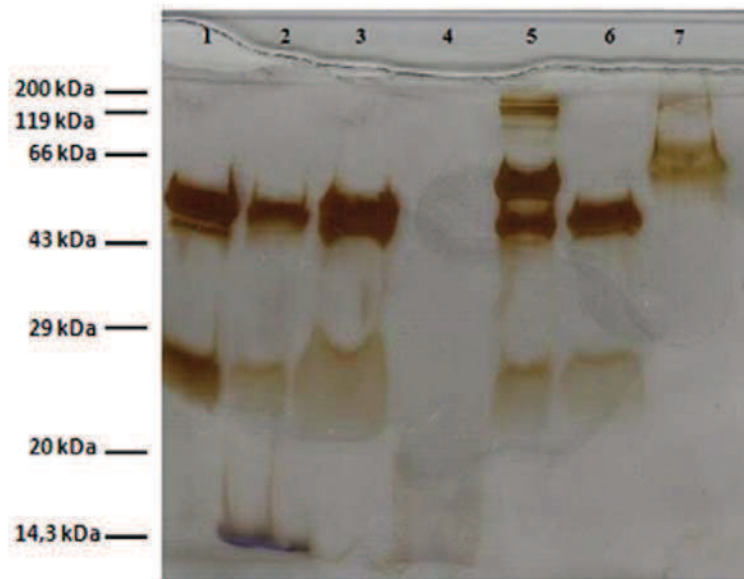
Figure 9. SDS-PAGE of HCP spiking experiment. Silver-staining. Lanes: (1) mAb04c, standard; (2) mother liquor with mAb04c and lysozyme; (3) washed mAb04c crystals from mother liquor with lysozyme; (4) the supernatant from the crystallization with lysozyme; (5) mother liquor with mAb04c and BSA; (6) washed mAb04c crystals from mother liquor with BSA; (7) the supernatant from the crystallization with BSA.

With the success of the HCP spiking test, we attempted to purify mAb04c from the culture supernatant through one-step crystallization. The supernatant was conditioned and concentrated by diafiltration / ultrafiltration and centrifugation as described above. The volume of crystallization suspension was scaled up from 2 µl to 40 µl in a Crystalbridge™ (20 µl protein solution plus 20 µl reservoir). The reservoir was also scaled correspondingly to 20 ml to keep the ratio constant.

Figure 10. Micrograph of crystalline mAb04c crystallized from clarified culture supernatant. Crystallization condition: sitting drop. Reservoir: 0.1 M imidazol, 0.2 M calcium acetate, 9 % w/v PEG 8000. 20 µL clarified culture supernatant (8.3 mg/ml mAb04c) plus 20 µl reservoir, RT. Scale bar 100 µm.

Similar to results of the HCP spiking test, crystals became visible after 2 days (Figure **10**). After 5 days the harvested crystals were redissolved in 20 µl 100 mM Sodium Acetate pH 4. On SDS-PAGE using Coomassie staining (Figure **11**), the concentration of contaminating proteins was considerably reduced (lane 2). A sample of IgG purified by protein A chromatography is shown as a benchmark reference (lane 3). The purity and amount of mAb in each fraction was then accessed by HPLC-SEC (Table 4). Before crystallization, the purity of mAb04c in solution (8.3 mg/ml in 20 µl supernatant) was 42 % of total protein according to peak integration. The analysis of redissolved crystals (2.6 mg/ml mAb in 20 µl buffer) showed that no significant oligomer arose from crystallization (Figure **12**). The purity was increased significantly to 90 % of total protein. Still, only 31.3 % of the mAb originally present in the culture supernatant was recovered in crystals, while the larger portion (67.5 %) was still found in the crystallization supernatant. In comparison, the yield of crystalline mAb04c that had undergone a prior protein A purification was 95 % with no detectable product in the mother liquor.
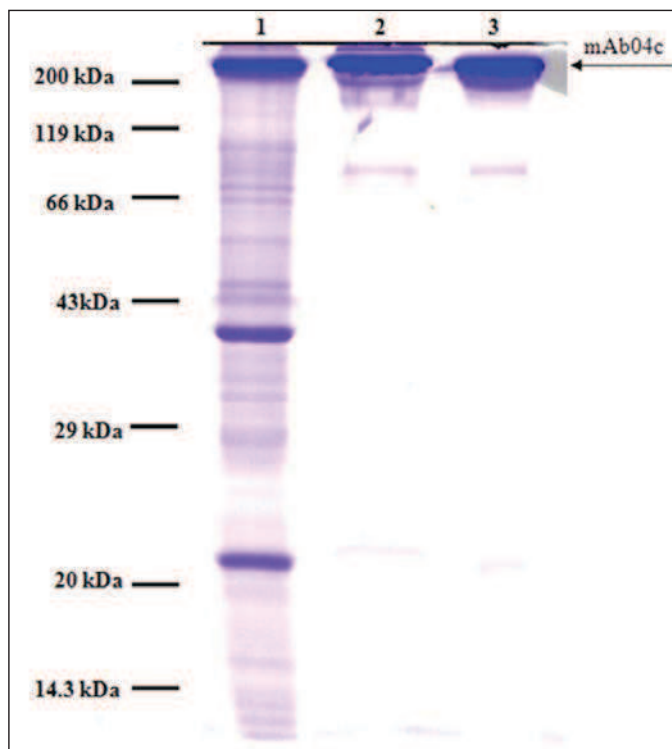
Figure 11. Coomassie blue stained none-reducing SDS-PAGE of mAb04c before and after crystallization or protein A purification. 7 µg of IgG was loaded per lane. Lanes: (1) clarified mAb04c culture supernatant; (2) washed mAb04c crystals, redissolved in 100 mM sodium acetate pH 4.0; (3) mAb04c, purified via protein A chromatography.

Table 4. Purity and Recovery of crystallized mAb04c

Fraction	Amount of mAb04c (µg)	Recovery (%)	Purity (%, estimated)
Clarified culture supernatant	166	100	42
washed mAb 04c crystals[*]	52	31.3	90
supernatant from the crystallization	112	67.5	10

[*] Protein redissolved in 100 mM sodium acetate pH 4.0
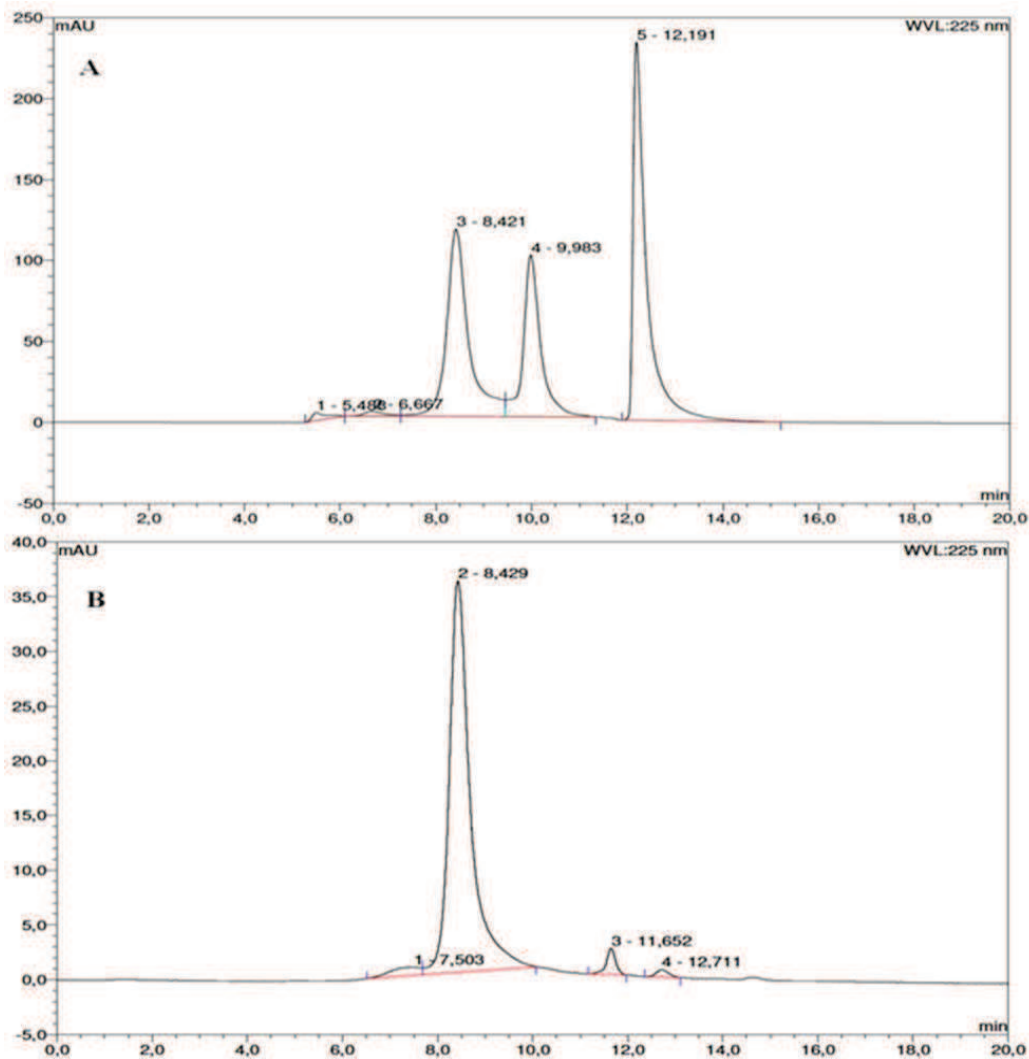
Figure 12. SE-Chromatogram of the sample before and after crystallization. Elution buffer: 0.05 M Tris/0.15 M NaCl, pH 7; flow rate: 1 ml/min; wavelength: 225 nm. (A) Clarified mAb04c culture supernatant. Peak 3: mAb04c, 8.42 min; Peak 4: Contaminating Protein, 9.98 min; Peak 5: Histidine in buffer, 12.19 min. (B) washed mAb04c crystals, redissolved in 100 mM sodium acetate pH 4.0. Peak 2: mAb04c, 8.43 min.

The binding ability of mAb04c to protein A before and after crystallization was determined via Biacore[®]. The association rate constants (k_a) were compared to evaluate a potential affinity loss. Before crystallization, k_a was determined to 3.35×10^6 L/ (mol*s), while after crystallization k_a was 4.81×10^6 L/ (mol*s). Apparently, crystallization had no influence on the affinity of the Fc-Region for protein A.

In spiking experiments, T7 bacteriophage and chromosomal DNA were added to the mAb solution before crystallization in order to challenge the ability of the crystallization process to remove non-protein impurities. Results are summarized in Table 5. LRV (Log reduction value) was 1.4 for DNA and 2.2 for T7 phage.

Table 5. Results of DNA and phage spiking

	Spiking concentration	Concentration in re-dissolved crystals	LRV
T7 phage [PFU/mg mAb]	6.4×10^7	4.5×10^5	2.2
DNA [μg/mg mAb]	25	1.1	1.4

In the present work, we examined the possibility of establishing crystallization as a process step for purification and formulation of a monoclonal antibody. High yields were achieved when crystallization was introduced after chromatographic purification, but not when conditioned cell culture supernatant was used as starting material. Interestingly, crystallization from culture supernatant was nevertheless possible and resulted in efficient removal of contaminants.

We frequently observed that within the crystallization region (area labeled by triangles in Figure **8**), protein initially precipitated directly after mixing (Figure **13**a), while crystals were detectable under the microscope only after a 3-4 hour lag period (Figure **13**b & Figure **13**c). This effect is known from literature. Even when the crystalline form of protein is more stable than its amorphous form, slow nucleation can delay the formation of crystals with respect to amorphous precipitate [18, 19]. Precipitate concentration will then decrease at the same time as crystals grow. Two models have been proposed to explain the growth of crystals from precipitates: phase transition and Oswald ripening [20]. Phase transition is a process where crystals form at the expense of a solid amorphous phase, whereas Oswald ripening describes growth of a few crystals at the expense of many microcrystals [21]. Ng et al. [20] reported that both processes can occur simultaneously. Unfortunately, the birefringence method described above is not applicable to microcrystals smaller than the

microscope resolution limit. In lack of a method distinguishing between amorphous precipitate and microcrystals, we could not decide which of the above processes was dominant.
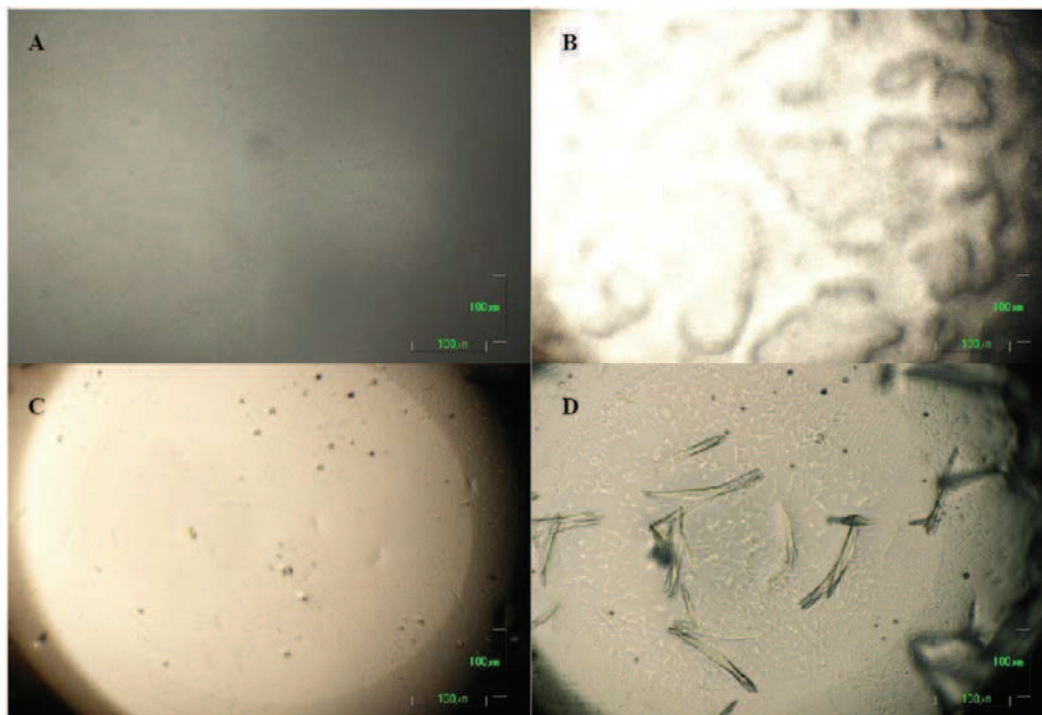
Figure 13. Time course of microbatch crystallization. Protein: 8 mg/ml mAb04c, crystallization buffer: 8 % (w/v) PEG 8000, 0.2 M calcium acetate 0.1 M imidazol, pH 7.0, RT. Time after mixing: (A) 0 hrs, (B) 2 hrs, (C) 10 hrs, (D) 70 hrs. Scale bar 100 μm.

To our knowledge, this is the first determination of the solubility limit at equilibrium for an IgG protein. Ahamed et al. [9] describe an apparent solubility limit in a system where precipitate, but not crystals formed. In comparison to their findings, we found a much lower solubility limit. This could of course be attributed to using a different protein, but Ahamed et al. point out that they would expect a lower solubility limit at equilibrium, i.e. in the presence of crystals as opposed to precipitate. The same antibody was studied by Lewus et al. [10] recently, and crystallization conditions were now identified at a different pH. However, here the solubility limit was not determined unequivocally as concentrations measured in the supernatant decreased over the course of 2 months (Figure. 4 of above reference). The large gap found in our experiments between equilibrium solubility and zone of spontaneous crystallization appears unexpected at first sight, but might be a feature

of IgGs in general. However, similar studies on other model antibody systems will have to be performed before this view can be corroborated. From a practical point of view, our result means that in a continuous process using heterogeneous nucleation, protein should be crystallizable at much lower protein concentration such as 2 mg/ml and at precipitant concentrations of 7 % PEG 8000 or even lower.

Removal of protein contaminations and virus was successful and comparable to Protein A chromatography. DNA removal however was marginal. This may be due to adsorption of DNA to the crystal surface by electrostatic interaction (mAb04c is positively charged at the pH of crystallization). We found that reducing the spiking concentration to 2.5 μg DNA/mg mAb, resulted in 0.35 μg DNA/mg mAb (data not shown), i.e. in an even lower LRV.

Recovery yield of crystallized mAb that had undergone prior protein A purification reached 95 %. This is expected when crystallization conditions are far above the solubility limit as revealed by the phase diagram. However, such high yields could not be achieved when cell culture supernatant was subjected to crystallization. Here the recovery of ~30 % indicated that either solubility of mAb had dramatically increased due to other compounds present in the culture supernatant, or crystallization had simply slowed-down. Microscopic examination indicated that onset of crystal formation was significantly delayed when culture supernatant was used instead of purified antibody: in the latter case, crystals could already be detected after 10 hrs, whereas the same process took 48 hrs starting from culture supernatant. Still, crystal shapes were similar in both cases.

Significant nucleation is the primary requirement for crystal formation. The nucleation rate depends in principle on the solubility of the protein, the degree of supersaturation and the interfacial free energy (γ) between solute and solution [22]. The first two contributions are not expected to be significantly influenced by the presence of impurities. As for the interfacial free energy, from thermodynamic aspect, an increase of the nucleation rate should be observed when impurities are present in the solution [22], because any adsorption onto the nucleus decreases γ [23]. However, kinetically, adsorbing impurities can keep the nucleus at a subcritical size [22]. The nucleation rate hence can be drastically reduced. It was reported that impurities present at 10^{-5} mol/L can decrease the nucleation

rate by ten orders of magnitude [24]. Biostelle et al. [22] point out that there is a competition between the adsorption kinetics of the impurities and the adsorption and integration kinetics of the solute, hence, a longer nucleation time is needed.

Moreover, this competition may further affect the growth of crystals when nuclei develop and begin to transform into crystals. Impurities can adsorb to the surface of the growing crystal, inhibit the addition of free molecules and thereby decrease the growth rate. Because of the negative effect of impurities in both stages of crystallization, the observed delay in mAb04c crystal formation in the presence of contaminating protein was not unexpected. In our work we did not study which stage was prone to be affected by the presence of impurities.

A low recovery rate (31.3 %) was observed, when mAb04c was crystallized from culture supernatant. In a future scaled-up process, nucleation and crystallization rates will have to be controlled e.g. by seeding, feeding protein during crystallization or evaporating solvent. Therefore the yield currently obtained should be subject to significant improvement when working at larger scale.

Conclusion

Protein crystallization has the potential to be introduced as a purification step in downstream processing of mAbs, although our present results so far show that it will likely be more useful in a later purification step and not in initial capturing of the product. Here we demonstrate purification of a monoclonal antibody in a single crystallization step from clarified cell culture supernatant to > 90 % purity, though with yet unsatisfactory yield. Aggregate formation was negligible as shown by SE-HPLC and binding activity to Protein A was not affected by crystallization. The current crystallization time of several days required to reach equilibrium is partly due to the shortcomings of vapor diffusion and should be subject to considerably improvement in a seeded batch process. Current work is focused on up-scaling and optimization of the process with respect to higher yields. We are well aware that at present only a handful of intact IgGs have been successfully crystallized and that there is no generic method available to identify crystallization conditions rapidly

for new antibodies. However, the recent results of Lewus et al. [10], who were able to crystallize an antibody where previously no crystallization conditions have been found [9], are encouraging. More work on a larger set of target mAbs will have to be done before the usefulness of this method can be evaluated in a broader context.

References

1. Klyushnichenko V (2003) Protein crystallization: From HTS to kilogram-scale. *Curr Opin Drug Discovery Dev*. 6: 848-854.

2. Peters J, Minuth T, Schroeder W (2005) Implementation of a crystallization step into the purification process of a recombinant protein. *Protein Expression Purif*. 39: 43-53.

3. Myerson AS, Toyokura K (1990) Crystallization as a separation process. ACS Symposium Series 438. American Chemical Society, Washington, DC

4. Jacobsen C, Garside J, Hoare M (1997) Nucleation and growth of microbial lipase crystals from clarified concentrated fermentation broths. *Biotechnol Bioeng*. 57: 666-675.

5. Judge RA, Johns MR, White ET (1995) Protein purification: The recovery of ovalbumin. *Biotechnol Bioeng*. 48: 316-323.

6. Brange J (1987) Galenics of insulin. *Springer-Verlag*, Berlin. 103   P.

7. Basu SK, Govardhan CP, Jung CW, Margolin AL (2004) Protein crystals for the delivery of biopharmaceuticals. *Expert Opin Biol Ther*. 4: 301-317.

8. Pikal MJ and Rigsbee DR (1997) The stability of insulin in crystalline and amorphous solids: Observation of greater stability of the amorphous form. *Pharm Res*. 14: 1379-1387.

9. Ahamed T, Esteban BNA, Ottens M, Van Dedem GWK, Van der Wielen LAM et al. (2007) Phase Behavior of an intact monoclonal antibody. *Biophys J*. 93: 610-619.

10. Lewus RA, Darcy PA, Lenhoff AM, Sandler SI (2011) Interactions and phase behavior of a monoclonal antibody. *Biotechnol Prog*. 27: 280-289.

11. Kuznetsov YG, Malkin AJ, McPherson A (2001) The liquid protein phase in crystallization: a case study-intact immunoglobulins. *J Crys Grow*. 232: 30-39.

12. McPherson A (1999) Crystallization of biological macromolecules. *Cold Spring Harbor Laboratory Press*. 1st edition. 586 P.

13. George A and Wilson WW (1994) Predicting Protein Crystallization from a Dilute Solution Property. *Acta Cryst*. D50: 361-365.

14. Bonnete F and Vivares D (2002) Interest of the normalized second virial coefficient and interaction potentials for crystallizing large macromolecules. Acta Cryst. D58: 1571-1575.

15. Bergfors TM (2009) Protein crystallization. *Second Edition*. *International University Line*. 474 P.

16. Panec M, Katz DS (2006) MicrobeLibrary-Plaque assay protocols. Available: http://archive.microbelibrary.org/asmonly/details.asp?id=2336

17. Vitzthum F, Geiger G, Bisswanger H, Brunner H, Bernhagen J (1999) A quantitative fluorescence-based microplate assay for the determination fo double-stranded DNA using SYBR Green I and a standard ultraviolet transilluminator gel imaging system. *Anal Biochem*. 276: 59-64.

18. Shenoy B, Wang Y, Shan W, Margolin AL (2001) Stability of crystalline proteins. *Biotechnol Biotech*. 73(5): 358-369.

19. Brange J. Langkjaer L, Havelund S, Volund A (1992) Chemical stability of insulin. 1. Hydrolytic degradation during storage of pharmaceutical preparations. *Pharm Res*. 9: 715-726.

20. Ng JD, Lorber B, Witz J, Théobald-Dietrich A, Kern D et al. (1996) The crystallization of biological macromolecules from precipitates: evidence for Ostwald ripening. *J. Crystal Growth*, 168: 50-62.

21. Mullin JW (1993) Crystallization. *3rd edtion. Butterworth-Heinemann: Oxford, UK*. 600 P.

22. Boistelle R, Astier JP (1988) Crystallization mechanisms in solution. *J Crystal Growth*. 90: 14-30.

23. Lacmann R, Stranski IN (1958) Growth and perfection of crystals. *Wiley, New York*. 427 P

24. Naono H, Miura M (1965) The effect of sodium triphosphat on the nucleation of strontium sulfate. *Bull Chem Soc Japan*. 38: 80-83.

4

Influence of Protein Impurities on the Crystallization of a Monoclonal Antibody

Zang Y, Eisenkolb M, Kiefer H

Institute of applied Biotechnology, Biberach University of applied sciences

Abstract

Large-scale crystallization of pharmaceutically active antibodies has been considered as a possible purification step, and feasibility at small scale has been demonstrated for a number of cases. Here we investigate the robustness of crystallization with regard to the presence of different unrelated proteins over a wide concentration range. Spiking crystallization batches with four model proteins reveals considerably different influences on the time course and yield of antibody crystallization: Protein impurities showing attractive interactions with the antibody in solution as detected by static light scattering analysis inhibit crystal growth at much lower concentration than proteins exhibiting repulsive interactions. At the crystallization condition used, electrostatic properties most likely dominated these interactions and could be used to predict the influence of the impurities on crystallization. The results provide important hints on process operations that should be implemented in downstream processing prior to a crystallization step.

Key words: impurity, protein crystallization, antibody, electrostatic interaction

Introduction

Therapeutic antibodies have seen an enormous success since first introduced in 1986, with currently about 30 antibody drugs approved for the US market [1]. When compared to small-molecule drugs, production of recombinant antibodies is much more costly. It has been estimated that up to 90 percent of the total production cost is taken up by the downstream process, where proteins are purified by chromatographic and filtration methods. Competition and the rise of biosimilars have started to exert strong economic pressure onto manufacturers who are evaluating alternative, more economic purification methods. Crystallization at industrial scale has recently attracted increasing interest as a possible alternative that might replace at least one chromatography unit operation [2, 3]. In our own work [4], we determined the phase diagram of an IgG that crystallized at low ionic strength in the presence of polyethylene glycol (PEG). However, in this system, both the crystallization rate and the final yield strongly depended on the purity of the starting material: If the antibody was purified by protein A chromatography prior to crystallization, crystals formed rapidly and high yields of crystalline protein were obtained reproducibly. If, on the other hand, the antibody was crystallized directly from concentrated cell culture supernatant low yields paralleled by slow crystal growth were observed.

Most of the published work on protein crystallization has been conducted with X-ray structure analysis in mind, where single, well-diffracting crystals are critical for success, while yield and scalability are of minor concern. The single most important factor affecting protein crystallization is certainly the target protein to be crystallized. However, all compounds other than the product can also affect growth rate and crystal yield when present in the starting material. Beneficial or deleterious effects of impurities on crystal growth are well documented in the case of small molecules [5, 6]. For macromolecular crystallization, the effect of impurities has been mostly studied on model proteins such as lysozyme [7-10], due to its easy access and crystallizability. Nevertheless, results from lysozyme cannot always be transferred to other proteins [11].

The protocol established in our paper cited above [4], allowed to crystallize the intact monoclonal antibody (mAb) mAb04c at micro liter scale over a period of two days yielding 95 % of crystalline mAb. When concentrated cell culture supernatant instead of a protein A eluate was used as the starting material, crystal yield and growth rate dropped to 30 % after 5 days of crystallization. The cell culture supernatant contained a significant fraction (~60%, w/w) of contaminating proteins including product-related impurities as evidenced by SE-HPLC. In the present report, we asked which properties of protein impurities might be responsible for inhibiting the crystallization process. To answer this question, we measured crystallization kinetics in the absence and presence of defined spiking proteins at varying concentrations, and at the same time investigated interactions between target protein (mAb) and protein impurities using light scattering. We explored a broad range of contaminant-to-product ratios that covers representative samples of cell culture supernatants used in industrial processes.

Materials and Methods

Antibody

Protein A-purified mAb04c (purity > 98 %), a monoclonal IgG4 type antibody derived from a CHO cell line was kindly provided by Boehringer Ingelheim Pharma GmbH (Biberach, Germany).

Sample preparation

Protein A-purified mAb was concentrated to the desired concentration in 50 mM Histidine buffer pH 7.0 with Vivaspin™ 500 centrifugal filter (30 kDa MWCO, Sartorius, Germany) by centrifugation (15000g, 4°C). Concentration of purified mAb was determined photometrically at 280 nm using a mass extinction coefficient of 1.47 [ml/ (mg·cm)].

Crystallization technique

Crystallization was carried out as described previously [4] using optimized conditions. 2.7 mg/ml (18 µM) mAb04c with and without added macromolecular impurities was crystallized in 25 mM Histidine, 25 mM Tris, 3.15 % (w/v) PEG 3350, pH 7.2 at room

temperature (ca. 21 °C). Protein was crystallized in parallel at micro batch (≤ 10 µl) as well as at batch (1 ml) scale. All mixtures were seeded by adding crystalline mAb04c to a final concentration of 2µg/ml to prevent nucleation processes from dominating the kinetics.

Spiking experiments with unrelated proteins

The effect of impurities on crystallization was investigated by spiking the crystallization batches with defined unrelated proteins at the molar ratios (**spiking protein: mAb**) indicated. Dependence of crystal yield on the concentration of added bovine serum albumin (BSA, Sigma, Germany) after 10 and 20 hours of crystallization, respectively, was investigated over a molar ratio range (BSA: mAb) of 0.29 to 7.7. Next, the antibody was crystallized in the presence of one out of four proteins (ovalbumin, lysozyme, cytochrome c, BSA) at a constant molar ratio of 3.7. Lysozyme, ovalbumin and cytochrome c were from Fluka (Switzerland).

1 ml batch experiments were carried out in 1.5 ml reaction tubes (Eppendorf, Germany) and were agitated in a test-tube rotator during the entire procedure. For visual inspection under microscope, 3 µl aliquots were withdrawn from each batch and transferred to microbatch plates (Greiner Bio-one, Germany). Crystallization rates were determined by measuring the time course of antibody concentration in the supernatant: 30 µl samples were taken from batch experiments at defined intervals and centrifuged at 15,000 g, 10 °C for 10 min. The supernatant was diluted with 120 µl of distilled water to prevent further crystallization. The IgG concentration in the samples was determined by Protein-A-HPLC on an HP1100 HPLC system (Agilent, Waldbronn, Germany) equipped with a pre-packed POROS® Protein A affinity column and a 1 mm guard column (Applied Biosystems, US). The equilibration buffer was 25 mM sodium phosphate 150 mM NaCl pH 7.4, the elution buffer was 25 mM sodium phosphate pH 3.0, the flow rate was 1 ml/min. Chromatograms were recorded at 225 nm, elution peaks integrated using the Chromeleon® software (Dionex, Sunnyvale, US) and compared to a mAb standard. The protein composition in the supernatant was analyzed by non-reducing SDS-PAGE on 12.5 % Laemmli gels and staining with Coomassie Blue.

Characterizing of protein-protein interaction via composition-gradient multi-angle static light scattering

Osmotic virial coefficients were determined as an indicator of attractive or repulsive interactions between product and contaminant. Composition gradient-multiangle static light scattering (CG-MALS) allows to measure self-virial coefficients (SVC) A_2 and the cross-virial coefficient (CVC) A_{11} for a two-component system simultaneously. A_2 describes interactions between molecules of the same type (i.e. mAb or impurity, respectively), while A_{11} describes the interaction between two different molecules. Positive virial coefficients are indicative of repulsive, negative coefficients of attractive interactions.

In CG-MALS, static light scattering intensity is measured as a function of protein concentration. For a two-component system, the concentration gradient has to be designed so that both SVCs of the individual components and the CVC can be extracted [12-14]. A Calypso™ II System for sample preparation and delivery connected to a Dawn-8® multi-angle static light scattering detector and an Optilab T-rEX™ refractive index (RI) detector for the determination of protein concentration were used. Instruments were from Wyatt, CA, USA.

All proteins were dissolved or diluted in buffer containing 25 mM Tris, 25 mM Histidine, pH 7.2 as stock solution, where mAb04c concentration was 2 mg/ml, and the concentrations of BSA and lysozyme were 6 mg/ml. All protein samples and buffer were filtered through 0.2 μm syringe filter (Sartorius, Germany). The mAb04c solution was mixed with BSA or lysozyme solution by the Calypso™ II System. Different compositions were obtained by varying the relative flow rates of the pumps and then injected into the SLS and RI detectors. Three segments were integrated in the programmed method (Figure **14**, mAb04c and BSA as an example): a concentration gradient of mAb alone, followed by a crossover composition gradient changing the ratio of concentration of mAb and BSA, and finally a concentration gradient of BSA.
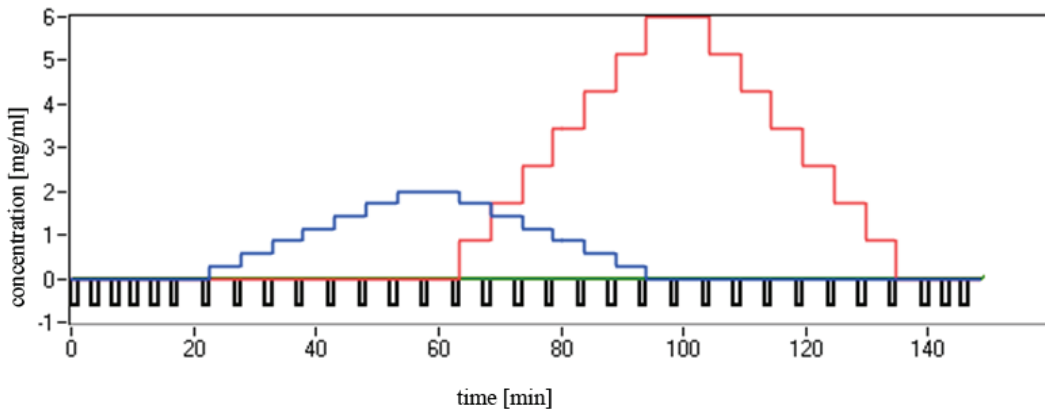
Figure 14. Experiment design for the characterization of nonspecific interaction between mAb04c and BSA using CG-MALS. Running buffer: 25 mM Tris, 25 mM Histidine, pH 7.2. The mAb04c solution was mixed with BSA solution by the Calypso™ II System: a concentration gradient of mAb alone, followed by a crossover composition gradient changing the ratio of concentration of mAb and BSA, and finally a concentration gradient of BSA. Both protein solutions were conditioned in running buffer. Blue line: concentration gradient of mAb04c; Red line: concentration gradient of BSA.

The other two spiking proteins, cytochrome c and ovalbumin, were not amenable to CG-MALS analysis. Cytochrome c absorbs light at the wavelength of the incident laser light (658 nm). Ovalbumin appeared to form large soluble aggregates in the running buffer: SLS analysis indicated an apparent molecular weight of ~ 350kDa instead of the expected 44 kDa, although the protein solution appeared clear. Both effects interfere with light scattering analysis.

Molecular weight, SVC and CVC were determined fitting the measured scattering intensities to equation (7) [15]:

$$\frac{R\left(c,\ \theta\right)}{K} = \left(\frac{dn}{dc^A}\right)^2 \frac{Mw^A c^A P\left(r_g^A, \theta\right)}{1 + 2A_2^A Mw^A c^A P\left(r_g^A, \theta\right)} + \left(\frac{dn}{dc^B}\right)^2 \frac{Mw^B c^B P\left(r_g^B, \theta\right)}{1 + 2A_2^B Mw^B c^B P\left(r_g^B, \theta\right)}$$

$$- 4\left(\frac{dn}{dc^A}\right)\left(\frac{dn}{dc^B}\right) A_{11} Mw^A Mw^B c^A c^B P\left(r_g^A, \theta\right) P\left(r_g^B, \theta\right) \qquad (7)$$

in which $R(c, \theta)$ is the excess Raleigh ratio at the angle θ (the angle between the scattering direction and the incident light); K is a constant that depends on the wavelength of incident light and solvent refractive index; dn/dc is the sample refractive index increment; and P (r_g,

θ) is the angular dependence of the scattered light on r_g, the radius of gyration of the sample; the indices A and B represent the two different proteins.

Results

Crystallization at varying impurity concentration

MAb04c was crystallized in seeded batch experiments as described in Methods in the absence and presence of added protein impurities. Figure **15** shows the dependence of crystal yield on the concentration of added bovine serum albumin at two time points. Pure antibody was crystallized to 95 % after 10 hours and to 98% after 20 h. Increasing the BSA concentration slowed down crystal formation considerably. At a molar ratio of BSA to antibody of 0.77 no crystals were visible after 10 h, while after 20 h, more than 90 % had crystallized. At a ratio of 7.7, no crystals formed even after 20h. Micrographs (Figure **16**) confirm that insoluble protein was always crystalline and never amorphous.
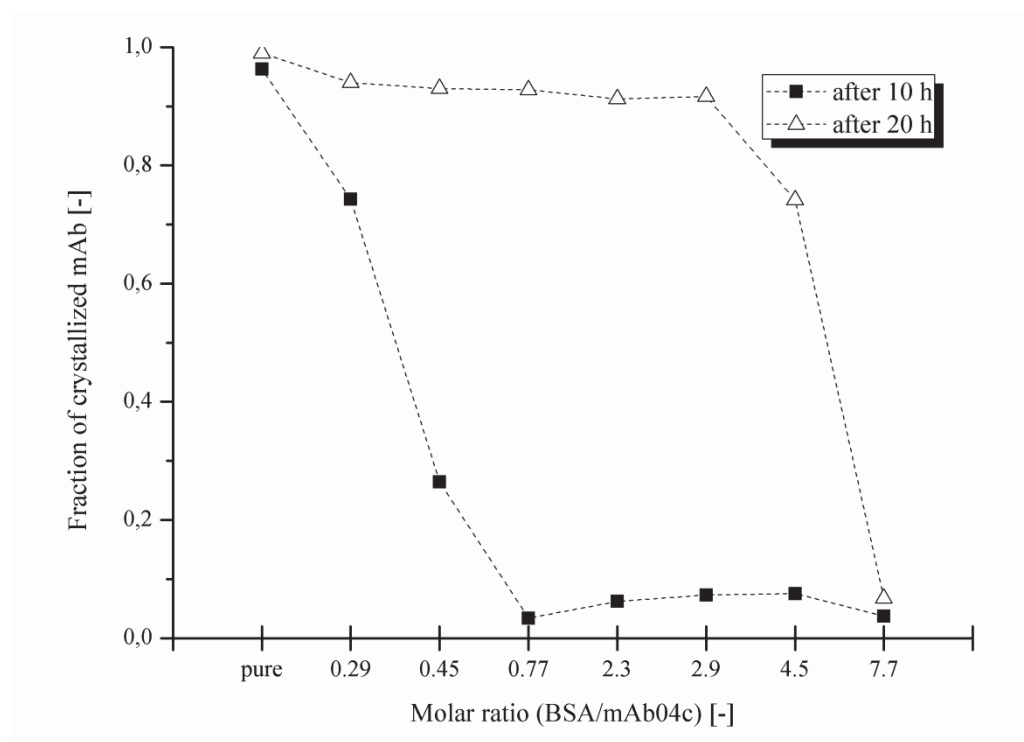
Figure 15. Influence of BSA amounts on the crystallization process of mAb04c. MAb04c was crystallized with BSA at molar ratios (BSA: mAb) of 7.7, 4.5, 2.9, 2.3, 0.77, 0.45, and 0.29. Fraction of crystallized mAb in each sample was determined after 10hrs and 20hrs.

To control whether crystals were formed from antibody and not from the spiking protein, supernatant samples were subjected to SDS-PAGE. In Figure **17**, the staining intensity of antibody in the supernatant decreased during crystallization while the intensity of the BSA band remained constant as expected. Although an incorporation of BSA in the mAb-crystals cannot be totally excluded, this result indicates that the crystals predominantly originated from antibody, even at a molar excess of BSA over mAb of 3.7.
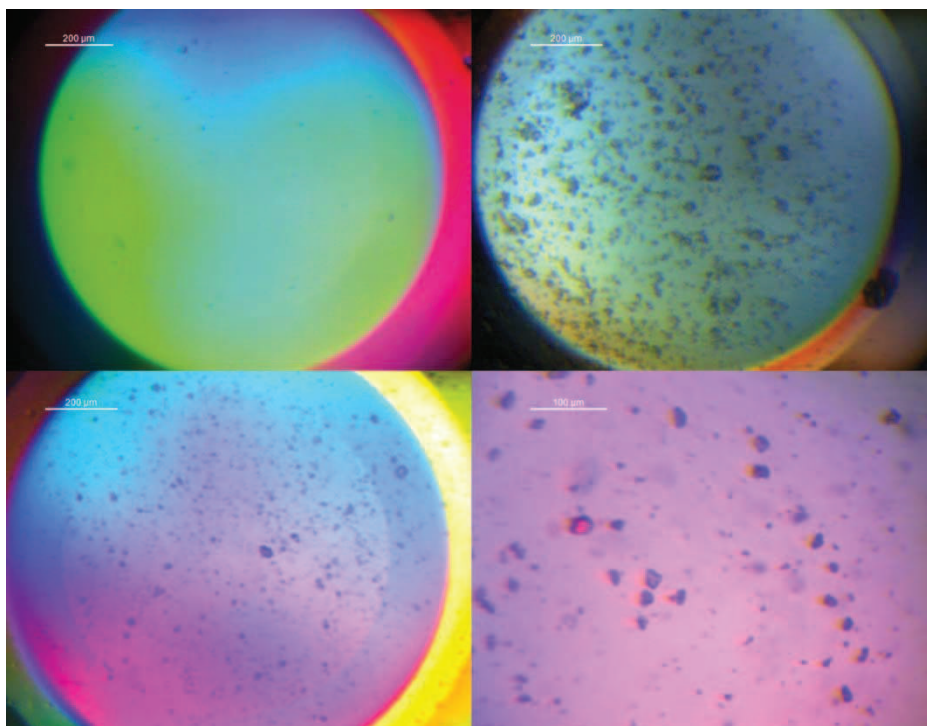
Figure 16. Optical micrographs of micro batches with BSA as examples of growth of protein crystals after a period incubation. Top left: initial conditions in batches, the black dots were seeds of mAb04c. Top right: in section of the batch with molar ratio of 0.29 after incubation of 20 hrs. Bottom left: inspection of the batch with molar ratio of 4.5 after incubation of 20 hrs. Bottom right: same sample as that in the bottom left, but with a higher magnification, the aggregate showed slight birefringence under polarized light demonstrating the protein crystalline. Scale bar in the top left, top right and bottom left =200 μm, 100 μm in the bottom left.
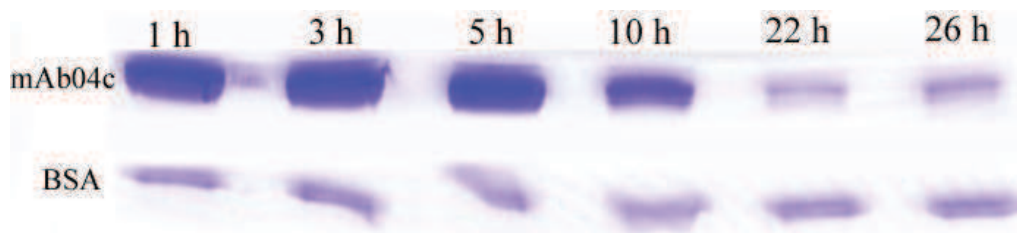
Figure 17. Time course of protein concentration in the supernatant of a batch with BSA (molar ratio 0.29) as impurity. 6.4 µl samples of supernatant after centrifugation from batch experiments were loaded. The staining intensity of BSA remained constant, while the intensity of mAb04c decreased over time, indicating that the observed crystals resulted from mAb04c. The skewed band of BSA at 5 hours could be caused by uneven gel.

Crystallization kinetics in the presence of different spiking proteins

Following this first experiment, four model contaminants representing a range of different molecular weights and isoelectric points (Table **6**) were mixed with mAb04c in separate batches. The molar ratio was 3.7 throughout the experiments.

Table 6. Molecular weights (MW) and isoelectric points (pI) of mAb04c and the spiking proteins.

Molecule	MW, kDa	pI	Resource
mAb04c	150	8.2-8.5	kindly provided by Boehringer Ingelheim
BSA	66	4.7	Malamud D and Drysdale JW, 1978 [16]
ovalbumin	44	4.4-4.6	Beeley JA et al. 1972 [17]
lysozyme	14.3	10.7	product information
cytochrome c	12.3	10.6	Keilin D and Hartree EF, 1945 [18]

The time courses of crystallization are presented in Figure **18**. In the presence of lysozyme and cytochrome c as well as in the control experiment without contaminant the main decrease of mAb04c concentration in the supernatant occurs in a period of 3 to 5 hours after mixing. Equilibrium (ca. 0.25 mg/ml) is reached after 10 hours. Crystallization batches containing ovalbumin or BSA precipitated immediately after mixing, which resulted in lower mAb-concentrations in the supernatant during the first 5 hours compared

to the other batches. However, precipitate later dissolved and mAb concentration in the supernatant increased again for the next 5 hours. Time to equilibrium was about 22 hours for the batch containing ovalbumin and about 30 hours for the batch containing BSA.
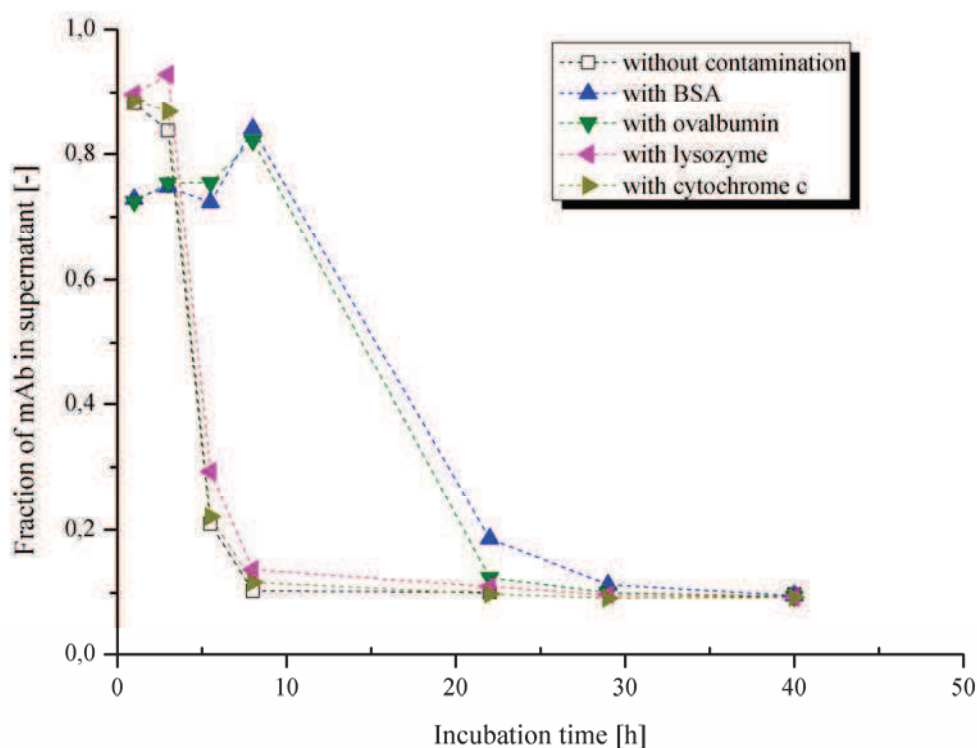
Figure 18. Time courses of mAb concentration in the supernatant of batches with and without the spiking proteins. Molar ratio (spiking protein: mAb) was 3.7. At this molar ratio, crystallization of mAb04c was suppressed in the first 10 hours by the presence of ovalbumin and BSA, whereas no obvious inhibition was found by lysozyme and cytochrome c.

Interactions between antibody and the spiking proteins in solution

As shown in Figure **18**, two proteins (lysozyme and cytochrome c) had only a very small effect on crystallization kinetics, while the other two considerably slowed down the process. We speculated that inhibition of crystallization could be due to adsorption of the contaminant protein to the surface of growing crystals. To investigate the interaction of mAb and contaminant in solution, we performed CG-MALS experiments as described in the methods section. Figure **19** presents the analysis data for the determination of virial

coefficients using CG-MALS. In Zone II, mAb04c was mixed with spiking protein at different ratio to investigate the CVC. The fitted results of the MALS data are presented in Table **7**. Analysis of the data yields a CVC value A_{11} of +2.94E-4 mol· ml/g^2 for mAb04c-lysozyme system and -1.19E-4 mol· ml/g^2 for mAb04c-BSA system.
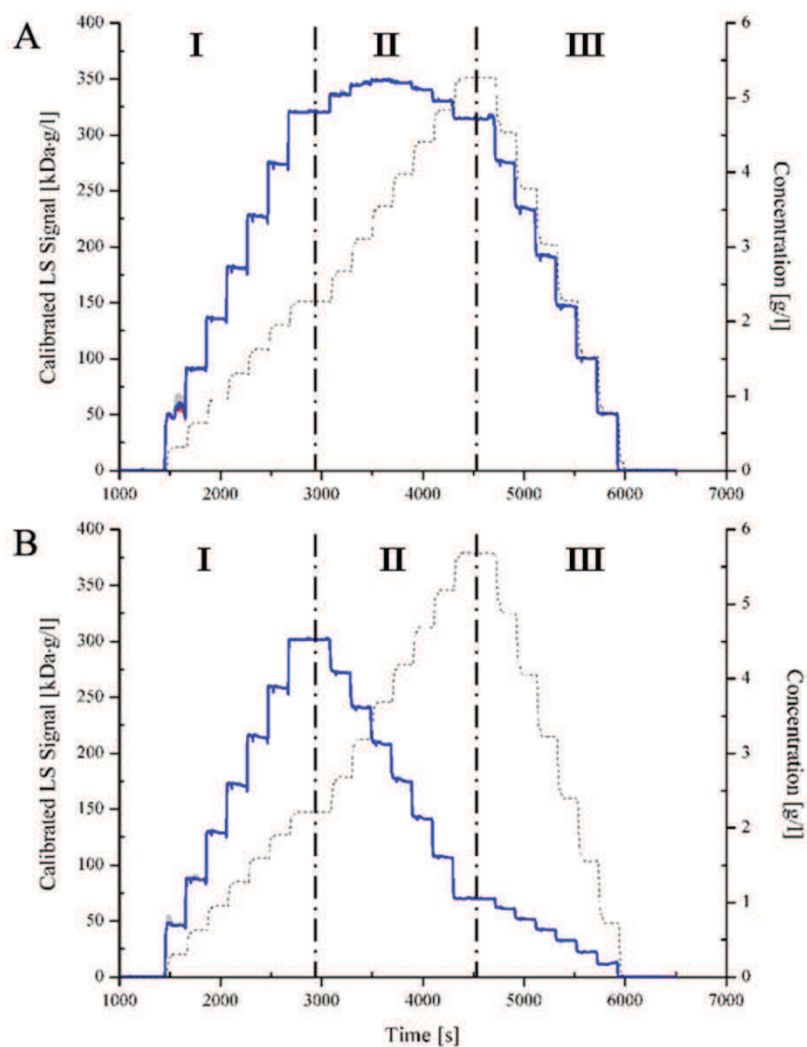
Figure 19. Analysis data from CG-MALS for the determination of virial coefficients. Solid line: light scattering signal; dashed line: concentration signal. Three segments were incorporated in each experiment: a concentration gradient of mAb04c alone (zone I), followed by a crossover composition gradient changing the ratio of test proteins (zone II), and a concentration gradient of BSA in A and lysozyme in B (zone III). All components were conditioned in 25 mM Tris, 25 mM Histidine, pH 7.2. Duration before 1000 s was preparation phase and was thus not shown here.

Table 7. Fitting results of the CG-MALS data. A_2 is the second self-virial coefficient. A_{11} is the cross-virial coefficient. The negative A_{11} in mAb04c-BSA system indicated attractive interactions between mAb04c and BSA molecules, and the positive A_{11} in mAb04c-lysozyme system suggested repulsive interactions between mAb04c and lysozyme.

	mAb04c-BSA System		mAb04c-lysozyme System	
	mAb04c	BSA	mAb04c	Lysozyme
A_2 (SVC)	+1.81E-4	+1.83E-4	+1.32E-4	+1.52E-3
A_{11} (CVC)	-1.19E-4		+2.94E-4	

Discussion

In the hierarchy of parameters governing growth of protein crystals, purity and homogeneity are amongst the most important [7, 19, 20]. For soluble proteins, a large-scale study [21] demonstrated that 229 proteins with purity levels of more than 95 % could be crystallized in 59% of all instances, whereas for protein samples exhibiting less than 95% purity the crystallization success rate was reduced to 37%. The yield of crystalline protein was not determined in this study, though. As a consequence, the ratio of contaminant to product is a critical factor in protein crystallization and has to be carefully controlled in an industrial process. In our present work, we investigate molar ratios of contaminant to mAb04c ranging from 0.29 to 7.7, which corresponds to a purity of mAb04c between 23% - 89% (w/w total protein). In comparison, the purity of mAb04c in culture supernatant was 40% according to SE-HPLC [4]. The purity range of our experimental setup therefore addresses crystallization at an early stage in the downstream process.

As expected, the presence of macromolecule impurity elicited an inhibitory effect on mAb04c crystallization in a concentration-dependent manner. Impurities can adsorb to the surface of a growing crystal and impede the addition of desired components [22-25]. Indeed, even when the mAb04c to BSA ratio was still about 3 (a molar ratio of 0.29 in Figure **15**), crystal growth rate had decreased significantly. Adsorption of the impurity to active growth sites on the crystal are a likely explanation, as reported previously for small molecules [25]. On the other hand, if the impurity concentration exceeds that of the target protein (e.g. molar ratio >4.5 in Figure **15**), crystallization could also be slowed down by reduced mass transport of the target protein from the bulk solution to the crystal surface.

This would be the case if target protein and impurity interact in solution. For BSA and ovalbumin, the latter might be the dominant effect.

Interestingly, the strong inhibition was not observed if crystallization of mAb04c was spiked with lysozyme or cytochrome c at a molar ratio of 3.7. Experiments similar to Figure **15** showed that notable inhibitory effect of lysozyme or cytochrome c only started at a molar excess of ten with respect to mAb04c (data not shown). Consequently, some mechanism appears to prevent these two proteins from inhibiting growth of crystals.

The negative CVC value of the mAb-BSA versus the positive CVC value of the mAb-lysozyme system indicates a strong attractive interaction between mAb and BSA, but a repulsive interaction between mAb and lysozyme in the crystallization buffer. This difference is most likely a consequence of the respective isoelectric points of the proteins investigated (Table **6**) and their resulting charge: mAb04c attracts BSA because of its opposite overall charge at pH 7.2, while mAb and lysozyme carry even charges and therefore repel each other. As the crystal's surface potential carries the same sign as the crystal forming molecule, attractive and repulsive interactions between growing crystal and soluble contaminant are expected to be the same as in solution. Also, at the low ionic strength used in our crystallization condition, electrostatic effects will not be attenuated. The crystallization kinetics in the presence of contaminants can therefore be mostly explained by electrostatic interactions between contaminant and target protein.

At very high excess concentration of lysozyme or cytochrome c, crystal growth might be impaired by a more viscous solution, leading to decreased diffusion rates and decreased mass transfer to the crystal surface.

A practical consequence of our finding is that a process step able to remove compounds interacting strongly with the product in solution should precede crystallization. For the system investigated here this could be an anion exchange chromatography operated in flow-through mode, which would remove only contaminants of opposite charge. This step would be fast to implement and not require much fine-tuning.

To our knowledge, the present report is the first describing inhibition of crystallization caused by electrostatic interactions. We are well aware that under different crystallization

conditions, such as the use of ionic precipitants, other interactions might become dominant. Even there the interaction analysis in solution might be a useful tool for designing a process step that enhances subsequent crystallization

Conclusion

In this work, we investigated how crystal growth of an intact monoclonal antibody is affected by protein impurities. The results suggest that the molar ratio of impurity to product as well as the interaction between product and impurity in solution were the two most important factors affecting crystallization kinetics and yield. The slowdown of crystallization rate was correlated with molar ratio of impurity to target protein, which was within expectation. Protein impurities with the same charge prefix as the product showed only minor inhibitory effects, probably due to electrostatic repulsion from the crystal surface. This might explain why some impurities influence crystallization at excess concentrations below 1 ppm, whereas others have to be present at fairly large concentrations before showing any effect [26, 27]. Interactions in solution as measured by SLS correlated with the inhibitory effect on crystallization. Whether this method has general predictive power will have to be shown by using the same approach for other proteins and crystallization conditions.

References

1. Chon JH and Zarbis-Papastoitsis G (2011) Advances in the production and downstream processing of antibodies. *New Biotechnol*. **28**: 458-463.

2. Klyushnichenko V (2003) Protein crystallization: From HTS to kilogram-scale. *Curr Opin Drug Discovery Dev*. **6**: 848-854.

3. Peters J, Minuth T, Schroeder W (2005) Implementation of a crystallization step into the purification process of a recombinant protein. *Protein Expression Purif*. **39**: 43-53.

4. Zang Y, Kammerer B, Eisenkolb M, Lohr K, Kiefer H (2011) Towards protein crystallization as a process step in downstream processing of therapeutic antibodies: Screening and optimization at microbatch scale. *PLoS ONE*. **6(9)**: e25282

5. Chernov AA (1984) Modern Crystallography III, Crystal Growth. *Springer Berlin*.

6. Myerson AS, Toyokura K (1990) Crystallization as a separation process. *Am Chem Soc Symp* Series 438.

7. Lorber B, Skouri M, Munch JP and Giege R (1993) The influence of impurities on protein crystallization: the case of lysozyme. *J Crystal Growth*. **128**: 1203-1211

8. Abergel C, Nesa MP, Fontecilla-Camps JC (1991) The effect of protein contaminants on the crystallization of turkey egg white lysozyme. *J Crystal Growth*. **110**: 11-19

9. Skouri M, Lorber B, Giege R, Munch JP, Candau JS (1995) Effect of macromolecular impurities on lysozyme solubility and crystallizability: dynamic light scattering, phase diagram and crystal growth studies. *J Crystal Growth*. **152**: 209-220

10. Caylor CL, Dobrianov I, Lemay SG, Kimmer C, Kriminski S, et al. (1999) Macromolecular impurities and disorder in protein crystals. *Proteins*. **36**: 270-281

11. Chayen NE, Saridakis E (2001) Is lysozyme really the ideal model protein? *J Crystal Growth*. **232**: 262-264

12. Attri A, Minton AP (2005) Composition gradient static light scattering (CG-SLS): a new technique for rapid detection and quantitative characterization of reversible macromolecular hetero-associations in solution. *Anal. Biochem*. 346: 132-138

13. Kameyama K, Minton AP (2006) Rapid quantitative characterization of protein interactions by composition gradient static light scattering. *Biophys. J*. **90**: 2164-2169

14. Some D, Hanlon A, Sockolov K (2008) Characterizing protein-protein interactions via static light scattering: reversible heteroassociation. *Amer. Biotechnol. Lab*. **26**:18-20.

15. Some D, Hitchner E, Ferullo J (2009) Characterizing protein-protein interactions via static light scattering: Nonspecific interactions. *Am. Biotechnol. Lab*. **27**: 2

16. Malamud, D. and Drysdale, JW (1978) Isoelectric points of proteins: A table. *Anal. Biochem.*, **86**: 620-647

17. Beeley, JA, Stevenson SM, Beeley JG (1972) Polyacrylamide gel isoelectric focusing of proteins: Determination of isoelectric points using an antimony electrode. *Biochim. Biophys. Acta*. **285**: 293-300

18. Keilin D and Hartree EF (1945) Purification and properties of cytochrome c. *Biochem J*. **39**: 289-292

19. Ducruix A and Giege R (1992) Crystallization of Nucleic Acids and Proteins: A Practical Approach. *IRL Press at Oxford University Press, Oxford*.

20. Giege R, Dock AC, Kern D, Lorber B, Thierry JC, et al. (1986) The role of purification in the crystallization of protein and nucleic acids. *J Crystal Growth*. **76**: 554-561

21. Geerlof A, Brown J, Coutard B, Egloff MP, Enguita FJ, et al. 2006. The impact of protein characterization in structural proteomic. *Acta Crystallogr., Sect. D: Biol. Crystallogr*. 62: 1125-1136

22. Land TA, Martin TL, Potapenko S, Palmore GT, De Yoreo JJ (1999) Recovery of surfaces from impurity poisoning during crystal growth. *Nature*. **399**: 442-445

23. McPherson A, Malkin AJ, Kuznetsov YG, Koszelak S (1996) Incorporation of impurities in to macromolecular crystals. *J Cryst Growth*. 168:74-92

24. Plomp M, McPherson A, Malkin AJ (2003) Repair of impurity-poisoned protein crystal surfaces. *Proteins*. **50**: 486-495

25. Sangwal K (1996) Effects of impurities on crystal growth processes. *Prog Cryst Growth Charact*. **32**:3-43

26. Mullin JW. (1993) Crystallization. *3rd edtion. Butterworth-Heinemann: Oxford, UK*. 600 P.

27. Rosenberger F (1986) Inorganic and protein crystal growth-similarities and differences. *J Crystal Growth*. **76**: 618-636

5

The effect of osmolytes on thermal and kinetic stability of lysozyme

Eisenkolb M, Zang Y, Marrahí AS, Witt A, Kiefer H

Institute of applied Biotechnology, Biberach University of applied sciences

Abstract

Seeded fibrillation of hen egg-white lysozyme at low pH was established as a model system of protein aggregation. The stabilization potency of osmolyte additives was tested using fluorescent dyes. The experimental setup allowed determining both shifts of the protein melting point T_m as well as aggregation kinetics under identical solvent conditions. A set of 21 compounds representing the three known osmolyte substance classes (polyols, amino acids and methylamines), was chosen and their thermal and kinetic stabilizing potencies were determined as a function of osmolyte concentration. A correlation of both stabilizing effects was clearly distinguishable, but so were deviations from perfect correlation. In general, polyols increased both thermal and kinetic stability in a concentration-dependent manner while most compounds of the amino acid and methylamine groups lead to destabilization. An attempt to correlate the observed stabilization effects with molecular mass and pKa values of the compounds revealed some weak structure function relationships. We tentatively interpreted our data by a volume exclusion effect dominating in the case of added polyols, while preferential binding appears to be responsible for destabilization by amino acids and methylamines. It also becomes evident that additional molecule-specific properties influence the stabilization potency of compounds tested. Additional model systems allowing controlled formation of different types of aggregates and larger sets of stabilizers should reveal information that could be used to design novel molecules that surpass the stabilizing properties of naturally occurring osmolytes.

Introduction

Aggregation of industrially produced proteins is a major problem resulting in activity loss and, in the case of pharmaceutical proteins, in safety issues due to immunogenic adverse reactions. It is therefore good practice to take measures during the downstream process to prevent aggregate formation and to remove aggregates [1]. The situation is complicated by the fact that aggregation can follow different pathways that may or may not include structural changes of the protein molecule. Examples of aggregation processes include precipitation by salting-out (reversible, structure is preserved), fibrillation in neurodegenerative diseases (irreversible, structure changes to beta-sheet), spontaneous aggregate formation during storage of biopharmaceuticals (reversible or irreversible, may include structural changes) etc. [1, 2]. Often, a rate-limiting step at the early onset of aggregation is the formation of nuclei, rendering this process highly auto-catalytic. Therefore, considerable effort is made to remove even trace amounts of aggregates, which otherwise would reduce stability and shelf-life of purified proteins.

Storage solvents for proteins are optimized not only by varying pH and ionic strength, but also by exploring the stabilizing effect of excipients added to the solvent. Among those is the group of osmolytes, naturally occurring, small organic molecules that many species have evolved in order to cope with osmotic, heat or desiccation stress [3]. The majority of osmolytic compounds belong to three substance classes: polyhydric alcohols and sugars (polyols), amino acids and their derivatives and methylamine compounds [3]. Most of these compounds have been shown to increase thermal stability of proteins as reflected by a shift of T_m, the midpoint of the unfolding transition, to higher values [4-8]. Those protecting osmolytes are presumed to act by their preferential exclusion from the protein surface, thus favouring compaction of the protein. From a thermodynamic point of view, the denatured state is at a higher Gibbs potential in the presence of osmolytes than in their absence, resulting in an increase of the Gibbs free energy of unfolding [8, 9] and therefore in higher protein stability.

The effect of osmolytes on thermal stability has been studied extensively [3-6, 8, 10, 11]. However, increased thermal stability does not necessarily correlate with extended shelf life of protein products. The latter can result partially or completely from kinetic

inhibition of aggregation and has a large impact in industrial applications. It is less clear, which of the osmolyte compounds can also act as kinetic stabilizers, i.e. inhibit or slow down protein aggregation. In some reports, this question has been addressed: Osmolytes were able to slow down insulin fibrillation [12] or to increase the storage half-life of human recombinant growth factor [6]. However, we are not aware of any systematic studies correlating thermal and kinetic stabilization by osmolytes.

Under some experimental conditions, osmolytes can even exhibit protein-destabilizing properties (reviewed in [13]). One parameter strongly influencing whether an osmolyte reacts in a protective or denaturing way is the solvent pH: For instance, TMAO is a potent stabilizer at neutral pH but destabilizes proteins at low pH [14]. A similar ph-dependency has also been reported for glycine betaine on α-lactalbumin [15]. Also polyols, while showing no influence on protein stability at pH 7.0 were able to increase ΔG_{D0} at low pH values [16]. Protein destabilization may as well occur at very high osmolyte concentrations [5, 17], where the modestly favourable interactions between apolar parts of the osmolyte and hydrophobic side chains become more significant, resulting in exposure of hydrophobic residues and unfolding [5]. Finally, part of the action of osmolytes can be protein-specific: The strength of protection from thermal denaturation can vary as different physico-chemical properties between the studied proteins lead to differences in protein-solvent interaction [18]. That is, opposite effects have been reported for glycine betaine depending on the examined protein: While the osmolyte exhibits destabilizing properties on α-lactalbumin at pH values below 5.0, T_m and ΔG_{D0} of RNase A are instead increased at equal or even lower pH values [15].

Destabilizing effects have been attributed tentatively to preferential binding of the osmolyte to the protein surface and can lead to a reduction in the Gibbs free energy of unfolding [13]. However, the opposite may also occur, i.e. preferential binding can result in increased protein stability [19], depending on whether binding is energetically more favourable to the folded or unfolded state of the protein.

Previously published work often focuses on rather small sets of osmolytes, those compounds often belonging to different substance classes [6, 10, 11]. Conclusions about common effects within and differences between compound classes are difficult to draw

from those data, even if taken together, since experimental conditions such as pH, solvent composition and protein type critically determine the osmolytes' impact on stability. As a result, general effects tend to get hidden behind variations caused by different experimental setups. To overcome this problem, we decided to focus on a single model for protein aggregation, lysozyme, and to include 21 selected osmolytes from all three compound groups. Lysozyme can be transformed into fibrils under defined conditions [20], and the system can be manipulated to yield reaction kinetics amenable to high throughput measurements. Obviously, any conclusion drawn from our data might be specific for the test system used and doesn't have to apply for other proteins or other aggregation mechanisms. In addition to kinetic measurements, we also investigate the effect of the same osmolytes on T_m under identical solvent conditions to allow for comparison of thermodynamic and kinetic stabilization effects. Stabilization potential within a substance group is finally correlated with molecule characteristics (molecular weight (MW) and pKa value), revealing some weak structure function relationships.

In a similar study, we recently investigated the effect of 18 polyols, amino acids and methylamines on the kinetic stability of glucagon to understand how intrinsically disordered proteins were affected by osmolytes [21].

Materials and Methods

Preparation of protein and osmolyte solutions

A representative sample of 21 osmolytes was selected from Table 6.1 in Hochachka and Somero [22]. The selected compounds are listed in Table **8** and include compounds of the polyol, methylamine and amino acid classes of osmolytes. Choline-O-sulfate (COS) and proline betaine were synthesized according to Schmidt and Wagner [23] and King, respectively [24]. All other chemicals were purchased from AppliChem (Darmstadt, Germany) and Sigma-Aldrich (Taufkirchen, Germany) and were of the highest purity available.

Table 8. List of included osmolytes

Substance class	Osmolyte	Abbr.[1]	Molecular weight	pKa value[2]
Polyols	Trehalose	tre	342.3 g/mol	
	Mannitol	man	182.2 g/mol	
	Sorbitol	sor	182.2 g/mol	
	Erythritol	ery	122.1 g/mol	
	Myo-Inositol	myo	180.2 g/mol	
	Glucose	glc	180.2 g/mol	
	Glycerol	glyc	92.1 g/mol	
Amino acids and derivatives	Glutamine	gln	146.2 g/mol	2.15
	Proline	pro	115.2 g/mol	1.94
	Alanine	ala	89.1 g/mol	2.47
	Glycine	gly	75.1 g/mol	2.31
	Serine	ser	105.1 g/mol	2.03
	Taurine	tau	125.2 g/mol	-1.49
	Beta-alanine	ß-ala	89.1 g/mol	4.08
	Ectoine	ect	142.2 g/mol	2.75
	Hydroxyectoine	OH-ect	158.2 g/mol	2.48
Methylamines	Betaine	bet	117.2 g/mol	2.26
	Sarcosine	sarc	89.1 g/mol	2.06
	Choline-O-sulfate	COS	183.3 g/mol	-1.88
	Trimethylamine-N-oxide	TMAO	75.1 g/mol	4.66
	Proline betaine	pro bet	179.6 g/mol	2.26

[1] Abbreviations are used in figure legends. [2] pKa values were calculated using Marvin [28].

Osmolytes were dissolved in 0.1 M glycine, pH 2.5 and pH value was adjusted to 2.5 where necessary. All solutions were sterile-filtered with a 0.22 μm filter prior to use.

Hen egg white lysozyme (Sigma-Aldrich # 62971) was dissolved in 0.1 M glycine, pH 2.5, and filtered as above. Protein concentration was calculated from A_{280} measurement using an extinction coefficient of 2.48 L·mol^{-1}·cm^{-1}.

For experiments at neutral pH, osmolytes and lysozyme were dissolved in 0.1 M sodium phosphate, pH 7.0 and treated as above.

Fibril seed stock was prepared by sonication: fibrillated lysozyme solutions (2 mg/ml) were subjected to sonication pulses of 50 % power for 3x10 s (Bandelin, Berlin, Germany, Sonopuls HD2070, sonotrode MS 72). Aliquots were stored until use at -20 °C.

Fibrillation of lysozyme

Lysozyme fibrillation was induced on the basis of Morshedi *et al*. [20]. However, protein and seed concentration as well as temperature was optimized to shorten the time needed for complete fibrillation and to allow for high throughput experiments.

All experiments were carried out in triplicates in 96 well plates (Roche, Mannheim, Germany, #04729692001). 100 μl samples containing 5 mg/ml lyoszyme, 40 μg/ml fibril seed stock, varying concentrations of osmolyte and 40 μM ThT (Sigma-Aldrich, Taufkirchen) were incubated without agitation at 75 °C in a Roche LightCycler 480. ThT fluorescence was monitored over a time course of 100 hrs (excitation 450 nm, emission 500 nm). Fluorescence reached a plateau in all experiments, which was used as endpoint for lag time calculations. No increased ThT fluorescence was observed when protein was omitted from the reaction, thus excluding the possibility of direct osmolyte-ThT-interaction.

Due to its autocatalytic nature, fibrillation usually follows a sigmoidal time course [25]. Lag time, for our experiments defined as the time required to reach 5% of the fluorescence endpoint intensity, can be used as an indicator of kinetic stability [12, 21, 26]. For some osmolytes (beta-alanine, TMAO and proline betaine), the sigmoidal curve shape could not be resolved even at the highest possible observation rate (one data point per 10 seconds).

For consistency, the 5% time point was used anyway as the lag time. The seed stock prepared as above apparently was not entirely stable, even when stored as frozen aliquots. We observed decreasing fibrillation lag times upon longer storage (data not shown). This problem was accounted for by including control experiments lacking osmolyte on each microtiter plate. For comparability, all results are presented relative to the control lag time on the same plate, the control lag time always set as 100 %.

Differential Scanning Fluorimetry

Thermal stability was investigated by measuring melting points (T_m) using a slight modification of the method introduced by Niesen *et al*. [27]. Experiments were performed in triplicate on a Roche LightCycler 480 in 96 well plates. In a reaction volume of 50 µl a final concentration of 0.8 mg/ml lysozyme was mixed with varying osmolyte concentrations. SYPRO Orange (Invitrogen, Darmstadt, Germany, 5000x in DMSO) was diluted 1000 fold in the assay. Melting points were derived from the inflexion point of the melting curves.

Results

Kinetic measurement of lysozyme fibrillation

Induced fibrillation of lysozyme as described under Methods was used as a model system to investigate the influence of osmolytes on fibrillation kinetics. Fibril formation was monitored by fluorescence measurement of the fibril-specific dye Thioflavin T. For most experiments fluorescence followed a sigmoidal time course leading to a maximum value, confirming previously published results [25]. An "overshoot" of the curve as observed e.g. for glucagon fibrillation [21] was not detected here. In the presence of a few osmolytes (beta-alanine, TMAO, proline betaine) kinetics appeared to deviate from sigmoidal shape and gave rise to a steep increase from the start of the experiment. This was probably due to the instrument's upper limit of time resolution. Lag time, corresponding to the time where 5% of the maximum fluorescence had been reached, was used as an indicator of fibrillation velocity [21]. Since kinetics was strongly dependent on the added

fibril seed stock, each series of experiments included a triplicate control lacking osmolyte additive. All data within a series are presented as percentage of this control.

Effect of osmolyte additives on fibrillation kinetics

When lag times were plotted vs. osmolyte concentration, an apparently linear increase was observed for compounds of the polyol group, while for the majority of the other compounds, a non-linear decrease was apparent. For consistency and comparability, all data were plotted as log (lag time) vs. concentration and subjected to linear regression (Figure **20**). This did not affect coefficients of determination negatively even in the case of polyols (polyol average adjusted r^2 = 0.935 for linear and adj. r^2 = 0.937 for half-logarithmic fits). The slope of the regression line was then used as a measure of kinetic stabilization potency of the respective compound. The variation of stabilization potency within osmolyte substance classes is described by the ratio of the highest and lowest observed concentration effect.

Polyols slow down fibrillation

For all compounds of the polyol group, lag times increased with polyol concentration, indicative of a stabilizing effect (Figure **20**A). Experiments were highly reproducible, as shown by error bars, and substantial variation of stabilization potency within this compound group was observed. Within the polyol group, the stabilization potency varied by a factor of 13.5 between myo-Inositol with the highest and glucose with the lowest effect.

Amino acids and methylamines accelerate fibrillation

In contrast to polyols, most compounds of the amino acid and methylamine group decreased lag times, i.e. acted as kinetic destabilizers (Figure **20**B and C). Beta-alanine and proline betaine were the strongest destabilizers in the amino acid and methylamine groups, respectively. Two compounds, namely COS and taurine, did not affect lag times significantly at any concentration measured. The destabilization potency of the other osmolytes varied by a factor of 3.4 for amino acids or 4.5 for methylamines, respectively.
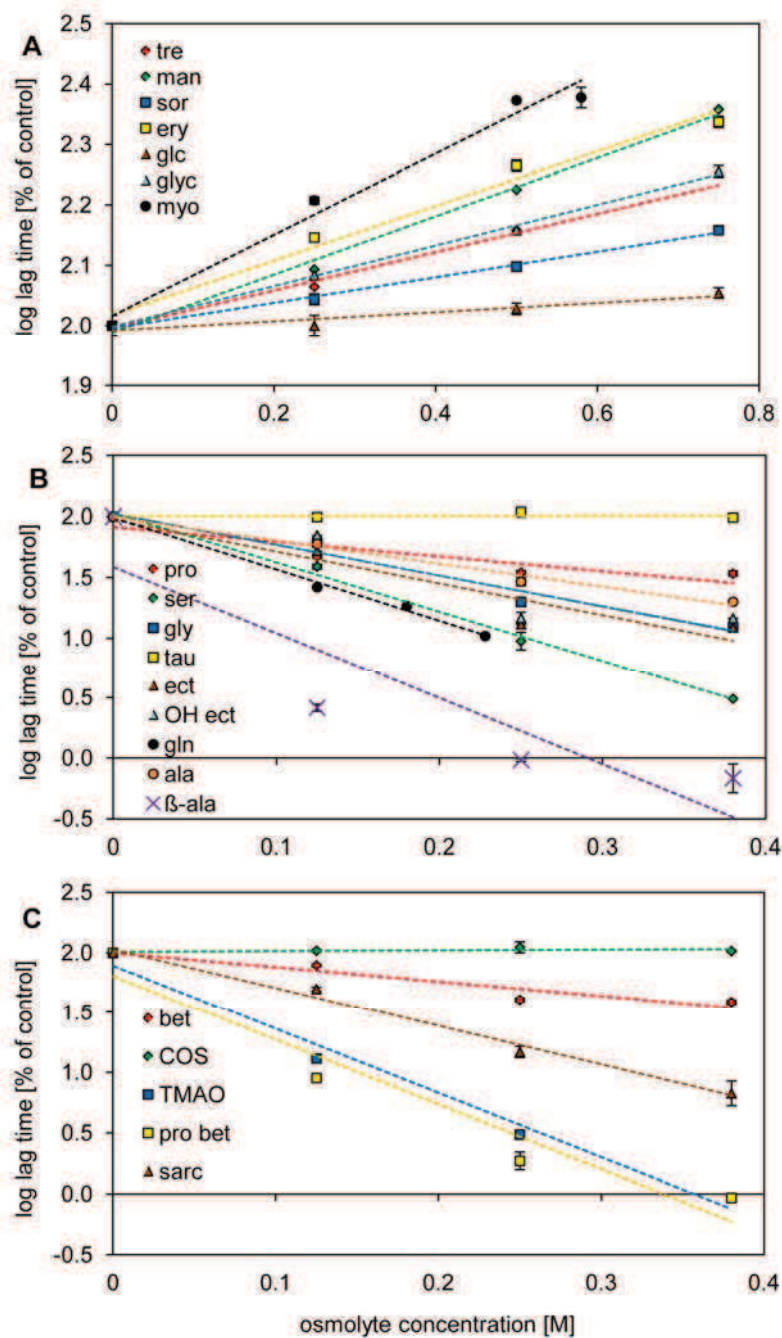
Figure 20. Concentration-dependent effect of osmolytes on kinetic stability at pH 2.5. Half-logarithmic plot of lag times versus osmolyte concentration (A) Polyols, (B) amino acids, (C) methylamines. Slopes of regression lines represent kinetic stabilization potency of the respective osmolyte (see Table 10 in supplementary material for potency values, their errors and coefficients of determination). Destabilizing osmolytes show negative slopes. Error bars are included. Control lag time is always set as 100 %, which equals a value of 2 in a logarithmic transformation.

Effect of osmolyte additives on thermal stability

The determination of thermal stability is the most frequently used method to study the effects of osmolytes on protein stability, although it is not automatically related to aggregation kinetics. We therefore determined the influence of increasing osmolyte concentrations on the unfolding temperature (T_m) of lysozyme by differential scanning fluorimetry [27]. Solvents used were identical to those in the fibrillation model, i.e. all measurements were recorded at pH 2.5. The melting point of the osmolyte-lacking control was determined at 59.1 °C ($\pm$ 0.2 °C). Thermal stabilization potency was determined by plotting log (T_m) vs. osmolyte concentration and calculating the slope of the regression line in analogy to the kinetic stabilization potency introduced above. As for the fibrillation experiments, logarithmically transformed data yielded the highest coefficients of determination. The relationship between T_m and osmolyte concentration was broadly similar to that between lag time and osmolyte concentration: polyols increased T_m in an apparently linear fashion, while most of the other compounds decreased T_m, and concentration dependence was nonlinear (Figure **21**). However, when the compounds within substance groups were ranked according to their stabilization potency, compound-specific differences between kinetic and thermal stabilization potency became obvious.

<u>Polyols increase T_m</u>

Thermal stabilizing potency of polyols varied by a factor of 9.9 between the weakest and the strongest additive (Figure **21**A). Glycerol, while among the best stabilizers in fibrillation experiments, appeared as the least potent polyol in T_m experiments. On the other hand, myo-inositol, which proved by far to be the best kinetic stabilizer, was less prominent in thermal stabilization where differences between compounds were generally much smaller.
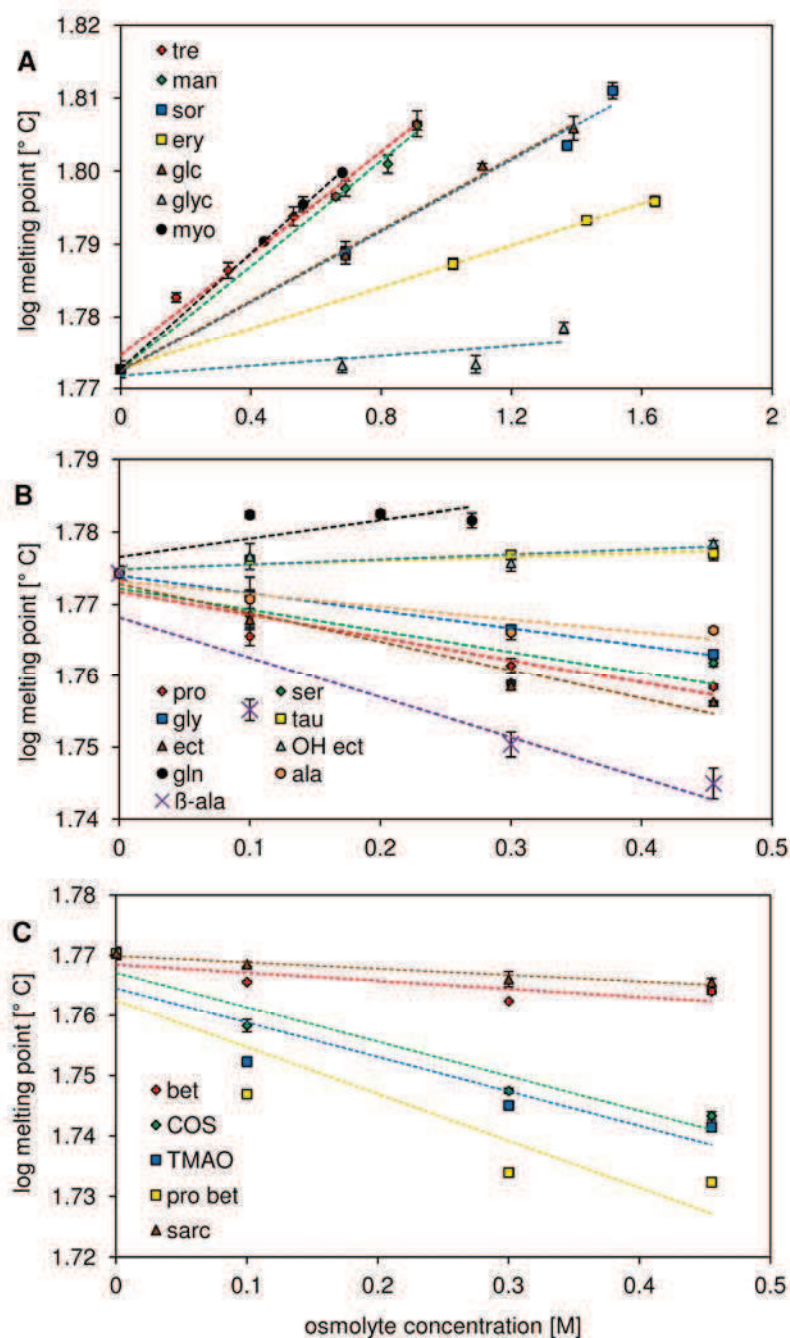
Figure 21. Concentration-dependent effect of osmolytes on thermal stability at pH 2.5. Half-logarithmic plot of T_m vs. osmolyte concentration. (A) Polyols, (B) amino acids, (C) methylamines. Slopes of regression lines represent thermal stabilization potency of the respective osmolyte (see Table 10 in supplementary material for potency values, their errors and coefficients of determination). Destabilizing osmolytes show negative slopes. Error bars are included. Control melting point was measured at 59.1 °C (± 0.2 °C), which equals a value of 1.77 in a logarithmic transformation.

Amino acids and methylamines decrease T_m

In contrast to the stabilizing effect of polyols and similar to the results obtained in fibrillation experiments, addition of most amino acids and methylamines led to decreasing melting points (Figure **21**B and C). For the class of amino acids, beta-alanine again had by far the highest impact, decreasing T_m by almost 4 °C at the highest concentration. Two osmolytes, namely hydroxyectoine and taurine, showed nearly no effect. In contrast to fibrillation experiments even a weak thermal stabilizer was found with glutamine.

Of the methylamine class, betaine was the least potent destabilizer, while proline betaine had the strongest (factor 7.0) destabilizing effect. COS, which did not affect lag times, led to a small decrease in T_m.

The destabilizing effect of amino acids and methylamines in both experiments may appear unexpected since osmolytes have generally been known to stabilize proteins. We hypothesized that our results could be caused by the low pH of 2.5 at which the experiments were conducted. In a second set of experiments, we therefore measured the effect of osmolytes on Tm at pH 7.0, buffered with 0.1 M sodium phosphate. Indeed, at neutral pH, we observed a stabilizing effect of almost all osmolytes as described earlier [5, 6, 8], proline betaine being the only exception with a very low destabilizing effect (Figure **22**). As we haven't been able to develop a lysozyme fibrillation protocol at neutral pH yet, those T_m data could not be correlated with corresponding kinetic experiments, though.
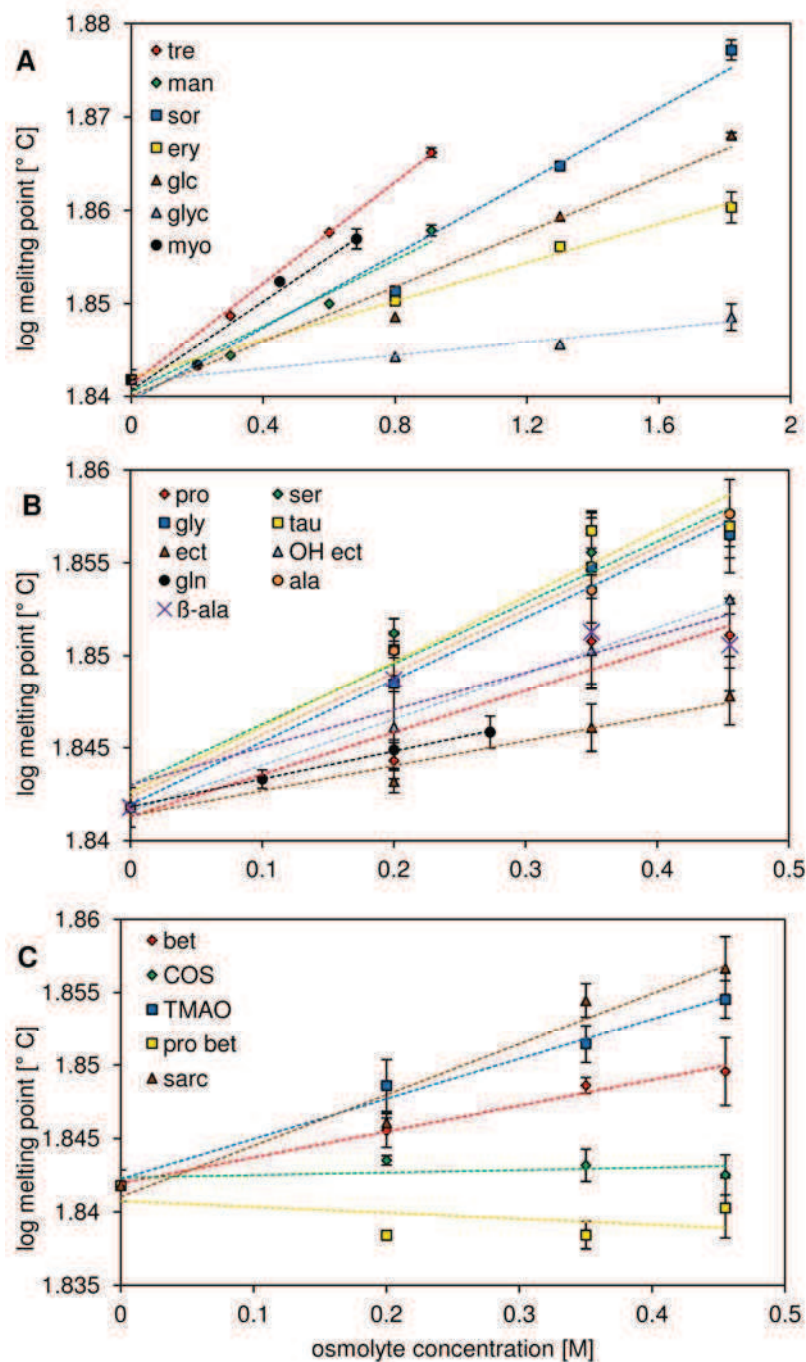
Figure 22. Concentration-dependent effect of osmolytes on thermal stability at pH 7.0. Half-logarithmic plot of T_m vs. osmolyte concentration. (A) Polyols, (B) amino acids, (C) methylamines. Slopes of regression lines represent thermal stabilization potency of the respective osmolyte (see Table 11 in supplementary material for potency values, their errors and coefficients of determination). Error bars are included. Control melting point was measured at 69.5 °C (± 0.2 °C), which equals a value of 1.84 in a logarithmic transformation.

Osmolytes exhibit similar effects on thermal and kinetic stability.

To enable comparison of kinetic and thermodynamic stabilization potency, the slopes of Figure **20** and Figure **21** were normalized with respect to myo-Inositol for polyols, proline betaine for methylamines and beta-alanine for the amino acid group. In Figure **23**, the normalized slopes of kinetic data are correlated with normalized slopes of T_m measurements. Both for stabilizing as well as for destabilizing compounds, a weak correlation between the two effects is evident (adj. $r^2 = 0.59$ for y = x).
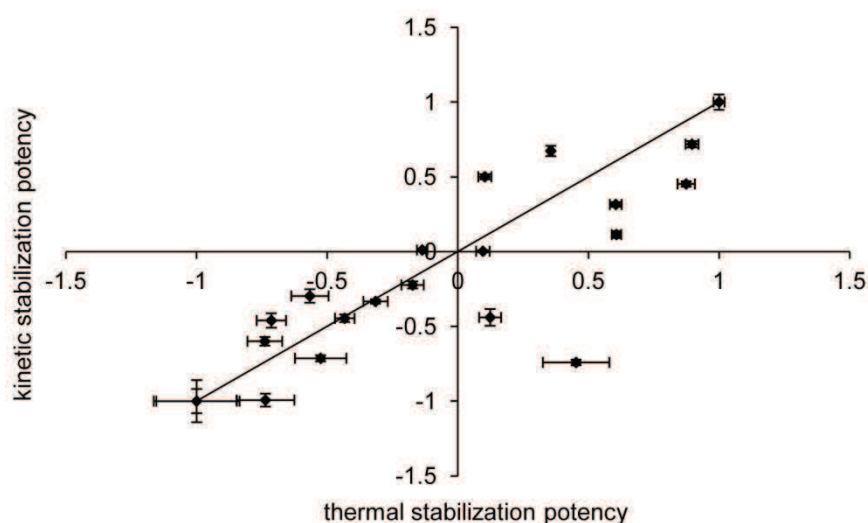
Figure 23. Correlation of kinetic and thermal stabilization potency. Slopes of the regression lines from Figure 20 and Figure 21 were normalized as described in the text, resulting in a value of 1/-1 for the osmolyte with the highest stabilization/destabilization potency within a substance class. Values from T_m measurements are plotted on the x-, those from fibrillation experiments on the y-axis. Fitting the curve to y=x gained an adj. r^2 of 0.59.

Molecular properties important for stabilization / destabilization

As a next step in our analysis, we attempted to identify molecular properties of the osmolytes that correlate with their effects on T_m or aggregation kinetics, respectively. Single and double linear regressions (the latter only for amino acids and methylamines) for kinetic and thermal stabilization potency vs. MW and pKa were performed (see Table **8,** for MW and pKa values of compounds). pKa values were calculated from osmolyte structure using the software Marvin [28] as no other single source of pKa values for all

osmolytes was available. Stabilizing polyols were analyzed separately from the primarily destabilizing amino acid and methylamine group, as the mostly opposite effects make a common mechanism unlikely. Results are summarized in Table **9**. Molecular weight has no significant influence on the effect of amino acids and methylamines, whereas a high pKa value strongly correlates with high destabilization potency. The impact of pKa values is more pronounced in fibrillation experiments. For the group of amino acids and methylamines, coefficients of determination are also higher in kinetic experiments. For the polyol group, we observe a correlation of MW and stabilization proficiency, but only in melting point experiments, where high MW polyols are more efficient in maintaining thermal stability (see also Figure **24** in supplementary material).

Table 9: Osmolyte effect and molecule characteristics: Correlation of slopes with molecular weight (MW) and pKa value

			Thermal stabilization potency		Kinetic stabilization potency	
			Regression coefficient x 10^{-4}	adj. r^2	Regression coefficient x 10^{-3}	adj. r^2
Amino acids / methylamines	DLR[1]	MW	0.18 (± 2.5)		-8.6 (± 11)	
		pKa	-76 (± 51)	0.08	-940 (± 230)	0.56
	SLR[2]	MW	2.0 (± 2.2)	-0.012	14 (± 15)	-0.0011
	SLR[2]	pKa	-78 (± 42)	0.16	-850 (± 200)	0.58
Polyols	SLR[2]	MW	1.1 (± 0.54)	0.34	-0.33 (± 1.1)	-0.18

Values were obtained via [1] double linear regression or [2] single linear regression.

Discussion

The effect of osmolytes on thermal stability of proteins and its underlying molecular mechanisms have been investigated by several authors in the past [4–6, 8, 9]. With respect to protection of proteins from aggregation, systematic work is less abundant. Published reports mostly deal with application-oriented case studies and a limited set of additives that reduce or slow down aggregation [12, 29-31]. In our present work, we examine a larger set

of osmolytes using a single test system of protein aggregation. We then directly compare thermal and kinetic stabilization propensities of osmolytes and tentatively correlate those properties to two selected structural features, MW and pKa.

Our main findings are: (i) thermal and kinetic stabilization correlate in general. (ii) However, there are significant deviations from this correlation making the prediction of aggregation inhibition from T_m measurements uncertain. These deviations are not caused by experimental noise, but instead significant as evidenced by error bars not reaching the diagonal. (iii) As a conclusion, compound-specific properties must significantly contribute to stabilization potency. Part of these molecule-specific effects can be attributed to molecular mass (increase of melting points with large polyols) and pKa value (destabilizing effect of zwitterionic compounds increases with pKa). (iv) Zwitterionic substances that increase T_m at neutral pH can decrease T_m at acidic pH. (v) Polyols enhance kinetic and thermal stability, the latter even more at low pH values than at neutral pH.

It is not too surprising that the correlation between thermal and kinetic stabilization is not perfect. Some aggregation mechanisms, including fibrillation investigated here, require at least partial unfolding or misfolding of the target protein to proceed [1]. However, the mechanisms destabilizing the native structure of a protein could also reduce their bias to aggregate. Well-known examples are urea or guanidinium, which lower T_m, i.e. promote unfolding, and inhibit aggregation [32, 33]. Both effects can be attributed to the chaotropic effect resulting in a weakening of hydrophobic interactions [34].

Thermal stability might therefore serve as an indicator for kinetic stability but cannot securely predict aggregation kinetics. A positive but also imperfect relationship between the osmolyte effect on melting points and aggregation kinetics was also found by Chen and Arakawa in a study on human keratinozyte growth factor [6]. They conclude that while thermal denaturation is a rate-limiting step in aggregation kinetics, additional direct interactions between osmolytes and protein must also contribute to a prolonged protein shelf life.

The effects of osmolytes on protein stability have been attributed to a combination of volume exclusion (preferential hydration) and preferential binding to the protein surface

[13, 14]. Volume exclusion is generally favouring the compact protein structure over a (partially) unfolded structure taking up more volume. The volume exclusion effect therefore always stabilizes folded proteins such as lysozyme. For natively unfolded proteins, e.g. glucagon, the same effect can promote the formation of aggregates as long as the aggregates are more compact than the soluble form [21 and references therein].

For the polyol group, both a preferential binding to the native state as well as a volume exclusion effect seem possible, as all compounds act as stabilizers. However, the present data do not allow us to determine the dominating mechanism. As the volume exclusion effect should correlate with total volume taken up by the solute, we expected a positive correlation between stabilizing potency and molecular mass as previously shown for various sugar osmolytes [35]. However, only a small correlation was observed for thermal stability experiments, letting us conclude that molecule-specific effects surmount volume exclusion. This is especially true for the kinetic experiment, where stabilizing potency of four monosaccharides with the same MW differ over one order of magnitude. We also find an increase in polyol stabilization potential at low pH compared to neutral pH as observed before for various polyols e.g. trehalose, sorbitol or glycerol [16, 18]. This effect has been attributed to increased preferential exclusion of the osmolytes: As a protein gets more hydrophobic at low pH values due to protonation of COO$^-$ groups [36], solvophobic interactions of the OH groups from protein and polyols occur [18].

Preferential binding on the other hand is generally associated with destabilization [13, 14, 22, 37]. However, when binding to the native form exceeds binding to the denatured protein, a stabilizing effect is observed [19].

Since destabilization of globular proteins has only been reported with preferential binding so far, we suggest this as the underlying mechanism for the observed effects with most amino acids and methylamines. At our experimental pH, most of the amino acids and methylamines carry a net positive charge in contrast to neutral pH, were they are zwitterionic. Destabilizing properties can be related with osmolyte charge, as it was shown for TMAO [14, 38] and are partly explained by the perturbation of electrostatic interactions within a protein, hindering correct folding [38]. We find a positive correlation between pKa value and destabilization potential of osmolytes, and this correlation is most obvious

for compounds where the pKa lies far away from pH 2.5. Examples are TMAO with a high and taurine with a low destabilizing effect, corresponding to high or low pKa values, respectively. For compounds with a pKa value close to the experimental pH this relationship is less visible, possibly due to small errors in calculating the predicted pKa leading to large differences between predicted and actual charge of the molecule at pH 2.5. Direct electrostatic attraction between osmolyte and lysozyme might however not be the dominating interaction leading to preferential binding, as not only the compounds, but also the protein are positively charged at pH 2.5. Concerning amino acids and apart from our recent study on osmolyte impact on glucagon fibrillation [21], we are not aware of publications having witnessed low stability in the presence of this osmolyte group at low pH. In fact the opposite was reported, as Taneja *et al.* observed a thermally stabilizing effect for moderately hydrophobic amino acids at pH 3.0 [4].

A more detailed understanding of osmolyte action on aggregate formation will require both molecular understanding of the aggregation mechanism as well as of the specific interaction of solute and protein surface. More model systems allowing controlled formation of different types of aggregates and even larger sets of stabilizers will be required to extract information that could be useful in designing novel molecules that surpass the stabilizing properties of naturally occurring osmolytes.

Supplementary Materials
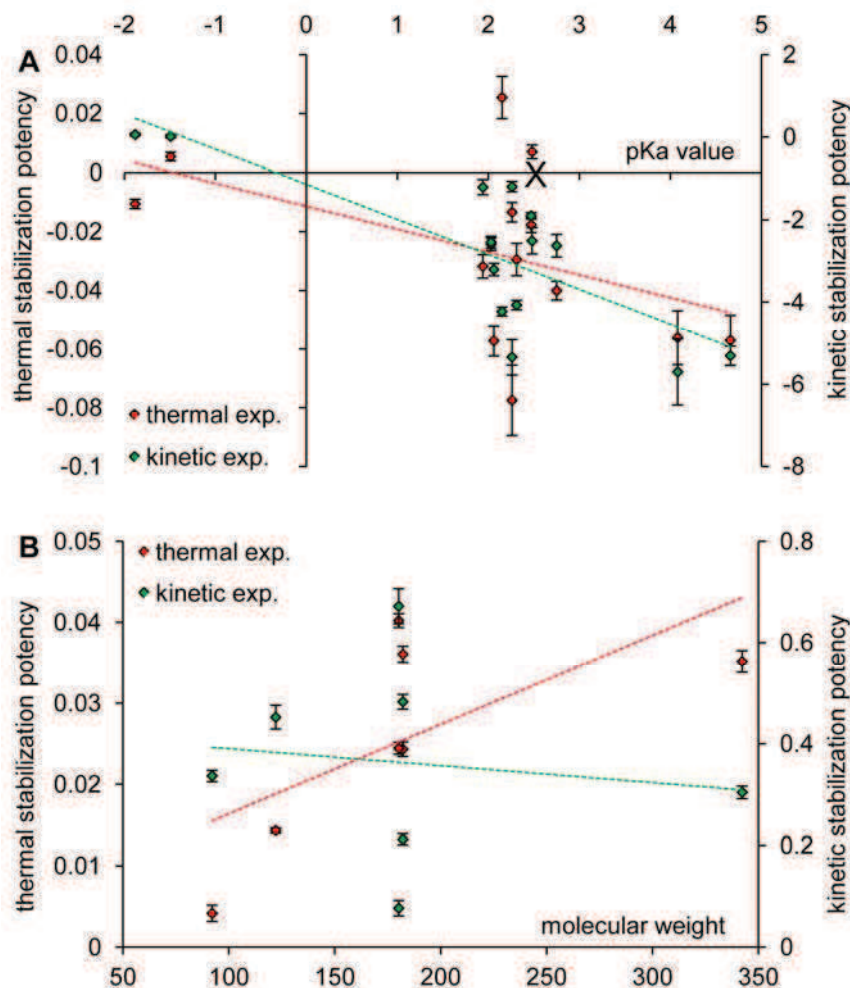
Figure 24. Correlation of stabilization potency with molecule characteristics at pH 2.5. Plot of pKa value (A) and molecular weight (B) (x-axis) vs. stabilization potency (y-axes). As they generally share a destabilizing effect, results from the amino acids and methylamines group are combined in (A), where a high pKa value is associated with higher destabilization potential. The experimental pH of 2.5 is marked as X on the x-axis. In (B), showing results for polyols, the regression of molecular weight with stabilization potency is only significant in thermal experiments. No diagram is shown relating molecular weight of amino acids and methylamines, as the correlation was not significant in both experiments.

Table 10: Comparison of concentration-dependent osmolyte effect in thermal and kinetic experiments at pH 2.5

		Thermal stabilization potency		Kinetic stabilization potency	
		Regression coefficient $\times 10^{-2}$	adj. r^2	Regression coefficient $\times 10^{-2}$	adj. r^2
Polyols	Trehalose	3.5 (± 0.13)	0.98	30 (± 1.2)	0.98
	Mannitol	3.6 (± 0.10)	0.99	48 (± 1.4)	0.99
	Sorbitol	2.4 (± 0.10)	0.99	21 (± 1.0)	0.97
	Erythritol	1.4 (± 0.03)	0.99	45 (± 2.3)	0.97
	Glucose	2.4 (± 0.07)	0.99	7.6 (± 1.5)	0.69
	Glycerol	0.42 (± 0.10)	0.54	34 (± 1.1)	0.99
	Myo-Inositol	4.0 (± 0.09)	1.0	67 (± 3.5)	0.97
Amino acids and derivatives	Proline	-3.2 (± 0.40)	0.85	-120 (± 19)	0.79
	Serine	-2.4 (± 0.21)	0.92	-250 (± 15)	0.96
	Glycine	-2.9 (± 0.55)	0.71	-410 (± 12)	0.99
	Taurine	0.54 (± 0.15)	0.54	1.4 (± 4.0)	-0.09
	Ectoine	-4.0 (± 0.32)	0.94	-260 (± 27)	0.89
	Hydroxyectoine	0.69 (± 0.24)	0.41	-250 (± 32)	0.85
	Glutamine	2.5 (± 0.72)	0.51	-420 (± 11)	0.99
	Alanine	-1.8 (± 0.26)	0.80	-190 (± 7.9)	0.98
	Beta-Alanine	-5.6 (± 0.92)	0.77	-570 (± 8.0)	0.82
Methyl-amines	Betaine	-1.3 (± 0.33)	0.58	-120 (± 13)	0.89
	COS	-1.1 (± 0.16)	0.80	5.7 (± 3.7)	0.12
	TMAO	-5.7 (± 0.86)	0.80	-530 (± 23)	0.98
	Proline Betaine	-7.8 (± 1.2)	0.79	-540(± 43)	0.93
	Sarcosine	-5.7 (± 0.52)	0.92	-320 (± 15)	0.98

Table 11: Concentration-dependent osmolyte effect in thermal experiments at pH 7.0

		Thermal stabilization potency	
		Regression coefficient $\times 10^{-2}$	adj. r^2
Polyols	Trehalose	2.7 (± 0.07)	0.99
	Mannitol	1.8 (± 0.14)	0.94
	Sorbitol	2.0 (± 0.15)	0.94
	Erythritol	1.0 (± 0.05)	0.98
	Glucose	1.3 (± 0.15)	0.87
	Glycerol	0.36 (± 0.04)	0.87
	Myo-Inositol	2.4 (± 0.19)	0.94
Amino acids and derivatives	Proline	2.3 (± 0.31)	0.83
	Serine	3.3 (± 0.31)	0.91
	Glycine	3.4 (± 0.29)	0.93
	Taurine	3.5 (± 0.33)	0.91
	Ectoine	1.4 (± 0.20)	0.80
	Hydroxyectoine	2.5 (± 0.24)	0.90
	Glutamine	1.5 (± 0.22)	0.80
	Alanine	3.4 (± 0.18)	0.97
	Beta-Alanine	2.0 (± 0.48)	0.61
Methylamines	Betaine	1.8 (± 0.22)	0.85
	COS	0.17 (± 0.19)	-0.02
	TMAO	2.7 (± 0.23)	0.93
	Proline Betaine	-0.40 (± 0.30)	0.07
	Sarcosine	3.5 (± 0.30)	0.92

References

1. Mahler HC, Friess W, Grauschopf U, Kiese S. (2009) Protein Aggregation: Pathways, Induction Factors and Analysis. *J. Pharm. Sci.* 98: 2909-2934.

2. Philo JS, Arakawa T. (2009) Mechanisms of protein aggregation. *Curr. Pharm. Biotechnol.* 10(4): 348-51.

3. Yancey PH, Clark ME, Hand SC, Bowlus RD, Somero GN. (1982) Living with Water Stress: Evolution of Osmolyte Systems. *Science.* 217: 1214-1222.

4. Taneja S, Ahmad F. (1994) Increased thermal stability of proteins in the presence of amino acids. *Biochem. J.* 303: 147-153.

5. Santoro MM, Liu Y, Khan SMA, Hou L-X, Bolen DW. (1992) Increased Thermal Stability of Proteins in the Presence of Naturally Occurring Osmolytes. *Biochemistry.* 31: 5278-5283.

6. Chen BL, Arakawa T. (1996) Stabilization of Recombinant Human Keratinocyte Growth Factor by Osmolytes and Salts. *J. Pharm. Sci.* 85: 419-422.

7. Gekko K, Koga S. (1983) Increased Thermal Stability of Collagen in the Presence of Sugars and Polyols. *J. Biochem.* 94: 199-205.

8. Arakawa T, Timasheff SN. (1985) The stabilization of proteins by osmolytes. *Biophys. J.* 47: 411-414.

9. Bolen DW. (2001) Protein Stabilization by Naturally Occurring Osmolytes. In: Murphy KP, editor. Methods in Molecular Biology: Protein Structure, Stability and Folding. Totowa: Humana Press. Vol. 168, pp 17-36.

10. Jamal S, Poddar NK, Singh LR, Dar TA, Rishi V, *et al*. (2009) Relationship between functional activity and protein stability in the presence of all classes of stabilizing osmolytes. *FEBS. J.* 276: 6024-6032.

11. Attri P, Venkatesu P, Lee MJ. (2010) Influence of Osmolytes and Denaturants on the Structure and Enzyme Activity of α-Chymotrypsin. *J. Phys. Chem., B*. 114: 1471-1478.

12. Nayak A, Lee CC, McRae GJ, Belfort G. (2009) Osmolyte Controlled Fibrillation Kinetics of Insulin: New Insight into Fibrillation Using the Preferential Exclusion Principle. *Biotechnol. Progr.* 25: 1508-1514.

13. Singh LR, Kumar PN, Dar TA, Kumar R, Ahmad F. (2011) Protein and DNA destabilization by osmolytes: The other side of the coin. *Life Sci.* 88: 117-125.

14. Singh R, Haque I, Ahmad F. (2005) Counteracting Osmolyte Trimethylamine N-Oxide Destabilizes Proteins at pH below Its pKa. *J. Biol. Chem*. 280: 11035-11042.

15. Singh LR, Dar TA, Rahman S, Jamal S, Ahmad F. (2009) Glycine betaine may have opposite effects on protein stability at high and low pH values. *BBA Proteins Proteom* 1794: 929-935.

16. Haque I, Singh R, Moosavi-Movahedi AA, Ahmad F. (2005) Effect of polyol osmolytes on Delta G(D), the Gibbs energy of stabilisation of proteins at different pH values. *Biophys. Chem*. 117: 1-12.

17. Hincha DK. (2006) High concentrations of the compatible solute glycinebetaine destabilize model membranes under stress conditions. *Cryobiology*. 53: 58-68.

18. Kaushik JK, Bhat R. (2003) Why Is Trehalose an Exceptional Protein Stabilizer? An analysis of the thermal stability of proteins in the presence of the compatible osmolyte trehalose. *J. Biol. Chem*. 278: 26458-26465.

19. Xie G, Timasheff SN. (1997) The thermodynamic mechanism of protein stabilization by trehalose. *Biophys. Chem*. 64: 25-43.

20. Morshedi D, Rezaei-Ghaleh N, Ebrahim-Habibi A, Ahmadian S, Nemat-Gorgani M. (2007) Inhibition of amyloid fibrillation of lysozyme by indole derivatives-possible mechanism of action. *FEBS J*. 274: 6415-6425.

21. Macchi F, Eisenkolb M, Kiefer H, Otzen DE. (2012) The Effect of Osmolytes on Protein Fibrillation. *Int. J. Mol .Sci.* 13: 3801-3819.

22. Hochachka PW, Somero GN. (2002) Water-Solute Adaptations: The Evolution and Regulation of the Internal Milieu. In: Hochachka PW, Somero GN. Biochemical Adaptation: Mechanism and Process in Physiological Evolution. New York: Oxford University Press. pp. 217-287.

23. Schmidt E, Wagner W. (1904) Ueber Cholin , Neurin und verwandte Verbindungen (2. Mittheilung). II. Cholin. Justus Liebigs Ann Chem 337: 51-62.

24. King H. (1941) 2-Acetyl-1-methylpyrrolidine. *J. Chem. Soc*. 64: 337-339.

25. Lee CC, Nayak A, Sethuraman A, Belfort G, McRae GJ. (2007) A three-stage kinetic model of amyloid fibrillation. *Biophys. J.* 92: 3448-3458.

26. Varughese MM, Newman J. (2012) Inhibitory Effects of Arginine on the Aggregation of Bovine Insulin. *J. Biophys.* 2012: 1-7.

27. Niesen FH, Berglund H, Vedadi M. (2007) The use of differential scanning fluorimetry to detect ligand interactions that promote protein stability. *Nat. Protoc*. 2: 2212-2221.

28. Marvin. (1991) Bio-Xplor, Version 1.0. New York: Biostructure Inc.

29. Wang W. (2005) Protein aggregation and its inhibition in biopharmaceutics. *Int. J. Pharm*. 289: 1-30.

30. Baynes BM, Trout BL. (2004) Rational Design of Solution Additives for the Prevention of Protein Aggregation. *Biophys. J*. 87: 1631-1639.

31. Carpenter JF, Kendrick BS, Chang BS, Manning MC, Randolph TW. (1999) Inhibition of stress-induced aggregation of protein therapeutics. *Meth Enzymol*. 309: 236-255.

32. Orsini G, Goldberg ME. (1978) The renaturation of reduced chymotrypsinogen A in guanidine HCl. Refolding versus aggregation. *J. Biol. Chem*. 253: 3453-3458.

33. Maeda Y, Koga H, Yamada H, Ueda T, Imoto T. (1995) Effective renaturation of reduced lysozyme by gentle removal of urea. *Protein Eng*. 8: 201-205.

34. Hamada H, Arakawa T, Shiraki K. (2009) Effect of Additives on Protein Aggregation. *Curr. Pharm. Biotech*. 10: 400-407.

35. Poddar NK, Ansari ZA, Singh RK, Moosavi-Movahedi AA, Ahmad F. (2008) Effect of monomeric and oligomeric sugar osmolytes on DeltaGD, the Gibbs energy of stabilization of the protein at different pH values: is the sum effect of monosaccharide individually additive in a mixture? *Biophys. Chem*. 138: 120-129.

36. Kuhn LA, Swanson CA, Pique ME, Tainer JA, Getzoff ED. (1995) Atomic and Residue Hydrophilicity in the Context of Folded Protein Structures. *Proteins Struct. Func.t Genet*. 23: 536-547.

37. Street TO, Bolen DW, Rose GD. (2006) A molecular mechanism for osmolyte-induced protein stability. *PNAS*. 103: 13997-14002.

38. Granata V, Palladino P, Tizzano B, Negro A, Berisio R *et al.* (2006) The effect of the osmolyte trimethylamine N-oxide on the stability of the prion protein at low pH. *Biopolymers*. 82: 234-240.

6

Summary

Pharmaceutical proteins constitute an important class of products in the biotech industry. Among them, monoclonal antibodies have become a driven force for the growth of the whole market, because of their broad application in clinical diagnostics and therapeutics. For the recovery of these products from fermentation broths, several preparative modes of chromatography are employed. Some of them, such as protein A chromatography, are costly and have limited scalability. The present thesis explores the possibility to implement crystallization, which is one of the oldest purification techniques used in chemical technology, in the early downstream process. **Chapter 3** focuses on exploring the phase diagram of a monoclonal antibody to identify optimized crystallization conditions with regard to yield and purity. **Chapter 4** is concerned with analyzing the impact of contaminating proteins on the crystallization process. **Chapter 5** deals with the competing process of protein aggregation, which can prevent crystallization if not controlled by the addition of stabilizers. A lysozyme fibrillation model system was used to test a set of naturally occurring osmolytes for their stabilizing potency.

The successful development of crystallization as a purification step for a monoclonal antibody presented in **Chapter 3** shows that crystallization has the potential to be introduced as a purification step for mAbs. After identifying crystallization conditions, protein solubility was studied as a function of the concentration of target protein BImAb04c and of the precipitant PEG. The solubility limit in this system was determined by preparing saturated solution in equilibrium with crystalline protein and measuring the protein concentration in the supernatant. By applying the resulting phase diagram, batch crystallization could be performed and scaled by carefully choosing operation conditions in the metastabile zone. In spiking experiments, BImAb04c could be crystallized in the presence of lysozyme or BSA. Analysis of crystallization samples by SDS-PAGE after

crystallization indicated that most of the spiking proteins were excluded from the crystals. In further experiments, crystallization conditions were adapted to crystallize the antibody directly from concentrated clarified cell culture supernatant. As a result, BImAb04c achieved a purity of more than 90% in a single crystallization step at small scale. In addition, aggregate formation was negligible during the whole process. But with a low recovery rate of about 30 % even after 5 days of incubation time, crystallization cannot compete with the widely-used protein A chromatography as a capturing step. Still, it was shown in this chapter that protein crystallization has the potential to be introduced as a purification step for mAbs, but more likely as a later purification step and not for capturing.

It is known from crystallography that the presence of impurities is a critical problem, since impurities may incorporate into growing protein crystals and thus affect defect densities, morphology and diffraction resolution of crystals. For bulk protein crystallization, crystal growth rate is more relevant than crystal diffraction quality. In **Chapter 3**, it was demonstrated that the presence of protein impurities in fermentation broth slowed down crystallization process of BImAb04c significantly. In **Chapter 4**, crystallization of mAb04c was conducted in the presence of various model contaminant proteins. Spiking test with BSA indicated that the reduction of the crystallization rate correlated with the molar ratio of impurity to target protein. This could be expected, as protein impurities can bind to active growth site of the crystal and prevent the target protein from becoming incorporated into the crystal. This inhibition is likely to depend on the impurity concentration. Another spiking protein ovalbumin showed the similar inhibition as BSA. Meanwhile, two other spiking proteins, lysozyme and cytochrome c, did not inhibit crystallization at concentrations comparable to BSA and ovalbumin. CG-MALS experiments supported the view that this difference was probably due to different types of interaction (attractive vs. repulsive) between protein impurity and target. In the low ionic strength system tested here, electrostatic interactions would be sufficient to explain the observed differences. Although other interactions might become dominant under different crystallization conditions, this indicates that analysis of molecular interactions in solution might help to predict inhibitory effects of specific contaminants and design process steps that improve crystallization rate and yield. Here, an anion exchange chromatography

operated in flow-through mode preceding crystallization should improve the crystallization efficiency and raise the product yield.

Maintaining stability is a major issue during the production of biopharmaceuticals, because aggregation results in activity loss and immunogenic adverse reactions. In case of protein crystallization, amorphous aggregates compete with the formation of crystals. For these reasons, aggregation is to be avoided at all costs. Therefore, stabilization potency of different osmolytes classes (polyols, amino acids and methylamine groups) was examined additionally in **Chapter 5**, focusing on lysozyme as an example of a folded globular protein. In measuring melting points with differential scanning fluorimetry and aggregation kinetics (model system fibrillation) using the fluorescent dye thioflavin T, osmolyte effects are related to molecule characteristics and a possible connection between thermal stability and kinetic stability was investigated. It was found that polyols increased both thermal and kinetic stability in a concentration-dependent manner, whereas most compounds from the amino acids and methylamine groups led to destabilization. The latter can possibly be ascribed to charge-related preferential binding mechanisms, as the strength of impact is related to increasing compound pKa values and stabilizing effects of these osmolytes near neutral pH. Furthermore, it was observed that there was similar but not identical effects of particular osmolytes on both types of stability. Thus, kinetic stability cannot solely be predicted by melting points, which is used to measure thermal stability of proteins. This kind of analysis could be helpful for aggregation control and thereby, benefits protein crystallization.

Appendix

Experimental methods

1. **Crystallization through vapor diffusion**

Vapor diffusion is the most widely used approach for screening of crystallization conditions at present. The detailed mechanism of this method is discussed in **Chapter 2.1.2**. Two common procedures are involved in this method, and they are sitting-drop and hanging drop vapor diffusion, named according to position of sample droplet.

a. **Hanging-drop crystallization**

The 24 well crystallization plates (24 Well ComboPlate™, Greiner Bio-one, Germany) were applied for hanging-drop crystallization. Volume of 1 ml crystallization reagent was pipetted into reservoir of plate. A bead of vacuum grease (Bayer, Germany) was applied along the upper edge of the reservoir. Subsequently, 1-2 µl protein solution was mixed with an equivalent volume of crystallization reagent in the center of a siliconized 18 mm circle cover slide (Jena Bioscience, Germany). The cover slide was then inverted so the droplet if hanging from the cover slide, positioned and pressed gently down onto the bead of grease on the reservoir to keep it tight.

b. **Sitting-drop crystallization**

Sitting-drop crystallization was performed either directly in 96 well crystallization plate from Corning, USA, or 24 well ComboPlate™ with help of Crystalbridge™ (Greiner Bio-one, Germany). With a 96 well crystallization plate, volume of 100 µl crystallization reagent was pipetted into reservoir (large well of the plate). 1-1.5 µl protein solution was mixed with 1-1.5 µl crystallization reagent in the small well of plate. All reservoirs were then sealed with clear plate sealing tape (Greiner VIEWseal, Greiner Bio-one) after preparation. In the case of 24 well ComboPlate volume of 1 ml reagent was transferred into reservoir. A Crystalbridge was placed into the bottom of reservoir. Droplet (maximum 40

µl) composed of protein solution and crystallization reagent was prepared in the concave depression of the Crystalbridge. Reservoir was then sealed with glass cover slide.

2. Microbatch crystallization under Oil

Batch technique is a simple and one of the oldest crystallization techniques. In labor, microbatch (with a volume less than 10 µl) is commonly performed under paraffin oil, to prevent aqueous samples from evaporation. The 60 well Terasaki plate was employed for performance of microbatch crystallization. A volume of 5-6 ml 100 % paraffin oil (Hampton research, USA) was pipetted into a Terasaki plate. Droplet (up to 10 µl) composed of protein solution and crystallization reagent was then mixed in the cone-shape depression in the microbatch plate. Plate cover was finally placed over plate to prevent dust from entering experiment.

3. Seeding Techniques

Seeding is a technique widely applied in protein crystallization. Crystal from primary crystallization can be seeded in the new crystallization drop or batch, to improve quality and growth rate of crystals, or distinguish microcrystalline from amorphous precipitate during screening. Seeding can be homogeneous or heterogeneous, depending on whether the seeds are composed of the same components as the target protein or not. This work deals mostly with the homogeneous seeding. *Streak seeding* and *microseeding* are two most popular seeding approaches and were employed in this work.

a. Streak seeding

Streak seeding (Figure **25**) was mainly used for the screening of crystal-growth conditions or to diagnostic to confirm whether phase separation or amorphous precipitate is crystalline. Seeding Tool made of nature fiber (HR8-133, Hampton Research) was inserted into droplet and was dragged through microcrystalline or crushed crystal so that seed crystals could attached to the fiber. A straight line was drawn with the fiber across a fresh crystallization drop containing the protein sample and reagent adequate to support growth. Crystals appear along the streak line, if the streak seeding has been successful.
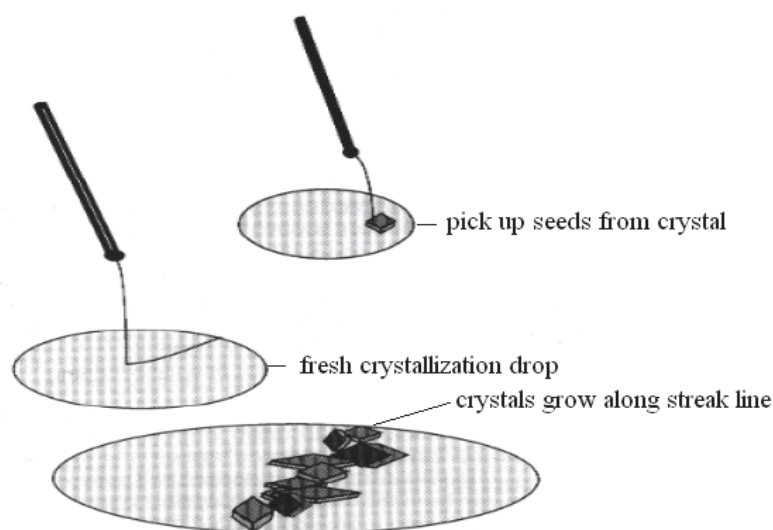
Figure 25. Schematic representation of the procedure for streak seeding. Crystal seed will be transported to a fresh crystallization drop with help of a probe made of nature fiber. New crystals can grow from these seeds if the conditions in droplet are suitable.

b. **Microseeding in solution**

Microseeding, illustrated in Figure **26**, was used to introduce a controlled number of crystal seeds into fresh mother liquor. Crystals were separated from the mother liquor by 10 min centrifugation at 4 °C and 10,000g and washed 3 times with reservoir solution, each volume of the wash reservoir being the same as that of the original sample of crystal suspension. The crystal suspension was then transferred into a microcentrifuge tube containing a Teflon Seed Bead™ (Hampton Research). Through vortex, a homogeneous stock solution of microseeds was generated with help of the bead. A series of dilutions were then performed to establish an appropriate dilution for Microseeding.
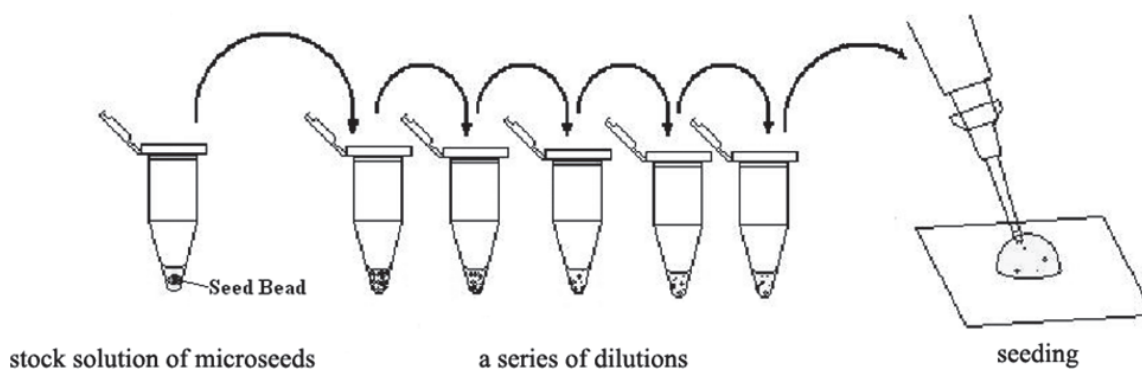
Figure 26. Schematic representation of microseeding method. A homogeneous stock solution of microseeds is generated by a Teflon bead. After a series of dilution, a controlled number of microcrystals are seeded in fresh mother liquor after a series of dilution.

4. **Analyzing protein-protein interaction via static light scattering**

The osmotic second virial coefficient A_2 is used to characterize overall protein-protein self interactions in one protein system, which is contributed by electrostatics, van der Waals interactions, excluded volumes, hydration forces, and hydrophobic effects. Similarly, the osmotic second cross virial coefficient A_{11} can also be employed to suggest cross interactions in multi-protein system. Through transformation of Equation (2) in **Chapter 2.2.2**, the virial coefficient for a single species in dilute solution can be expressed as:

$$\frac{R(\theta)}{K^* \cdot c} = \frac{M \cdot c \cdot P(\theta)}{1 + 2A_2 \cdot M \cdot c \cdot P(\theta)} \qquad (8)$$

Therefore, determination of the A_2 consists of measurement of the excess Rayleigh ratio $R(\theta)$ over several values of protein concentration c, construction of Zimm plot, and fitting the data. Likewise, the second cross virial coefficient A_{11} of a two-protein system may be determined by measuring $R(\theta)$ at a series of compositions of the two soluble proteins A and B—changing the ratio $c^A{:}c^B$—and fitting the results to following equation (Some D, et al. 2009):

$$\frac{R(\theta)}{K^*} = \frac{M^A c^A P^A(\theta)}{1+2A_2^A M^A c^A P^A(\theta)} + \frac{M^B c^B P^B(\theta)}{1+2A_2^B M^B c^B P^B(\theta)} \tag{9}$$

$$-4A_{11}M^A M^B c^A c^B P^A(\theta)P^B(\theta)$$

The determination of virial coefficient is a time-consuming and tedious process if carried out manually. In this work, an automated composition-gradient multiangle static light scattering (CG-MALS) was employed for the characterization of the A_2 and A_{11} in solution. The whole system (Figure **27**) includes an automated composition gradient system (Calypso™ II), a static light scattering instrument (Dawn®-8), and a differential refractive index detector (Optilab® T-rEX). All the instruments are from Wyatt Technology, USA.
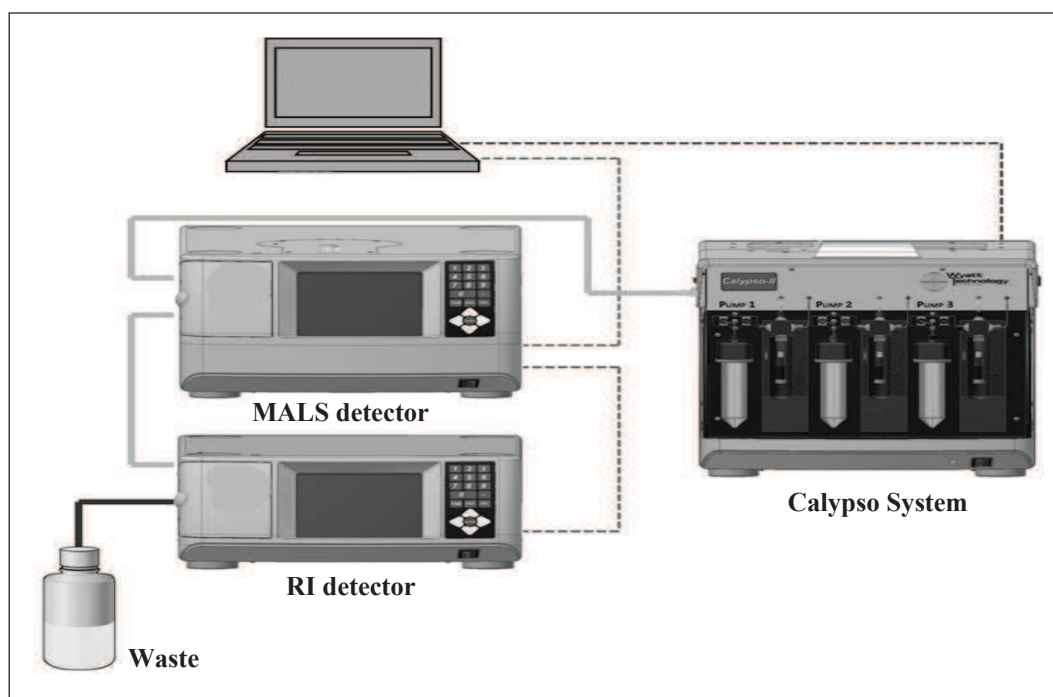
Figure 27. The CG-MALS system composed of a composition gradient pump system, a static light scattering detector and a concentration detector. Solid lines indicate fluid connections. Dashed lines indicate electrical connections.

The Calypso system is an automated composition delivery system composed of three computer controlled syringe pumps linked to reservoirs. The pumps are operated separately through control software. Therefore, up to three solutions can be mixed by pumping through a static mixer and achieve then different compositions. Since light scattering detector is very sensitive to large particles, in-line filter (0.1 µm, Millipore, US), is assembled after each pump to prevent large aggregates and particles, which are generated by mechanical motion of syringes and valves, from disturbing light scattering signals.

A multiangle light scattering (Dawn-8) was employed for the measurement of scattered light intensity of particles in different angle. The laser wavelength is 658 nm. The detector has photodiode detectors at eight scattering angles, ranged from 23°-155°, and scattering volume of 0.07 µl.

The Optilab T-rEX differential refractive index (RI) detector was served as online concentration detector. The refractive index of solution is related to concentration of the solute. Therefore, knowing the slope of the dependence of refractive index of protein solution on its concentration, i.e. the *dn/dc* value, concentration of protein can be determined. For most proteins in aqueous buffers the *dn/dc* is 0.185 mL/g, which is an advantage of RI detector compared to UV detector, since determination of extinction coefficient of protein is not required. The RI detector has a flow cell separated into two parts, that is, the reference cell and the sample cell. Both parts were flushed with reference fluid (running buffer) before the experiments. The reference cell was closed, when baseline stayed constant. Fluid was then directed through the sample cell. Any differences of RI between the two cells lead to change of signal peak area. To obtain accurate concentration data, protein solutions were dialyzed against the running buffer used in the experiment sufficiently, well-degassed and filtrated through 0.2 µm syringe filter (Sartorius, Germany).

5. Determination of protein melting points with the LightCycler 480

Protein melting points was determined with a Roche LightCycler 480 using SYPRO Orange (5000× in DMSO, Invitrogen, Germany) as fluorescence dye. With increased temperature, proteins exhibit unfolding and expose their hydrophobic regions, which can interact with SYPRO Orange in solution. The fluorescence signal rises then with an increase of the exposed hydrophobic regions.

In a reaction volume of 50 µl, a final concentration of 0.8 mg/ml lysozyme was mixed with varying osmolyte concentrations in 96 well LightCycler plates (white, opaque). SYPRO Orange was diluted 1000 fold in each assay. The plates was then sealed with clear plate sealing tape (Greiner VIEWseal, Greiner Bio-one) and shaken for 1 min at 400 rpm. Change of fluorescence signal was monitored (excitation 483nm, emission 568 nm) by LightCycler with increased temperature. Melting points were derived from the inflexion point of the melting curves. All experiments were carried out in triplicates

Bibliography

Abergel C, Nesa MP, Fontecilla-Camps JC. (1991) The effect of protein contaminants on the crystallization of turkey egg white lysozyme. *J Crystal Growth*. 110: 11-19.

Aehle W. (2007) Enzymes in Industry: Production and Application. *Wiley-VCH Verlag*. 3rd Edition. p 59.

Aggarwal S. (2010) What's fueling the biotech engine? *Nat. Biotechnol*. 28: 1165-1171.

Ahamed T, Esteban BNA, Ottens M, Van Dedem GWK, Van der Wielen LAM, et al. (2007) Phase Behavior of an intact monoclonal antibody. *Biophys J*. 93: 610-619.

Ahrer K, Buchacher A, Iberer G, Josic D, Jungbauer A. (2003) Analysis of aggregates of human immunoglobulin G using size-exclusion chromatography, static and dynamic light scattering. *J. Chromatogr., A*. 1009: 89-96.

Albercht AC. (1957) Intermolecular correlation in light scattering from dilute polymer solutions. *J. Chem. Phys*. 27: 1014-1023.

Anderson WF, Boodhoo A, Mol CD. (1988) The importance of purity in the crystallization of DNA binding immunoglobulin F_{ab} fragments. *J. Cryst. Growth*, 90: 153-159.

Anicetti V. (2009) Biopharmaceutical Processes: A glance into the 21st century. *Bioprocess Inter*. 7: 4-9.

Arakawa T, Timasheff SN. (1985) The stabilization of proteins by osmolytes. *Biophys. J*. 47: 411-414.

Arakawa T, Kita Y, Shiraki K, Ohtake S. (2011) The mechanism of protein precipitation by salts, polymers and organic solvents. *Gobal. J. Anal. Chem*. 2: 152-167.

Arosio P, Barolo G, Müller-Späth T, Wu H, Morbidelli M. (2011). Aggregation stability of a monoclonal antibody during downstream processing. *Pharm. Res*. 28: 1884-1894.

Asakura S, Oosawa F. (1954) On interactions between two bodies immersed in a solution of macromolecules. *J. Chem. Phys*. 22: 1255-1256.

Asakura S, Oosawa F. (1958) Interactions between particles suspended in a solution of macromolecules. *J. Poly Sci*. 33:183.

Attri A, Minton AP. (2005) Composition gradient static light scattering (CG-SLS): a new technique for rapid detection and quantitative characterization of reversible macromolecular hetero-associations in solution. *Anal. Biochem*. 346: 132-138.

Attri P, Venkatesu P, Lee MJ. (2010) Influence of Osmolytes and Denaturants on the Structure and Enzyme Activity of α-Chymotrypsin. *J. Phys. Chem., B*. 114: 1471-1478.

Baldwin RL. (1996) How Hofmeister ion interactions affect protein stability. *Biophys. J.* 71: 2056-2063.

Ball V, Ramsden JJ. (1998) Buffer dependence of refractive index increments of protein solutions *Biopolymers*. 46: 489-492.

Basu SK, Govardhan CP, Jung CW, Margolin AL. (2004) Protein crystals for the delivery of biopharmecuticals. *Expert Opin. Biol. Ther*. 4: 301-317.

Baynes BM, Trout BL. (2004) Rational Design of Solution Additives for the Prevention of Protein Aggregation. *Biophys. J*. 87: 1631-1639.

Becker T and Lawlis VB. (1991) Subtilisin crystallization process. U.S. Patent 5,041,377, August 20, 1991.

Beeley, JA, Stevenson SM, Beeley JG. (1972) Polyacrylamide gel isoelectric focusing of proteins: Determination of isoelectric points using an antimony electrode. *Biochim. Biophys. Acta.* 285: 293-300.

Bergfors TM. (2009) Protein crystallization. *Second Edition*. *International University Line*. 2nd Edition. p 184.

Birch JR and Racher AJ. (2006) Antibody production. *Adv. Drug Deliv. Rev*. 58:671-685

Boistelle R, Astier JP. (1988) Crystallization mechanisms in solution. *J Crystal Growth*. 90: 14-30.

Bolen DW. (2001) Protein stabilization by naturally occurring osmolytes. *Meth. Mol. Biol*. 168: 17-36.

Bolen DW. (2004) Effects of naturally occurring osmolytes on protein stability and solubility: issues important in protein crystallization. *Methods*. 24: 312-322.

Bonnete F, Vivares D. (2002) Interest of the normalized second virial coefficient and interaction potentials for crystallizing large macromolecules. *Acta Cryst*. D58: 1571-1575.

Brange J. (1987) Galenics of insulin: The Physico-Chemical and Pharmaceutical Aspects of Isulin and Insulin Preparations. *Springer-Verlag*, Berlin.

Brange J. Langkjaer L, Havelund S, Volund A. (1992) Chemical stability of insulin. 1. Hydrolytic degradation during storage of pharmaceutical preparations. *Pharm Res*. 9: 715-726.

Budayova M, Bonnete F, Tardieu A, Vachette P. (1999) Interactions in solution of a large oligomeric protein. *J. Cryst. Growth*. 196: 210-219.

Carpenter JF, Kendrick BS, Chang BS, Manning MC, Randolph TW. (1999) Inhibition of stress-induced aggregation of protein therapeutics. *Meth Enzymol*. 309: 236-255.

Caspar DL, Cohen C and Longley W. (1969) Tropomyosin, crystal structure, polymorphism and molecular interactions. J. Mol. Biol. 41: 87.

Caylor CL, Dobrianov I, Lemay SG, Kimmer C, Kriminski S, et al. (1999) Macromolecular impurities and disorder in protein crystals. *Proteins: Struct., Funct., Genet*. 36: 270-281.

Chayen NE, Saridakis E. (2001) Is lysozyme really the ideal model protein? *J Crystal Growth*. 232: 262-264.

Chen BL, Arakawa T. (1996) Stabilization of recombinant human keratinocyte growth factor by osmolytes and salts. *J. Pharm. Sci*. 85: 419-422.

Chernov AA. (1984) Modern Crystallography III, Crystal Growth. *Springer Berlin*. 544 p.

Choi HS, Bae YC. (2009) Osmotic cross second virial coefficient of unfavorable proteins: modified Lennard-Jones potential. *Macromol. Res*. 17: 763-769.

Chon JH and Zarbis-Papastoitsis G. (2011) Advances in the production and downstream processing of antibodies. *New Biotechnol*. 28: 458-463.

Cohn EJ and Ferry JD. (1943) The interactions of proteins with ions and dipolar ions. In *Proteins, amino acids and peptides as ions and dipolar ions*. p. 586. Van Nostrand-Reinhold, Princeton, New Jersey.

Curitis RA, Blanch HW, Prausnitz JM. (2001) Calculation of phase diagrams for aqueous protein solutions. *J. Phys, Chem. B*. 105: 2445-2452.

Ducruix A and Giege R. (1992) Crystallization of Nucleic Acids and Proteins: A Practical Approach. *IRL Press at Oxford University Press, Oxford*. 331 p.

Ebel C, Faou P, Kernel B, Zaccai G. (1999) Relative role of anions and cations in the

Fahrner RL, Knudsen HL, Basey CD, Galan W, Feuerhelm D, et al. (2001) Industrial purification of pharmaceutical antibodies: development, operation and validation of chromatography processes. *Biotechnol. Genet. Eng. Rev.* 18: 301-327.

Feher G. (1986) Mechanism of nucleation and growth of protein crystals. *J. Cryst. Growth*. 76 :545-546.

Fennema OR. (1996) Food Chemistry. 3rd Edition. *Marcel Dekker Inc*. p373.

Fukumoto J, Iwai M, Tsujisaka Y. (1963) Studies on lipase. I. Purification and crystallization of a lipase secreted by *Aspergillus niger*. *J. Gen. Appl. Microbiol*.

Geerlof A, Brown J, Coutard B, Egloff MP, Enguita FJ, et al. (2006) The impact of protein characterization in structural proteomic. *Acta Crystallogr., Sect. D: Biol. Crystallogr*. 62: 1125-1136.

Gekko K, Koga S. (1983) Increased Thermal Stability of Collagen in the Presence of Sugars and Polyols. *J. Biochem.* 94: 199-205.

George A and Wilson WW. (1994) Predicting protein crystallization from a dilute solution property. *Acta Crystallogr. D*. 50: 361.

Giege R, Dock AC, Kern D, Lorber B, Thierry JC, et al. (1986) The role of purification in the crystallization of proteins and nucleic acids. *J. Crystal. Growth*. 76: 544-561.

Gilliland GL. (1988) A biological macromolecule crystallization database: A basis for a crystallization strategy. *J. Cryst. Growth*. 90: 51.

Granata V, Palladino P, Tizzano B, Negro A, Berisio R *et al.* (2006) The effect of the osmolyte trimethylamine N-oxide on the stability of the prion protein at low pH. *Biopolymers*. 82: 234-240.

Haas C and Drenth J. (1999) Understanding protein crystallization on the basis of the phase diagram. *J. Cryst. Growth*. 196: 388-394.

Hamada H, Arakawa T, Shiraki K. (2009) Effect of Additives on Protein Aggregation. *Curr. Pharm. Biotech*. 10: 400-407.

Haque I, Singh R, Moosavi-Movahedi AA, Ahmad F. (2005) Effect of polyol osmolytes on Delta G(D), the Gibbs energy of stabilisation of proteins at different pH values. *Biophys. Chem*. 117: 1-12.

Harries D, Rösgen J. (2008) A practival guide on how osmolytes modulate macromolecular properties. *Methodes Clee Biol*. 84: 679-735.

Hincha DK. (2006) High concentrations of the compatible solute glycinebetaine destabilize model membranes under stress conditions. *Cryobiology*. 53: 58-68.

Hitscherich C, Kaplan J, Allaman M, Wiencek J, Loll PJ. (2000) Static light scattering studies of OmpF porin: Implications for integral membrane protein crystallization. *Protein. Sci*. 9: 1559-1566.

Hochachka PW, Somero GN. (2002) Biochemical adaptation: Mechanism and Process in Physiological Evolution. *Oxford University Press*, New York. 480 p.

Hofmeister F. (1888) Zur Lehre von der Wirkung der Salze. *Naunyn-Schmiedebergs Arch. Exp. Pathol. Pharmakol*. 24: 247.

Hui A and Edwards A. (2003) High-throughput protein crystallization. *J. Struct. Biol*. 142: 154-161.

Huglin MB. (1972) Light scattering from polymer solutions. *Academic Press, London*. 885 p.

Jackewitz A. (2008) Reducing elution volumes with high capacity and improved mass transfer ion-exchange resins. *Bioprocess Int*. 6: 108-110.

Jacobsen C, Garside J, Hoare M. (1997) Nucleation and growth of microbial lipase crystals from clarified concentrated fermentation broths. *Biotechnol Bioeng*. 57:666-675.

Jakoby WB. (1971) Crystallization as a purification technique. *Meth. Enzymol*. 22: 248: 252.

Jamal S, Poddar NK, Singh LR, Dar TA, Rishi V, *et al*. (2009) Relationship between functional activity and protein stability in the presence of all classes of stabilizing osmolytes. *FEBS. J.* 276: 6024-6032.

Jancarik J and Kim SH. (1991) Sparse matrix sampling: A screening method for the crystallization of macromolecules. *J. Appl. Cryst*. 24: 409-411.

Judge RA, Johns MR, White ET. (1995) Protein purification: The recovery of ovalbumin. *Biotechnol Bioeng*. 48: 316-323.

Kameyama K, Minton AP. (2006) Rapid quantitative characterization of protein interactions by composition gradient static light scattering. *Biophys. J*. 90: 2164-2169.

Kaushik JK, Bhat R. (2003) Why Is Trehalose an Exceptional Protein Stabilizer? An analysis of the thermal stability of proteins in the presence of the compatible osmolyte trehalose. *J. Biol. Chem*. 278: 26458-26465.

Keilin D and Hartree EF. (1945) Purification and properties of cytochrome c. *Biochem J*. 39: 289-292.

King H. (1941) 2-Acetyl-1-methylpyrrolidine. *J. Chem. Soc*. 64: 337-339.

Kitazono A, Yoshimoto T, Tsuru D. (1992) Cloning, sequencing, and high expression of the prolin iminopeptidase gene from *Bacillus coagulans*. *J. Bacteriol*. 174: 7919-7925.

Klyushnichenko V. (2003) Protein crystallization: From HTS to kilogram-scale. *Curr Opin Drug Discovery Dev*. 6: 848-854.

Koszelak S, Martin D, Ng J, MePherson A. (1991) Protein crystal growth rates determined by time lapse microphotography. *J. Cryst. Growth*. 110: 177.

Kuhn LA, Swanson CA, Pique ME, Tainer JA, Getzoff ED. (1995) Atomic and Residue Hydrophilicity in the Context of Folded Protein Structures. *Proteins Struct. Func.t Genet*. 23: 536-547.

Kundrot CE. (2004) Which strategy for a protein crystallization project? *Cell. Mol. Life. Sci*. 61: 525-536.

Kurihara K, Miyashita S, Sazaki G, Nakada T, Durbin SD, et al. (1999) Incorporation of impurity to a tetragonal lysozyme crystal. *J. Cryst. Growth*. 196: 285-290.

Kuznetsov YG, Malkin AJ, Glantz W, McPherson A. (1996) In situ atomic force micorscopy studies of protein and virus crystal growth mechnanisms. *J. Cryst. Growth*. 168: 63.

Kuznetsov YG, Malkin AJ, Land TA, DeZoreo JJ, Barba de la Rosa AP, et al. (1997) Molecular resolution imaging of macromolecular crystals by atomic force microscopy. *Biophsy. J.* 72: 2357.

Kuznetsov YG, Malkin AJ, McPherson Alexander. (2001) The liquid protein phase in crystallization: a case study-intact immunoglobulins. *J Crys Grow*. 232: 30-39.

Lacmann R, Stranski IN. (1958) Growth and perfection of crystals. *Wiley, New York*. 427 p.

Lain B, Cacciuttolo MA, Zarbis-Papastoitsis G. (2009) Development of a high-capacity Mab capture step based on cation exchange chromatography. *Bioprocess Int*. 7: 26-34.

Land TA, Malkin AJ, Kuznetsov YZ, McPherson A, DeYoreo JJ. (1995) Mechanisms of protein crystal growth: An atomic force microscopy study of canavalin crystallization. *Phys. Rev. Lett.* 75: 2774.

Land TA, Martin TL, Potapenko S, Palmore GT, De Yoreo JJ. (1999) Recovery of surfaces from impurity poisoning during crystal growth. *Nature*. 399: 442-445.

Lee CC, Nayak A, Sethuraman A, Belfort G, McRae GJ. (2007) A three-stage kinetic model of amyloid fibrillation. *Biophys. J.* 92: 3448-3458.

LeVine H III. (1993) Thioflavine T interaction with synthetic Alzheimer's disease beta-amyloid peptides: detection of amyloid aggregation in solution. *Protein Sci*. 2: 404-410.

Lewus RA, Darcy PA, Lenhoff AM, Sandler SI. (2011) Interactions and phase behavior of a monoclonal antibody. *Biotechnol Prog*. 27: 280-289.

Lodish H, Berk A, Zipursky SL, et al. (2000) Molecular Cell Biology, section 2.2: Noncovalent Bonds. 4th edition. *New York: W. H. Freeman.*

Lorber B, Skouri M, Munch J, Giege R. (1993) The influence of impurities on protein crystallization: the case of lysozyme. *J. Crystal. Growth*. 128: 1203-1211.

Macchi F, Eisenkolb M, Kiefer H, Otzen DE. (2012) The Effect of Osmolytes on Protein Fibrillation. *Int. J. Mol .Sci.* 13: 3801-3819.

Maeda Y, Koga H, Yamada H, Ueda T, Imoto T. (1995) Effective renaturation of reduced lysozyme by gentle removal of urea. *Protein Eng*. 8: 201-205.

Mahler HC, Friess W, Grauschopf U, Kiese S. (2009) Protein Aggregation: Pathways, Induction Factors and Analysis. *J. Pharm. Sci*. 98: 2909-2934.

Malamud, D. and Drysdale, JW. (1978) Isoelectric points of proteins: A table. *Anal. Biochem.*, 86: 620-647.

Malkin AJ, Chernov AA, McPherson A. (1993) Crystallization of satellite tobacco mosaic virus. I. Nucleation phenomena. *J. Cryst. Growth*. 126: 544.

Malkin AJ, Kuznetzov YG, Land TA, DeYoreo JJ, McPherson A. (1995) Mechanisms of growth for protein and virus crystals. *Nat. Struct. Biol*. 2: 956.

Malkin AJ, Kuznetsov YG, McPherson A. (1996a) Defect structure of macromolecular crystals. *J. Struct. Biol*. 117: 124.

Malkin AJ, Kuznetsov YG, McPherson A. (1996b) Incorporation of microcrystals by growing protein and virus crystals. *Protein Struct. Funct. Genet*. 24: 247.

Malkin AJ, Kuznetsov YG, Glantz W, McPherson A. (1996c) Atomic force microscopy studies of surface morphology and growth kinetics in thaumatin crystallization. *J. Phys. Chem*. 100: 11736.

Marvin. (1991) Bio-Xplor, Version 1.0. New York: Biostructure Inc.

Matthews BW. (1968) Solvent content of protein crystals. *J. Mol. Biol*. 33:491.

McPherson A. (1991) A brief history of protein crystal growth. *J. Cryst. Growth*. 110: 1.

McPherson A. (1993) Virus and protein crystal growth on earth and in microgravity. *J. Phys. D: Appl. Phys*. 26: B104-B112.

McPherson A, Malkin AJ, Kuznetsov YZ, Koszelak S. (1996) Incorporation of impurities into macromolecular crystals. *J. Cryst. Growth*. 168: 74-92

McPherson A. (1999) Crystallization of biological macromolecules. *Cold Spring Harbor Laboratory Press*. 1st edition. 586 p.

Moon YU. (2011) Osmotic pressures and second virial coefficients for aqueous saline solutions of lysozyme. *Fluid Phase Equilibria*. 168: 229-239.

Morshedi D, Rezaei-Ghaleh N, Ebrahim-Habibi A, Ahmadian S, Nemat-Gorgani M. (2007) Inhibition of amyloid fibrillation of lysozyme by indole derivatives-possible mechanism of action. *FEBS J*. 274: 6415-6425.

Mullin JW. (1993) Crystallization. *3rd edtion. Butterworth-Heinemann: Oxford, UK*. 600 p.

Myerson AS, Toyokura K. (1990) Crystallization as a separation process. ACS Symposium Series 438. American Chemical Society, Washington, DC.

Naono H, Miura M. (1965) The effect of sodium triphosphat on the nucleation of strontium sulfate. *Bull Chem Soc Japan*. 38: 80-83.

Nayak A, Lee CC, McRae GJ, Belfort G. (2009) Osmolyte controlled fibrillation kinetics of insulin: New insight into fibrillation using the preferential exclusion principle. *Biotechnol. Progr*. 25: 1508-1514.

Neal BL, Asthagiri D, Lenhoff AM. (1998) Molecular origins of osmotic second virial coefficients of proteins. *Biophys. J*. 75: 2469-2477.

Niesen FH, Berglund H, Vedadi M. (2007) The use of differential scanning fluorimetry to detect ligand interactions that promote protein stability. *Nat. Protoc*. 2: 2212-2221.

Ng JD, Lorber B, Witz J, Théobald-Dietrich A, Kern D, Giegé R. (1996) The crystallization of biological macromolecules from precipitates: evidence for Ostwald ripening. *J. Crystal Growth*, 168: 50-62.

Ng JD, Kuznetsov YG, Malkin AJ, Keith G, Goege R, et al. (1997) Visualization of nucleic acid crystal growth by atomic force microscopy. *Nucleic Acids Res*. 25: 2582.

Nilsson MR (2004) Techniques to study amyloid fibril formation in vitro. *Methods*. 34: 151-160.

Orsini G, Goldberg ME. (1978) The renaturation of reduced chymotrypsinogen A in guanidine HCl. Refolding versus aggregation. *J. Biol. Chem*. 253: 3453-3458.

Panec M, Katz DS. (2006) MicrobeLibrary-Plaque assay protocols. Available: http://archive.microbelibrary.org/asmonly/details.asp?id=2336

Pechenov S, Shenoy B, Zang MX, Basu SK, Margolin AL. (2004) Injectable controlled release formulations incorporating protein crystals. *J. Control. Release*. 96: 149-158.

Peters J, Minuth T, Schroder W. (2005) Implementation of crystallization step into the purification process of a recombinant protein. *Protein. Expr. Purif*. 39: 43-53.

Pey AL, Rodriguez-Larrea D, Bomke S, Dammers S, Godoy-Ruiz R, et al. (2008) *Proteins*. 71: 165-174.

Philo JS, Arakawa T. (2009) Mechanisms of protein aggregation. *Curr. Pharm. Biotechnol.* 10(4): 348-51.

Pikal MJ and Rigsbee DR. (1997) The stability of insulin in crystalline and amorphous solids: Observation of greater stability of the amorphous form. *Pharm Res*. 14: 1379-1387.

Pitts JE, Ussitalo JM, Mantafounis D, Nugent PG, Quinn DD, et al. (1993) Expression and characterisation of chymosin pH optima mutants produced in *Trichoderma reesei*. *J. Biotechnol*. 28: 69-83.

Plomp M, McPherson A, Malkin AJ. (2003) Repair of Impurity-Poisoned Protein Crystal Surfaces. *Proteins: Struct., Funct., Genet*. 50: 486-495.

Poddar NK, Ansari ZA, Singh RK, Moosavi-Movahedi AA, Ahmad F. (2008) Effect of monomeric and oligomeric sugar osmolytes on DeltaGD, the Gibbs energy of stabilization of the protein at different pH values: is the sum effect of monosaccharide individually additive in a mixture? *Biophys. Chem*. 138: 120-129.

Price WN, Chen Y, Handelman SK, Neely H, Manor P, et al. (2009) Understanding the physical properties controlling protein crystallization based on analysis of large-scale experimental data. *Nat Biotechnol*. 27: 51-57.

Przybycien TM. (1998) Protein-protein interactions as a means of purification. *Curr. Opin. Biotechnol*. 9: 164-170.

Podzimek S. (2011) Light Scattering, Size Exclusion Chromatography and Asymmetric Flow Field Flow Fractionation. 1st Edition. *John Wiley & Sons, Inc*. 372 p.

Ries-Kautt M and Ducruix A. (1989) Relative effectiveness of various ions on the solubility and crystal growth of lysozyme. *J. Biol. Chem*. 264: 745.

Rodriguez-Larrea D, Minning S, Borchert TV, Scanchez-Ruiz JM. (2006) Role of salvation barriers in protein kinetic stability. *J. Mol. Biol*. 360: 715-724.

Rosenberger F. (1986) Inorganic and protein crystal growth-similarities and differences. *J Crystal Growth*. 76: 618-636.

Roussel A, Serre L, Frey M, Fontecilla-Camps JC. (1990) Rapid access to an uupdated biological macromolecule crystallization database through artificial intelligence. *J. Cryst. Growth*. 106: 405-409.

Sanchez-Ruiz JM. (2010) Protein kinetic stability. *Biophys Chem*. 148: 1-15.

Sangwal K. (1996) Effects of impurities on crystal growth processes. *Prog Cryst Growth Charact*. 32:3-43.

Santoro MM, Liu Z, Khan SMA, Hou LX, Bolen DW. (1992) Increased thermal stability of proteins in the presence of naturally occurring osmolytes. *Biochemistry*. 31: 5278-5283.

Saunders AJ, Davis-Searles PR, Allen DL, Pielak GJ, Erie DA. (1999) Osmolyte-induced changes in protein conformational equilibria. *Biopolymers*. 53: 293-307.

Sekhon BS. (2010) Biopharmaceuticals: an overview. *Thai. J. Pharm. Sci*. 34: 1-19.

Shenoy B, Wang Y, Shan W, Margolin AL. (2001) Stability of crystalline proteins. *Biotechnol Biotech*. 73(5): 358-369.

Schmidt E, Wagner W. (1904) Ueber Cholin , Neurin und verwandte Verbindungen (2. Mittheilung). II. Cholin. Justus Liebigs Ann Chem 337: 51-62.

Shukla AA, Etzel MR, Gadam S. (2007) Process Scale Bioseparations for the Biopharmaceutical Industry. *CRC Press*. 1st Edition. p 575.

Shukla AA, Hubbard B, Tressel T, Guhan S, Low D. (2007) Downstream processing of monoclonal antibodies-Applecation of platform approaches. *J. Chromatogr. B*. 848: 48.

Singh R, Haque I, Ahmad F. (2005) Counteracting Osmolyte Trimethylamine N-Oxide Destabilizes Proteins at pH below Its pKa. *J. Biol. Chem*. 280: 11035-11042.

Singh LR, Dar TA, Rahman S, Jamal S, Ahmad F. (2009) Glycine betaine may have opposite effects on protein stability at high and low pH values. *BBA Proteins Proteom*. 1794: 925-935.

Skouri M, Lorber B, Giege R, Munch JP, Candau JS. (1995) Effect of macromolecular impurities on lysozyme solubility and crystallizability: dynamic light scattering, phase diagram and crystal growth studies. *J Crystal Growth*. 152: 209-220.

Some D, Hanlon A, Sockolov K. (2008) Characterizing protein-protein interactions via static light scattering: reversible heteroassociation. Amer. Biotechnol. Lab. 26: 18-20.

Some D, Hitchner E, Ferullo J. (2009) Characterizing protein-protein interactions via static light scattering: Nonspecific interactions. *Am. Biotechnol. Lab*. 27: 2.
Sekhon BS. 2010. Biopharmaceuticals: an overview. *Thai. J. Pharm. Sci*. 34: 1-19.

Street TO, Bolen DW, Rose GD. (2006) A molecular mechanism for osmolyte-induced protein stability. *PNAS*. 103: 13997-14002.

Tanaka S and Ataka M. (2002) Protein crystallization induced by polyethylene glycol: A model study using apoferritin. *J. Chem. Phys.* 117: 3504-3509.

Taneja S, Ahmad F. (1994) Increased thermal stability of proteins in the presence of amino acids. *Biochem. J*. 303: 147-153.

Upreti D. (2012) Snapshot on global market of therapeutic monoclonal antibody. http://talkbiotech.org/?p=189

Urmann M, Graalfs H, Joehnck M, Jacob LR, Frech C. (2010) Cation-exchange chromatography of monoclonal antibodies. *Mabs*. 2: 395-404.

Varughese MM, Newman J. (2012) Inhibitory Effects of Arginine on the Aggregation of Bovine Insulin. *J. Biophys*. 2012: 1-7.

Veesler S, Marcq S, Lafont S, Astier JP, Biostelle R. (1994) Influence of polydispersity on protein crystallization: A quasi-elastic light-scattering study applied to α–amylase. *Acta. Crystallogr. D*. 50: 355.

Vitzthum F, Geiger G, Bisswanger H, Brunner H, Bernhagen J. (1999) A quantitative fluorescence-based microplate assay for the determination fo double-stranded DNA using SYBR Green I and a standard ultraviolet transilluminator gel imaging system. *Anal Biochem*. 276: 59-64.

Walsh G. (2000) Biopharmaceutical benchmarks. *Nat. Biotechnol*. 18: 811-833.

Walsh G. (2003) Biopharmaceuticals: Biochemistry and Biotechnology. *John Wiley & Sons*. 3rd Edition.; Walsh G. 2001. Biopharmaceuticals and biotechnology medicines: an issue of nomenclature. *Eur. J. Pharm. Sci*. 15: 135-138.

Wang W. (2005) Protein aggregation and its inhibition in biopharmaceutics. *Int. J. Pharm*. 289: 1-30.

Weber PC. (1991) Physical principles of protein crystallization. *Adv. Prot. Chem*. 41: 1-36.

Weber PC. (1997) Overview of protein crystallization methods: Macromolecular crystallography. *Methods Enzymol*. 276A: 13.

Wen J, Arakawa Tsutomu. (2000) Refractive index of proteins in aqueous sodium chloride. *Ana. Biochem*. 280: 327-329.

Werner RG. (1998) Economy of mammalian cell culture derived biopharmaceuticals. *Med. Fra. Landbouww. Univ. Gent*. 63/4a.

Xie G, Timasheff SN. (1997) The thermodynamic mechanism of protein stabilization by trehalose. *Biophys. Chem*. 64: 25-43.

Yancey PH, Clark ME, Hand SC, Bowlus RD, Somero GN. (1982) Living with water stress: Evolution of osmolyte systems. *Science*. 217: 1214-1222.

Yang MX, Shenoy B, Disttler M, Patel R, McGrath M, et al. (2003) Crystalline monoclonal antibodies for subcutaneous delivery. *Proc. Natl. Acad. Sci.USA*. 100: 6934-6939.

Yoo EM, Chintalacharuvu KR, Penichet ML, Morrison SL. (2002) Myeloma expression systems. *J. Innunol. Methods*. 261: 1-20.

Zang Y, Kammerer B, Eisenkolb M, Lohr K, Kiefer H. (2011) Towards protein crystallization as a process step in downstream processing of therapeutic antibodies: Screening and optimization at microbatch scale. *PLoS ONE*. 6(9): e25282.

Zimm BH. (1948) The Scattering of Light and the Radial Distribution Function of High Polymer Solutions. *J. Chem. Phys.* 16: 1093-1099.

Curriculum Vitae

Personal information

Name	Yuguo Zang
Address	Riedlinger Street 7, 88400, Biberach, Germany
Date of birth	11.Jan.1980 Shanghai, China
Nationality	P. R China

Education

04/2009- now	Ph. D student at the Institute of applied Biotechnology, Biberach University of applied Sciences, Germany.
	Ph. D student at the Institute of Process Engineering in Life Sciences, Karlsruhe Institute of Technology; Germany
04/2004-12/2008	Studies of Molecular Biotechnology (diploma), Bielefeld University, Germany
09/1998-06/2002	Studies of Chemical technique and technology (Bachelor) in Eastchina University of science and technology, China

Scientific Publications

Paper

Zang Y, Kammerer B, Eisenkolb M, Lohr K, Kiefer H. (2011)
Towards Protein Crystallization as a Process Step in Downstream Processing of Therapeutic Antibodies: Screening and Optimization at Microbatch Scale
PLoS ONE 6(9): doi:10.1371/journal.pone.0025282

Zang Y, Eisenkolb M, Kiefer H. (2012)
Influence of Protein Impurities on the Crystallization of Monoclonal Antibody
Submitted to Process Biochemistry

Eisenkolb M, Zang Y, Marrahi AS, Witt A, Kiefer H. (2012)
The Effect of Osmolytes on Thermal and Kinetic Stability of Lysozyme
Submitted to PLoS ONE

Poster

Zang Y, Kammerer B, Eisenkolb M, Kiefer H. (2010)
Purification of a monoclonal antibody by crystallization.
BioProcess International Conference, Providence, 20.-24.9.2010.

Eisenkolb M, Zang Y, Witt A, Kiefer H. (2010)
Stabilization and crystallization of aggregation-prone biopharmaceutical proteins.
International Symposium on the Separation of Proteins, Peptides and Polynucleotides (ISPPP), Bologna, 5.-8.9.2010

Zang Y, Eisenkolb M, Kiefer H. (2011**)**
Large-Scale crystallization of a therapeutic antibody: phase behavior and kinetics of crystal formation
IX European Symposium of the Protein Society, Stockholm, 22.-26.05. 2011
I European Congress of Applied Biotechnology (ECAB), Berlin, 26.-29.9.2011.

Eisenkolb M, Zang Y, Kiefer H. (2011)
Preventing protein aggregation: A comparison of protein-stabilizing capabilities of naturally occurring osmolytes.
I European Congress of Applied Biotechnology (ECAB), Berlin, 26.-29.9.2011.

Kiefer H, Eisenkolb M, Zang Y. (2012)
Preventing protein aggregation by naturally occurring and designed osmolytes
Recovery of biological products XV, Vermont, 29.07-03-08.2012

Hubbuch J, Alten S, Cornehl B, Ebert S, Kiefer H, Kind M, Nirschl H, Nothelfer F, Schnabel N, Zang Y. (2012)
Protein crystallization-From phase diagrams to process
Recovery of biological products XV, Vermont, 29.07-03-08.2012